

GENETIC REGULATION OF OSTEOLASTIC CELLS IN REACTION TO A MAGNESIUM CORROSION ENVIRONMENT

Dissertation with the aim of achieving a doctoral degree at the Faculty of Mathematics,
Informatics and Natural Sciences
Department of Chemistry of University Hamburg

Dipl.-Biol. Anna Müller née Burmester

2016

Evaluators of the dissertation:

Prof. Dr. Regine Willumeit-Römer

Prof. Dr. Ulrich Hahn

Date of disputation: 15.07.2016

Declaration upon Oath

I hereby declare that except where reference to the literature as well as acknowledgement of collaborative research and discussions have been made, this PhD dissertation entitled “Genetic regulation of osteoblastic cells in reaction to a magnesium corrosion environment” represents my own original research work and effort and it has not been previously submitted, in whole or in part, to qualify for any other academic award.

Signed:

10.05.2016, Cologne

ABSTRACT

Magnesium-based implants exhibit several advantages, such as biodegradability and the enhancement of *in vivo* bone formation [1, 2]. Nonetheless, the degradation of magnesium may induce cell type-specific modifications of metabolism, which still remain unclear. To examine the mechanisms of osteoinduction, the reaction of bone-derived cells (U2OS, MG63, and SaoS2 cells and primary human osteoblasts (OB)) to magnesium (Mg) was analysed. Magnesium salt (MgCl_2) was used as the simplest model system. Additionally, magnesium-based extracts were then applied to create more realistic magnesium degradation conditions. In a third approach, the cells were incubated directly on magnesium metal to investigate the influence of direct contact on metabolism.

The relations between cell count, viability, and cell size and the presence of magnesium were investigated to analyse the effects on proliferation and differentiation. Additionally, the cells were seeded directly on top of pre-incubated magnesium samples, and the number of focal adhesions was analysed. Furthermore, the expression of genes involved in bone metabolism was determined by qPCR. The analysed conditions were verified with a proteomics approach analysing primary human osteoblasts.

As an *in vitro* model system, MgCl_2 yielded very heterogeneous results. Magnesium-based extracts indicated no particular stimulus, depending on the selected cell line. In contrast to these results, the experiments performed using primary human osteoblasts were remarkably different. Some osteoinductive reactions were detected for primary human osteoblasts:

- I. Increased cell counts after extract addition;
- II. Increased cell sizes in combination with augmented adhesion behaviour after MgCl_2 and extract exposure; and
- III. Bone remodelling gene expression patterns were observed for nearly all analysed conditions.

Thus, it can be concluded that magnesium induces enhanced *in vivo* bone formation in combination with other degradation factors.

Proteomics revealed distinct differences in the patterns obtained under the various conditions. Osteoinductive features were confirmed at the protein level. Most striking was the frequent occurrence of calcium (Ca) binding proteins and proteins involved in cell metabolism or cell structure.

In conclusion, the results obtained using the cell lines were heterogeneous and showed no specific stimulation after magnesium exposure, whereas a distinct osteoinductive effect could be demonstrated with primary human osteoblasts.

ZUSAMMENFASSUNG

Magnesium-basierte Implantate weisen eine Reihe von Vorteilen, wie z. B. die biologische Abbaubarkeit und die Verbesserung der Knochenbildung *in vivo*, auf [1, 2]. Nichtsdestotrotz kann der Magnesiumabbau im Körper zelltypspezifische Änderungen des Stoffwechsels induzieren, welche nach jetzigem Stand der Forschung noch ungeklärt sind. Um die Mechanismen der Osteoinduktion zu untersuchen, wurde die Reaktion von Knochenzellen (U2OS, MG63, SaoS2, primäre humane Osteoblasten (OB)) nach Magnesiumexposition (Mg) analysiert. Magnesiumchlorid ($MgCl_2$) wurde als das einfachste Modellsystem verwendet. Um Abbaubedingungen *in vivo* möglichst realistisch darzustellen, wurden zusätzlich magnesiumbasierte Extrakte verwendet. In einem dritten Schritt wurden die Zellen direkt auf dem Magnesium inkubiert, um den Einfluss des direkten Kontaktes auf den Stoffwechsel zu bestimmen.

Der Einfluss von Magnesium auf Zellzahl, Viabilität und Zellgröße wurde analysiert, um dessen Effekt auf die Proliferation und Differenzierung zu ermitteln. Die Zellen wurden direkt auf den vorinkubierten Magnesiumproben ausgesät und zusätzlich die Anzahl der fokalen Adhäsionen ermittelt. Zusätzlich wurde mittels qPCR die Expression von Genen bestimmt, die am Knochenstoffwechsel beteiligt sind. Die zuvor untersuchten Bedingungen wurden mit einem Proteomansatz und primären humanen Osteoblasten verifiziert.

$MgCl_2$ als *in vitro* Modellsystem wies sehr heterogene Ergebnisse auf. Magnesium-basierte Extrakte zeigten keinen besonderen Stimulus auf die verwendeten Osteosarkomzelllinien. Im Vergleich konnte bei Verwendung von primären humanen Osteoblasten ein gegenläufiges Bild gezeigt werden. Die Ergebnisse zeigen folgende Hinweise auf Osteoinduktion bei Verwendung von primären humanen Osteoblasten:

- I. Eine erhöhte Zellzahl nach Extrakt-Exposition;
- II. Erhöhte Zellgrößen in Kombination mit einem verstärkten Haftverhalten nach $MgCl_2$ und Extrakt-Exposition;
- III. Genexpressionsmuster, die den Knochenumbau unter fast allen analysierten Bedingungen begünstigen.

Diese Ergebnisse lassen den Schluss zu, dass Magnesium, in Kombination mit anderen Abbaufaktoren, die Knochenbildung *in vivo* induziert. Die Ergebnisse aus der Proteomanalyse zeigten deutliche Unterschiede in den Expressionsmustern unter den verschiedenen Bedingungen. Die osteoinduktiven Eigenschaften konnten auf Proteinebene bestätigt werden. Am Häufigsten zeigte sich ein erhöhtes Auftreten von Calcium (Ca)-bindenden Proteinen sowie von Proteinen, die am Zellstoffwechsel oder der Zellstruktur beteiligt sind.

Zusammenfassend sind die Ergebnisse, die mit den Zelllinien erzielt wurden heterogen und zeigten keine spezifischen Stimuli nach Magnesiumexposition, während bei primären Osteoblasten ein eindeutiger osterinduktiver Effekt zu sehen ist.

TABLE OF CONTENTS

1. Introduction	1
1.1 Magnesium as an implant material	1
1.2 Ossification	2
1.3 Cell lines and primary cells	4
1.4 The Role of magnesium in bone metabolism	5
2. Scope of the work.....	7
3. Materials & Methods.....	8
3.1 Materials	8
3.1.1 Buffer composition	8
3.1.2 Media	8
3.1.3 DNA ladders	8
3.1.4 Oligo-nucleotides	9
3.2 Cell culture	10
3.2.1 Cell lines	10
3.2.2 Cultivation and differentiation of primary human cells.....	10
3.3 Proliferation tests	12
3.4 Fluorescence microscopy	13
3.4.1 Cell size.....	14
3.4.2 Live/Dead staining	14
3.4.3 Focal adhesions	14
3.4.4 Cell/Green particle calculation from fluorescent images.....	15
3.5 Molecular biology methods	15
3.5.1 RNA extraction	15
3.5.2 cDNA synthesis	16
3.5.3 Polymerase chain reaction (PCR)	16
3.6 Proteomics	17
3.6.1 Cell preparation.....	17
3.6.2 2-D Gel electrophoresis	17
3.6.3 Tryptic in-gel digestion of proteins.....	18
3.6.4 Liquid chromatography–mass spectrometry (LC/MS)	19
3.7 Sample and extract preparation	19
3.7.1 Analytic tests for the examination of extract constitution (osmolality, pH, and magnesium concentration)	21

3.9 Statistical analysis.....	21
4. Results	22
4.1 Influence of magnesium chloride on osteoinductive features	22
4.1.1 Proliferating cells	22
4.1.2 Differentiating cells	30
4.2 Influence of magnesium-based extracts on osteoinductive features.....	34
4.2.1 Media and extract characterisation	35
4.2.2 Proliferating cells	37
4.2.3 Differentiating cells	41
4.3 Direct contact with the material and its influence on osteoinduction.....	44
4.4 Osteoinductive effects reflected in Proteomics	51
5. Discussion	57
5.1 Cell counts affected by magnesium.....	58
5.2 Viability influenced by magnesium exposure	60
5.3 Cell size affected by magnesium corrosion	62
5.4 Gene expression reveals osteoinductive properties	63
5.5 Suitable osteoblastic <i>in vitro</i> cell model for magnesium investigation	68
5.6 Proteomics confirmed phenotypic and genotypic studies for osteoinductive features...	69
6. Summary and Outlook	73
7. References	74
8. Abbreviations	90
9. List of Tables.....	93
10. List of Figures	95
11. Appendix	97
12. Publication list.....	124
12.1 Journal Articles.....	124
12.2 Conference contributions.....	124
13. Hazard statements and safety phrases	126
14. Acknowledgements	134

1. INTRODUCTION

1.1 MAGNESIUM AS AN IMPLANT MATERIAL

Magnesium-based implants are not an invention of recent decades but have been under intensive investigation since the 19th century [3]. Magnesium alloys have long been used as a stent material for cardiovascular applications. The first successful surgery was performed on a premature baby. The stent was implanted into the left pulmonary artery and degraded completely after five months [4]. In another study, degradable magnesium stents were implanted into the coronary arteries of 63 patients, and the results were comparable to those obtained with bare metal stents [5]. Moreover, a cannulated screw made of biodegradable magnesium was successfully tested in a clinical trial and was thus placed on the market. This screw showed analogous behaviour to titanium screws [6].

However, this material is not the clinical standard because the degradation mechanisms are not understood *in vitro* or *in vivo*. Although such implants exhibit several advantages over permanent implants, such as biodegradability and possible osteoinductive properties [7].

While the implant is degrading, the bone must absorb an increasing load, which is important for the stability of the bone. Moreover, the mechanical properties of magnesium, such as its density, modulus of elasticity and compressive yield strength, are similar to those of bone. In contrast, the mechanical characteristics of titanium are much higher. If the mechanical properties are similar to those of bone, the material does not absorb all of the operating strengths; thus, the healing process of the fracture is improved. An overview of the mechanical properties is presented in Table 1 [8].

Table 1. Mechanical properties of bone and biomaterials.

Properties	Natural bone	Magnesium	Titanium
density (g/cm^3)	1.8-2.1	1.74-2.0	4.4-4.5
elastic modulus (Gpa)	3-20	41-45	110-117
compressive yield strength (Mpa)	130-180	65-100	758-1,117
fracture toughness ($\text{MPam}^{1/2}$)	3-6	15-40	55-115

The main constituent of such degradable implants is magnesium, which is one of the most abundant cations in the human body [9]. This abundance increases the biocompatibility of these implants. Moreover, a second surgery to remove the implant is not necessary because the implants are biodegradable. The material will be completely reabsorbed from the surrounding tissue, and bone formation also appears to be enhanced [1, 2]. Many parameters provoke modifications of metal degradation behaviour (*e.g.*, the microstructure of magnesium and its alloys, temperature, pH, the composition of the corrosion medium or body

environment, the buffering capacity of the solutions, the existence of proteins in the medium or the adjustment of the flow rate of the environmental medium) [1, 2, 10-12]. Therefore, a change in one of these parameters can cause different results. Additionally, the presence of cells has a direct influence on the corrosion rate [10]. This issue is quite complicated to evaluate and has not been investigated in depth to date. In this study, a systematic examination of different magnesium models was conducted. The aim of this analysis was to determine the influence of magnesium corrosion on osteoinductive effects in bone-related cells.

1.2 OSSIFICATION

Ossification is the process of building new bone material. In the case of chondral ossification, which is responsible for the formation of long bones, new bone tissue is created out of the mesenchyme. The initial calcified tissue is built. Within this calcified matrix, the first vessels are developed. This site functions as the main centrum of ossification. Trabeculae are built by numerous chondrocytes. The matrix is replaced by increasing amounts of hardened bone. The periosteum is formed by a layer called the perichondrium. The periosteum produces osteogenic cells, such as osteoblasts, which build the medullary cavity. Secondary centroms of ossifications are developed towards the epiphysis. Figure 1 presents a schematic illustration of how ossification occurs. Bone is generated via the same mechanism after a fracture.

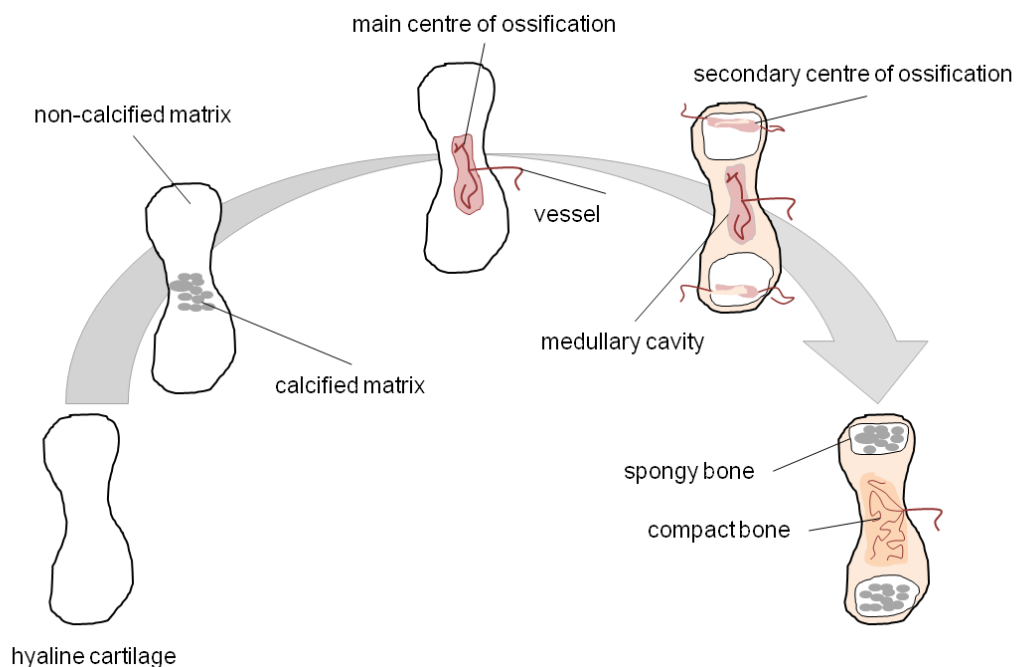


Figure 1. Schematic presentation of chondral ossification.

Presented is the process of bone generation from hyaline cartilage to compact bone. The origin is hyaline cartilage, and the bone tissue is built from ossification centres. Angiogenesis also occurs in the main centre of ossification. Image modified from Kanczler and Oreffo, 2008 [13].

To build new bone tissue, osteogenic cells are necessary. Osteoblasts belong to these cells. Osteoblasts originate from mesenchymal stem cells. Due to the induction of runt-related transcription factor 2 (Cbfa1), mesenchymal stem cells differentiate into pre-osteoblasts [14]. This stage of osteoblast differentiation is marked by cell proliferation. Increased expression of alkaline phosphatase can be observed in the immature osteoblast stage. This stage is marked by matrix maturation. The last step of osteoblast differentiation is marked by mineralization due to the increased expression of matrix-related genes, such as bone sialoprotein, osteocalcin, osteopontin and collagen 1 [15, 16].

Within the process of bone formation, bone resorption is also an important part of generating healthy bone. Osteoclasts are the main cells involved in this process. These cells originate from macrophages that were stimulated by macrophage colony-stimulating factor (M-CSF). The expression of receptor activator of NF- κ B (RANK) is increased in osteoclast precursor cells, and the protein is expressed on the outside of the cells and acts as a receptor for RANKL ligand (RANKL). Both of these factors are key molecules in osteoclast activation and differentiation [17]. If RANKL, which is expressed by immature osteoblasts, is capable of binding to RANK, the osteoblast precursor cells can further differentiate into mature osteoclasts. Mature osteoclasts are able to resorb bone tissue. Osteoprotegerin (OPG) is the antagonist of RANKL and inhibits its binding by blocking RANK. OPG is a decoy receptor for RANKL and inhibits the maturation of osteoclasts. Thus, the differentiation of osteoclasts is inhibited, leading to increased bone formation caused by an increased number of osteoblasts. The process of balanced bone formation and resorption is called the bone remodelling process. A schematic overview of the differentiation of osteoblasts and osteoclasts and the main genes involved in these progresses is presented in Figure 2.

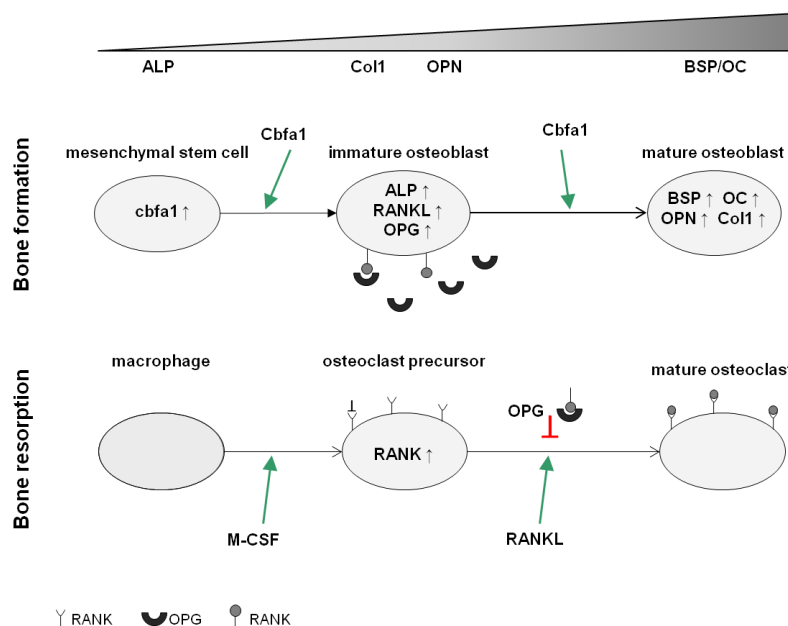


Figure 2. Schematic presentation of the genes involved in bone formation and resorption.

Presented are the processes of osteoblast and osteoclast differentiation, including the genes that are involved, with increased expression indicated by grey triangles. ALP: alkaline phosphatase; RANK: receptor activator of NF- κ B; RANKL: RANK ligand; BSP: bone sialoprotein; Cbfa1: runt-related transcription factor 2; OC: osteocalcin, OPN: osteopontin; OPG: osteoprotegerin; Col1: Collagen 1; and M-CSF: macrophage colony-stimulating factor.

1.3 CELL LINES AND PRIMARY CELLS

Cell lines are usually fast-growing, well-defined cells. For those reasons, cell lines are commonly applied in cell culture research. These cells were originally isolated from tumour tissue and were immortalised afterwards. Because of genetic modification, the cells do not have normal senescence control, exhibit an activated cell cycle and do not undergo apoptosis [18, 19]. Due to the enormous amount of tumour variation, a large number of cell lines are available. In the case of bone research, the MG63 cell line became a standard model in addition to primary human osteoblasts in recent decades [20-22]. Other human osteosarcoma-derived cell lines, such as SaoS2 and U2OS cells, are also used for *in vitro* tests. A literature search with relevant keywords for this study (*i.e.*, magnesium, U2OS, MG63, SaoS2 and primary human osteoblasts [23]) indicated that more than 60% of the identified publications were conducted with cell lines and only 39% were conducted with cells isolated directly from the investigated tissue (in this case, primary human osteoblasts). Although the percentage of publications that examined cell lines as bone models is very high, it remains debatable whether those cells are suitable cells for research concerning magnesium degradation.

It is obvious that primary cells, which are isolated directly from the tissue, exhibit different characteristics than cancer-derived immortalised cell lines. Primary human osteoblasts are still able to differentiate on their own. In contrast to cell lines, primary human osteoblasts exhibit senescence control, which is caused by telomerase shortening. The cells stop dividing after a few generations [24]. Osteosarcomas are tumours that consist of heterogeneous cell populations that are not all derived from bone [25]. Thus, the cell lines used in this study exhibit different characteristics, although they are all osteosarcoma-derived cell lines.

The first osteosarcoma cell line (U2OS) was established in 1964 [26]. In contrast to primary human osteoblasts, this cell line is no longer capable of differentiating on its own and building a calcified matrix [27, 28]. In addition, the proteomic profile of U2OS cells shows that they exhibit a more fibroblastic origin [29]. However, U2OS cells are not widely used in biomaterials research.

The second osteosarcoma-derived cell line (MG63) is the most well established cell line for biomaterials research [30-33]. Similar to U2OS cells, these cells are unable to build a calcified matrix [28, 34]. Furthermore, high concentrations of fibroblast-like interferon can be produced by MG63 cells [35]. Similar to primary human osteoblasts, MG63 cells are able to produce action potentials [36].

The third cell line (SaoS2) is known for its high mineralisation and proliferation characteristics [37, 38]. In contrast to the other two cell lines, SaoS2 cells are known to have osteoinductive potential *in vivo* [39].

In this study, a systematic, comparative analysis of all four cell types was performed. The reactions of proliferating and differentiating cells to enhanced extracellular magnesium concentrations were examined. The aim was to identify the most suitable and reliable cell model for investigating the effects of degrading magnesium materials *in vitro*.

1.4 THE ROLE OF MAGNESIUM IN BONE METABOLISM

Magnesium is one of the most common divalent cations in the human body [9]. Up to 60% of the magnesium in the body is stored in the bound form in the bones [40-42]. Skeletally bound magnesium serves as a reservoir because it is released under magnesium-deficient conditions [43]. Magnesium is not only important for bone but also exhibits many essential functions in the body [44, 45]. Due to its positive charge, magnesium stabilises nucleic acids, protein structures and cell membranes [46]. Magnesium is a cofactor for hundreds of enzymes and is important for various cell processes, such as protein synthesis, proliferation and apoptosis [11].

As a divalent cation, magnesium influences cell adhesion. Adhesion and spreading are stimulated by magnesium [47]. Magnesium was shown to influence integrin binding affinity [48, 49]. Integrins are a part of focal adhesions, which are multi-protein assemblies that connect the extracellular matrix to the cytoskeleton. This conjunction is mediated by the integrin family [50]. Furthermore, the overexpression of focal adhesion kinase (FAK) resulted in integrin-provoked cell migration in ovary cells [51].

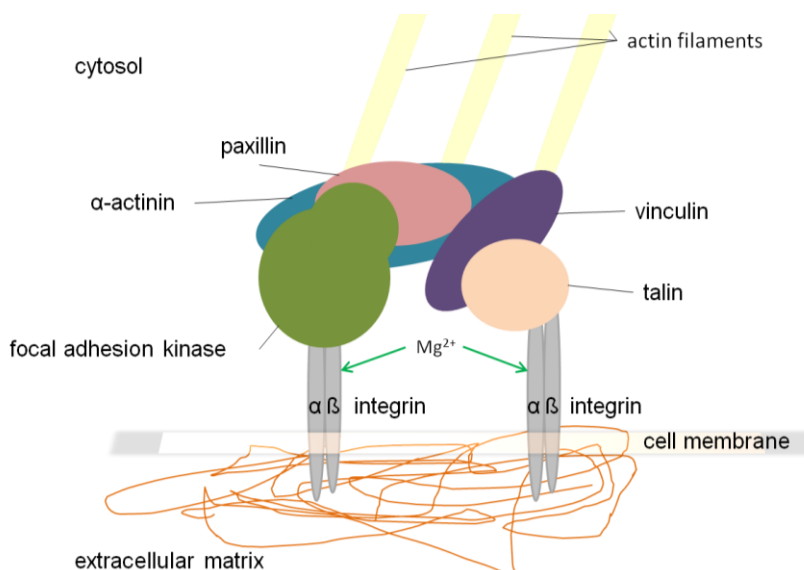


Figure 3. Schematic presentation of the focal adhesion complex.

The core assembly is within the cell and consists of talin, vinculin, paxillin and focal adhesion kinase. The integrins are the connections to the extracellular matrix, whereas the core assembly is bound to the cytoskeleton. Modified from Hammerschmidt und Wedlich, 2008 and Zebda et al. 2012 [52, 53].

Magnesium has great relevance for human health. The serum concentration of extracellular magnesium has been determined to be between 0.7 and 1.05 mmol/L (blood plasma) [45]. The kidneys and the intestine preserve homeostasis [54]. Magnesium imbalance is linked to various diseases. Magnesium deficiency, including chronic hypomagnesaemia (< 0.7 mmol/L Mg), is well studied [41, 44, 55]. Magnesium depletion leads to various dysfunctions in diverse areas of the body. Hypomagnesaemia affects not only bone metabolism but also the neuromuscular and cardiovascular systems [55]. Moreover, hypomagnesaemia is not an unusual disease, as up to 20% of patients are afflicted [41, 56]. If magnesium deficiency is not medicated, it will lead to osteoporosis [55, 57, 58]. One possible reason is that magnesium is important for transforming vitamin D into its active form. The active form of vitamin D is capable of inducing calcium absorption and thus mineralisation [59]. In addition, magnesium is a necessary cofactor for all enzymes that metabolise vitamin D [60, 61]. If magnesium is not available, these important pathways collapse. Castiglioni et al. provided a good overview of the correlation between magnesium and osteoporosis [62]. Additionally, a lack of magnesium was reported to lead to an increased number of osteoclasts [63].

Magnesium deficiency also influences the antagonists in bone metabolism: OPG and RANKL. Magnesium depletion provokes OPG/RANKL ratios that tend towards osteoclastogenesis (up to 16-fold in comparison to the control after a 50% magnesium nutrition diet in osteoblasts for six months), which would also lead to osteoporosis [58].

In contrast, very little is known about hypermagnesaemia (> 1.05 mmol/L Mg). This disease is caused primarily by increased and long-term oral ingestion. Common symptoms are lethargy and confusion, arrhythmias, and muscle weakness [41, 64]. However, biodegradable magnesium implants were shown to enhance bone formation *in vivo* [1, 2].

2. SCOPE OF THE WORK

The intention of this thesis was to investigate whether there is evidence that an osteoinductive effect occurs in cells of the bone system due to magnesium salt, magnesium-based extracts or direct contact with the material *in vitro*. The scope of the work was to investigate the following aspects:

- a) Determination of cell counts under different magnesium conditions with cell lines and primary human osteoblasts, as well as proliferating and differentiating cells;
- b) Cell viability in different magnesium-containing environments with cell lines and primary cells, as well as proliferating and differentiating cells;
- c) Analysis of cell sizes with cell lines and primary cells, as well as proliferating and differentiating cells, and analysis of focal adhesions of primary human osteoblasts in direct contact with degrading magnesium metal;
- d) Gene expression under different magnesium conditions with cell lines and primary cells, as well as proliferating and differentiating cells;
- e) Proteomics under different magnesium conditions with primary human osteoblasts; and
- f) Comparison of the different cell types in terms of the reaction to magnesium.

3. MATERIALS & METHODS

3.1 MATERIALS

3.1.1 BUFFER COMPOSITION

Phosphate-buffered saline, PBS

0.137 M	NaCl	Merck, Darmstadt, Germany
0.0027 M	KCl	Merck, Darmstadt, Germany
0.01 M	Na ₂ HPO ₄ x 2 H ₂ O	Sigma-Aldrich, Taufkirchen, Germany
0.00176 M	KH ₂ PO ₄	Merck, Darmstadt, Germany

Add 1 L of double-distilled H₂O, and adjust the pH to 7.4.

TRIS-Borat-EDTA-Puffer, TBE (for DNA agarose gel preparation)

0.089 M	tris(hydroxymethyl)aminomethane (Tris)	Sigma-Aldrich, Taufkirchen, Germany
0.089 M	boric acid	Sigma-Aldrich, Taufkirchen, Germany
0.002 M	ethylenediamine tetra acetic acid-Na ₂ (EDTA)	Merck, Darmstadt, Germany

Add 1 L of double-distilled H₂O, and adjust the pH to 8.3.

3.1.2 MEDIA

Different cell culture media were used for the various cell types investigated in this study. The media were purchased from Life Technologies (Darmstadt, Germany) and supplemented with 10% (v/v) foetal bovine serum (FBS; PAA Cell Culture Company, Linz, Austria). The compositions of these media are presented in Table 2. The values are provided by the manufacturer.

Table 2. Applied media and their compositions. DMEM GlutaMAX was used for primary human osteoblasts and MG63 cells, DMEM was used for U2OS cells and McCoy's 5A was used for SaoS2 cells.

	DMEM GlutaMAX	DMEM	McCoy's 5A
pH range:	6.8-7.2	7.0-7.4	6.9 - 7.1
glutamine:	GlutaMAX-I	L-Glutamine	L-Glutamine
osmolality:	320-360 mOsm/kg	320-360 mOsm/kg	280 - 320 mOsm/kg
concentrated:	1 x	1 x	1 x
culture environment:	CO ₂	CO ₂	CO ₂
phenol red indicator:	phenol red	phenol red	phenol red
supplementation required:	serum	serum	serum
buffering system:	sodium bicarbonate	sodium bicarbonate	sodium bicarbonate

3.1.3 DNA LADDERS

For the analysis of the correct DNA size of PCR products, a 1% (w/v) agarose gel (Sigma-Aldrich, Taufkirchen, Germany) gel containing 0.01% (v/v) GelRed (Biotium, Hayward, California, USA) was used. In addition, a size marker was applied (Quick-Load 100 bp DNA Ladder, New England Biolabs, Ipswich, Massachusetts, USA).

3.1.4 OLIGO-NUCLEOTIDES

The genes involved in bone and matrix formation were investigated, as well as housekeeping genes. Primer sequences were either selected from previous publications or designed with Primer3 (version 0.4.0 [65]). All primers were purchased from Eurofins MWG Operon (Ebersberg, Germany), and their sequences are presented in Tables 3 and 4.

Table 3. Reverse transcription-PCR (RT-PCR) primer sequences.

Gene	Abbreviation	RT-PCR-Primer (5'-3')	Ta [°C]	Product size
glyceraldehyde-3-phosphate dehydrogenase [66]	GAPDH	ACCACAGTCCATGCCATCAC TTCACCACCCTGTTGCTGTA	55	452
heparanase [67]	HPSE	TGGACCTGGACTTCTTCACC TTGATTCCTTCTTGGGATCG	53	216
alkaline phosphatase [66]	ALP	ACGTGGCTAAGAATGTCATC CTGGTAGGCGATGTCCTTA	53	475
receptor activator of NF-κB ligand [68]	RANKL	CAGGAGACCTAGCTACAGA CAAGGTCAAGAGCATGGA	49	418
bone sialoprotein [69]	BSP	AAGCAATCACCAAATGAAGACT TGAAATCGTTTTAAATGAGGATA	55	188
runt-related transcription factor 2 [70]	Cbfa1	CCCCACGACAACCGCACC CACTCCGCCCCACAAATCTC	55	289
osteocalcin [66]	OC	CATGAGAGCCCTCACA AGAGCGACACCCTAGAC	48	315
osteopontin [66]	OPN	CCAAGTAAGTCCAACGAAAG GGTGATGTCCTCGTCTGTA	55	347
osteoprotegerin [68]	OPG	AGACTTTCCAGCTGCTGA GGATCTCGCCAATTGTGA	49	469
collagen type 1	Col1	AAAGGCAATGCTCAAACACC TCAAAAACGAAGGGGAGATG	49	159
collagen type 2 [71]	Col2	GTGGAGCAGCAAGAGCAAGGA CTTGCCCCACTTACCAGTGTG	61	334
collagen type 10	Col10	TCAAAAAGGTGATCCTGGAG CCCTTTAGACCCAGGGAATC	55	181

Table 4. Real-time PCR (qPCR) primer sequences.

Gene	Abbreviation	qPCR-Primer (5'-3')	Ta [°C]	Product size
β -actin	β -Actin	CTTCCTGGGCATGGAGTC TGATCTTCATTGTGCTGGGT	60	134
glyceraldehyde-3-phosphate dehydrogenase	GAPDH	GTCGGAGTCAACGGATTTG TGGGTGGAATCATATTGGAA	60	143
alkaline phosphatase	ALP	CACCCACGTCGATTGCATCT TAGCCACGTTGGTGTGAGC	60	211
bone sialoprotein	BSP	TGGATGAAAACGAACAAGGCA AAACCCACCATTTGGAGAGGT	60	200
osteocalcin	OC	GGCAGCGAGGTAGTGAAGAG CTGGAGAGGAGCAGAACTGG	60	230
osteopontin	OPN	CTCCATTGACTCGAACGACTC CAGGTCTGCGAACTTCTTAGAT	60	230
osteoprotegerin	OPG	CGCTCGTGTTTCTGGACAT GGACATTTGTCACACAACAGC	60	112
receptor activator of NF- κ B ligand [72]	RANKL	ATACCCTGATGAAAGGAGGA GGGGCTCAATCTATATCTCG	60	202
alpha-actinin-1	ACTN1	TCAAGGCCCTGCTCAAGAAG GCTTCCCTTCGCTTCTGAGT	60	199
annexin A1	ANXA1	AGCGAAACAATGCACAGCGT CCCTTCATGGCAGCACGAAG	60	175
annexin A2	ANXA2	ACATTTTGACCAACCGCAGCAA GAGTCCTCGTCGGTTCACAG	60	208
annexin A4	ANXA4	AGCAATATGGACGGAGCCTTGA CAACAGGTGATTTCCGGTTCAG	60	230
endoplasmic reticulum chaperone	HSP90B1	ACCCACATCTGCTCCACGTG CGCGGGAAACATTCAAGGGG	60	179
myosin light chain 6B	MYL6	GCACACTGTCCTTTGGCCAC GCACACTGTCCTTTGGCCAC	60	171
protocadherin alpha-1	PCDHA1	ACATTAAATGCCTCTGATGCTGACG TACATCCAGCACTTTCACCAAACC	60	243

3.2 CELL CULTURE

3.2.1 CELL LINES

The osteosarcoma-derived cell lines U2OS, MG63 and SaoS2 were obtained from the European Collection of Cell Cultures (ECACC, Salisbury, United Kingdom).

3.2.2 CULTIVATION AND DIFFERENTIATION OF PRIMARY HUMAN CELLS

The primary human osteoblasts (OB) used in this study were derived either from artificial hip joints after hip replacement (Hospital in Eilbek; used for proliferation, viability and cell size

measurements, direct contact tests, and proteomics) or cruciate ligament operations (Hospital Universitätsklinikum Hamburg-Eppendorf; used for gene expression analysis with MgCl_2 ($\text{MgCl}_2 \cdot 6\text{H}_2\text{O}$ (Merck, Darmstadt, Germany); 0-25 mM in 5 mM steps) or magnesium-based extracts for 1 week); the latter cells were healthy primary human osteoblasts without an osteoporotic background. The isolation and culture of the cells was approved by the local ethics committee and carried out in accordance with the Declaration of Helsinki, as described previously [73].

Cancellous bone material was isolated from bone pieces and transferred to a cell culture flask. Cell culture medium was added to the cancellous particles. Incubation under cell culture conditions was performed until the cells reached approximately 90% confluence, and the cells were then passaged. Primary human osteoblasts were used up to the 3rd passage. The cell lines were used between the 4th and 10th passages. The cells were incubated with or without (as a control) the addition of MgCl_2 , extracts or direct contact with the material for 1 week, 2 weeks or 4 weeks, respectively. The medium was changed every 2 to 3 days.

For passaging, the cells were washed with PBS, and 0.05% Trypsin/EDTA (Life Technologies, Darmstadt, Germany) was added. The cells were then incubated for 5 min in the incubator. Trypsin is an enzyme that cuts extracellular proteins and thus detaches the cells from cell culture tissue. With the addition of cell culture medium, the enzyme is inactivated again. The cells were centrifuged at 250 x g (Labofuge 400R, Heraeus Instruments, Hanau, Germany), old medium was discarded afterwards and cells were resuspended in new medium. Pure magnesium samples were pre-incubated for 24 h in the corresponding cell culture medium containing 10% FBS (v/v) under cell culture conditions before the cells were seeded on top of the samples. The cells were allowed to adhere for 30 min prior to the addition of medium to the magnesium samples. As controls, mirror-polished titanium discs and cell culture plastic were used. Each experiment was performed using five independent cultures (n=5).

For cell differentiation, the media or extracts were supplemented with 10^{-8} M dexamethasone (Sigma-Aldrich, Taufkirchen, Germany), 5 mM L-ascorbic acid (L-AA, Sigma-Aldrich, Taufkirchen, Germany), and 10^{-8} M $1\alpha,25$ dihydroxyvitamin D3 (Vit-D3, Sigma-Aldrich, Taufkirchen, Germany) for 2 weeks and with the addition of 5 mM β -glycerolphosphate (β -GP, Sigma-Aldrich, Taufkirchen, Germany) for 2 additional weeks for primary human osteoblasts. The cell lines were incubated with the indicated components for 1 week (dexamethasone, L-AA, and Vit-D3) and one additional week (β -GP). An overview of the different incubation times and procedures is presented in Table 5 and Figure 4.

Table 5. Cell culture conditions for different exposure conditions.

	MgCl₂	Extract	Direct contact
sample pre-incubation	—	—	24 h
medium change	every 2-3 days	every 3-4 days	every 2-3 days
incubation time cell lines proliferation	1 week	1 week	1-2 weeks
incubation time cell lines differentiation	2 weeks	2 weeks	—
incubation time primary human osteoblasts proliferation	4 weeks	4 weeks	1-4 weeks
incubation time primary human osteoblasts differentiation	4 weeks	4 weeks	—

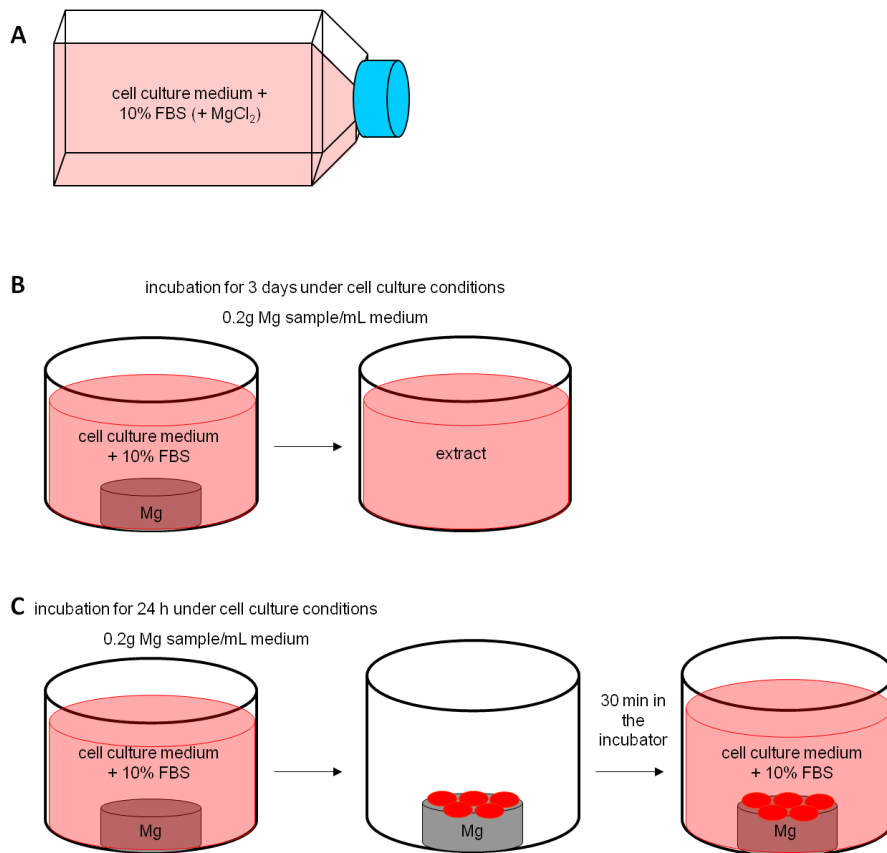


Figure 4. Overview of cell culture conditions.

Presented is a schematic summary of the cell culture systems used in this study. A) This figure represents the incubation of cells under control conditions or with the addition of MgCl₂. B). This figure shows the preparation of magnesium-based extracts before application to the cells. C) This figure demonstrates the procedure used to place the cells in direct contact with corroding magnesium material (Mg).

3.3 PROLIFERATION TESTS

The counted cells were incubated under different conditions for a period of time (Table 5). Afterwards, the proliferation (*i.e.*, cell count), viability and cell size of the cells in suspension was examined. The number of cells used in each experiment is shown in Table 6.

Table 6. Initial cell counts for the various proliferation experiments.

	U2OS	MG63	SaoS2	OB
MgCl ₂ proliferating	10 ⁴	10 ⁴	10 ⁴	10 ⁴
MgCl ₂ differentiating	10 ³	5.000	10 ⁴	10 ⁵
extract proliferating	10 ⁴	10 ⁴	10 ⁴	10 ⁶
extract differentiating	5.000	5.000	10 ⁴	10 ⁶

The cells were trypsinised, and the viable cell number, viability and mean diameter were determined using a CASY Model TT 150 µm system (Roche, Mannheim, Germany). Briefly, the pulse area analysis technique is used by the CASY system. The system uses the electric current exclusion method, which is based on the integrity of cell membranes. Intact cell membranes can exclude the electrical current, whereas damaged membranes are permeable to the electrical current. The size of the nucleus is measured. Every cell is analysed with hundreds of readings, resulting in a frequency of one million measurements per second for every object.

The quantification of dead and viable cells, with individual adjustments for each cell type, is performed simultaneously. The adjustments are presented in Table 7.

Table 7. CASY Model TT adjustments for different cell types.

	Cell debris	Dead cells	Living cells and cell aggregates	Sample volume
U2OS	< 7.25 µm	7.25 µm - 11.50 µm	> 11.50 µm	25.0 µL
MG63	< 7.75 µm	7.75 µm - 12.75 µm	> 12.75 µm	25.0 µL
SaoS2	< 7.00 µm	7.00 µm - 11.25 µm	> 11.25 µm	50.0 µL
osteoblasts	< 7.63 µm	7.63 µm - 14.88 µm	> 14.88 µm	200 µL

3.4 FLUORESCENCE MICROSCOPY

For fluorescence microscopy analysis, an Eclipse Ti-S microscope (Nikon GmbH, Düsseldorf, Germany) was employed, using the NIS-Elements Microscope Imaging Software (Nikon GmbH, Düsseldorf, Germany). The filters and the corresponding filter spectra are presented in Table 8.

Table 8. Fluorescent microscope filters and the corresponding spectra.

Filter	Excitation	Emission	Mirror
DAPI	325 - 375 nm	435 - 485 nm	400 nm
FITC	460 - 500 nm	510 - 560 nm	505 nm
TexasRed	533 - 588 nm	608 - 683 nm	595 nm

3.4.1 CELL SIZE

To visualise the shape of the adherent cells, fluorescence microscopy was used. Therefore, the cells were incubated on sterile glass slides that were previously covered with fibronectin overnight (10 ng/mL in PBS; Sigma-Aldrich, Taufkirchen, Germany) or incubated directly on the material. Formaldehyde (3.7% (v/v) in PBS; Sigma-Aldrich, Taufkirchen, Germany) was used to fix the cells. Incubation was carried out for 10 min at room temperature, followed by two washing steps with PBS for 1 min each. A mixture of 1% (v/v) bovine serum albumin (BSA, Life Technologies, Darmstadt, Germany) and 1 unit of Alexa Fluor 488 phalloidin (Life Technologies, Darmstadt, Germany) was added to stain the actin filaments. Incubation with this mixture was carried out at 37 °C for 20 min in the dark. The samples were washed twice with PBS for 1 min each. Then, 4,6-diamidino-2-phenylindole dihydrochloride (DAPI; Sigma-Aldrich Chemie, Taufkirchen, Germany) at a concentration of 5 µg/mL was added to stain the nuclei. The samples were incubated at 37 °C for 15 min in the dark. Images were collected immediately using an Eclipse Ti-S microscope.

3.4.2 LIVE/DEAD STAINING

Pure magnesium samples were pre-incubated for 24 h in the corresponding cell culture medium containing 10% FBS (v/v) under cell culture conditions before the cells were seeded on top of the samples (cell lines: 10^4 cells, primary human osteoblasts: 10^5 cells). The cells were allowed to adhere for 30 min prior to the addition of medium to the magnesium samples. After 1 week (cell lines) or 4 weeks (primary human osteoblasts) of direct contact with the implant material, the extract was decanted and kept. The samples were treated simultaneously with 2 µM ethidium homodimer-1 and 1.6 µM calcein-AM (LIVE/DEAD Viability/Cytotoxicity Kit for mammalian cells, Life Technologies, Darmstadt, Germany) in PBS for 20 min in the incubator. Afterwards, the previously decanted extract was added to the cells or samples, and images were collected immediately using an Eclipse Ti-S microscope. The assay is based on the fact that calcein-AM itself is not a fluorescent molecule. However, viable cells are able to cut the calcein with an esterase, which is then fluorescent (green). In contrast, ethidium homodimer-1 visualises dead or dying cells, as it is not able to permeate intact membranes and binds to DNA (red).

3.4.3 FOCAL ADHESIONS

To examine the adhesion of primary human osteoblasts via focal adhesions (FAs), vinculin was visualised as part of the FA. Therefore, $5 \cdot 10^4$ cells were incubated on cell culture plastic (control), on mirror-polished titanium discs and on pure magnesium samples, and the existence of FAs was determined after 1 day, 3 days, 1 week and 2 weeks. The staining was

conducted in accordance with the manufacturer's manual (FAK100 Actin Cytoskeleton/Focal Adhesion Staining Kit, Merck Millipore, Darmstadt, Germany). The cells were fixed with formaldehyde (4% (v/v) in PBS). The cells were permeabilised via supplementation with Triton X-100 (0.1% (v/v) in PBS, Sigma-Aldrich Chemie, Taufkirchen, Germany). A blocking solution was added (1% (v/v) BSA in PBS), followed by incubation with the primary antibody (anti-vinculin) at a concentration of 1:250 in a blocking solution for 1 h at room temperature in the dark. Afterwards, incubation with TRITC-conjugated phalloidin (1:500 in PBS) and the secondary antibody (1:100 in PBS; FITC-conjugated Goat Anti-mouse IgG (H+L); Jackson Immuno Research Laboratories, Inc., Newmarket, UK) was carried out concurrently for 45 min at room temperature in the dark. Finally, DAPI (1:1,000 in PBS) was added to stain the nuclei of the cells. Incubation was performed for 3 min at room temperature in the dark. Images were collected immediately using an Eclipse Ti-S microscope.

3.4.4 CELL/GREEN PARTICLE CALCULATION FROM FLUORESCENT IMAGES

The ImageJ software (National Institutes of Health, Bethesda, Maryland, USA) was applied to analyse the images. Before the adjustments of brightness and contrast were performed the region of interest (ROI) was defined manually. Then, the image was converted into an 8-bit image. The colour threshold was adapted to ensure that the pixels appeared black. If needed, the watershed tool was applied to separate the particles. Afterwards, the particles were analysed. Therefore, the smallest adjustments (0-Infinity) were used because the cells/focal adhesions were very small in the images.

3.5 MOLECULAR BIOLOGY METHODS

3.5.1 RNA EXTRACTION

The RNeasy Mini Kit (Qiagen, Hilden, Germany) was used to isolate total cellular ribonucleic acid (RNA). Isolation was performed in accordance with the manufacturer's manual. Therefore, up to $4 \cdot 10^6$ cells were washed twice with PBS and lysed via the addition of a buffer that contains guanidine thiocyanate (buffer RLT). A QIAshredder spin column (Qiagen, Hilden, Germany) was then used to homogenise the lysate. Then, ethanol (70% (v/v) in ddH₂O, Merck Millipore, Darmstadt, Germany) was added to the flow-through. This solution was applied to an RNeasy spin column (a silica-gel membrane) and washed with buffers RW1 and RPE. RNase-free water was added to the column to elute the total RNA. Finally, a NanoDrop 2000c Spectrophotometer (PEQLAB Biotechnologie GmbH, Erlangen, Germany) was used to determine the RNA concentration and integrity photometrically (at 260 nm and 280 nm).

3.5.2 *CDNA SYNTHESIS*

To obtain complementary deoxyribonucleic acid (cDNA), reverse transcription was performed as recommended by the manufacturer (Omniscript RT Kit, Qiagen, Hilden, Germany) using the corresponding buffer, 0.5 mM of each dATP, dGTP, dTTP and dCTP, 1 μ M of Oligo-dT primer, 4 units of the Omniscript Reverse Transcriptase and 10 units of RNase Inhibitor (Qiagen, Hilden, Germany). The incubation was carried out for 60 min at 37 °C.

3.5.3 *POLYMERASE CHAIN REACTION (PCR)*

a) *Reverse Transcriptase PCR (RT-PCR)*

cDNA was used as the template for RT-PCR. All enzymes, nucleotides, buffers and other chemicals for RT-PCR were obtained from Qiagen (*Taq* PCR Core Kit, Hilden, Germany). For each PCR approach, 2.5 units of *Taq* DNA Polymerase, 800 μ M of each dNTP, 20 pmol of each primer and a total concentration of 2.5 mM MgCl₂ were used. For the reaction of osteocalcin (OC), 4% (v/v) glycerol (Merck, Darmstadt, Germany) was added. The PCR program was carried out as follows in an Eppendorf Mastercycler (Hamburg, Germany):

initial denaturation	5 min	95 °C	1 cycle
denaturation	30 sec	95 °C	35 cycles
primer annealing	30 sec	see Table 3	35 cycles
elongation	45 sec	72 °C	35 cycles
additional elongation	7 min	72 °C	1 cycle

A 1% (w/v) agarose gel was used to visualise the PCR products. For the staining, 0.01% (v/v) GelRed was added. To prove that cDNA synthesis was successful, glyceraldehyde-3-phosphate dehydrogenase (GAPDH) was used as evidence.

b) *Real-time PCR (qPCR)*

To quantify the gene expression rate, qPCR was performed. Therefore, the SsoFast EvaGreen Supermix (Bio-Rad Laboratories GmbH, München, Germany), 10 pmol of each primer and cDNA were mixed. The qPCR program was carried out as follows with a CFX96 Thermal Cycler (Bio-Rad Laboratories GmbH, München, Germany):

initial denaturation	30 sec	95 °C	1 cycle
denaturation	5 sec	95 °C	60 cycles
primer annealing	15 sec	60 °C	60 cycles
elongation	30 sec	72 °C	60 cycles
melt curve	65 °C - 95 °C and 0.5 °C per step		

The CFX Manager Software 1.1 (Bio-Rad Laboratories GmbH, München, Germany) was used to analyse the results. GAPDH and β -actin were applied as internal controls (housekeeping genes) because both genes are expressed constitutively and were found to be the most reliable housekeeping genes [74]. The homogeneity of the housekeeping genes was surveyed via an examination of the target stability values. Gene expression was normalised to both housekeeping genes and also normalised to the control ($\Delta\Delta Cq$).

3.6 PROTEOMICS

3.6.1 CELL PREPARATION

After incubation under various conditions, the cells were washed with PBS and detached from the surface with 0.05% Trypsin/EDTA, followed by incubation for 5 min in the incubator. Afterwards, the cell culture medium was added to stop the reaction, and the cells were centrifuged at 250 x g. Afterwards, the medium was discarded and the cells were resuspended in an EDTA-free protease inhibitor buffer (cOmplete ULTRA Tablets, EDTA-free, Roche, Mannheim, Germany) and centrifuged again at 250 x g. The supernatant was removed, and the cell sediment was quick-frozen in liquid nitrogen. The cells were stored at -20 °C. Further processing was performed by the group of Prof. Dr. Hartmut Schlüter at Universitätsklinikum Hamburg-Eppendorf Hamburg (UKE) until spots could be cut out of the 2-dimensional electrophoresis (2-DE) gels. Finally, 1/10 of the sample was used for mass spectrometry-based proteomic analysis (liquid chromatography–mass spectrometry (LC/MS)).

3.6.2 2-D GEL ELECTROPHORESIS

The samples were used for 2-DE gel electrophoresis according to Proteome Factory's 2-D electrophoresis technique (Proteome Factory AG, Berlin, Germany), which is based on the protocol described by Klose and Kobalz [75] and adapted by Zimny-Arndt [76].

The cells were resuspended in a buffer containing 6 M urea, 3 M thiourea, 2% ampholytes, and 70 mM DTT (dithiothreitol). For isoelectric focusing (IEF) in the first dimension at 8,800 Vh, 100 μ g of total protein were disposed to vertical rod gels (pH 3 – 11). Then, these gels were added to 15% SDS-PAGE gels for the separation of the proteins in the 2nd dimension. The fixation of the SDS-PAGE gels was performed in 50% (v/v) ethanol and 10% (v/v) acetic acid in MS-H₂O (Merck Millipore, Darmstadt, Germany) for approximately 16 h. Afterwards, the gels were stained with mass spectrometry-compatible silver nitrate (FireSilver staining kit PS-2001, Proteome Factory AG, Berlin, Germany). Furthermore, the 2-DE gels were digitalised with a PowerLook 2100XL containing a transparency adapter at a resolution of 150 dpi. Further analysis was performed using the Delta2D software (DECODON GmbH, Greifswald, Germany).

3.6.3 TRYPTIC IN-GEL DIGESTION OF PROTEINS

After 2-DE gel electrophoresis, selected protein spots were cut out for tryptic in-gel digestion. The gel pieces were shifted to vials and dehydrated via the addition of 500 μ L of pure acetonitrile (Merck Millipore, Darmstadt, Germany). The vials were incubated for 10 min with shaking. The supernatant was then removed. The reduction of cysteine residues was achieved by adding 10 mM DTT (Sigma-Aldrich Chemie, Taufkirchen, Germany) dissolved in 100 mM swelling solution (ammonium bicarbonate (NH_4HCO_3), Sigma-Aldrich Chemie, Taufkirchen, Germany) in MS- H_2O to the samples, followed by an incubation for 30 min at 56 $^\circ\text{C}$. Afterwards, the supernatant was removed and dehydrated with 500 μ L of acetonitrile, followed by a 10 min incubation with shaking. The acetonitrile was removed, and the IAA solution (IAA solution: 55 mM iodacetamide, Sigma-Aldrich Chemie, Taufkirchen, Germany; dissolved in 100 mM NH_4HCO_3) was added to the gel pieces for alkylation. The samples were incubated in the dark at room temperature for 20 min. The supernatant was then removed. Then, 500 μ L of acetonitrile were added for 10 min, and the vials were shaken in parallel. The supernatant was removed, 250 μ L of wash solution (50 mM NH_4HCO_3 and 50% (v/v) acetonitrile) were added and the vials were incubated for 45 min with shaking. Afterwards, the supernatant was removed, and 500 μ L of acetonitrile were added to the gel pieces. The vials were incubated for 10 min with shaking. Then, the supernatant was removed, and 30 μ L of modified trypsin (Sigma-Aldrich Chemie, Taufkirchen, Germany) were added (final concentration: 13 ng/ μ L in digest buffer (50 mM NH_4HCO_3 in 10% acetonitrile/ H_2O (v/v))). The samples were incubated on ice for 90 min. Afterwards, the supernatant was removed, and digest buffer was added. The vials were incubated overnight at 37 $^\circ\text{C}$, the supernatant was transferred to new collection vials, and a peptide extraction solution (65% acetonitrile (v/v) + 5% formic acid (v/v) (Sigma-Aldrich Chemie, Taufkirchen, Germany) in MS- H_2O) was added to the gel pieces (peptide extraction solution:gel-volume = 2:1). Incubation was performed for 30 min at 37 $^\circ\text{C}$ with shaking. The supernatant was transferred to the collection tubes. Pure acetonitrile was added to the samples, and the vials were incubated for 15 min at 37 $^\circ\text{C}$ with shaking. The supernatant was added to the collection tubes. MS- H_2O was added to the gel pieces, and the samples were incubated for 15 min at 37 $^\circ\text{C}$ with shaking. The supernatant was added to the collection tubes. Peptide extraction solution was added to the samples, and the vials were incubated for 30 min at 37 $^\circ\text{C}$ with shaking. The supernatant was transferred to the collection tubes. The extracted digests were then spun in a centrifugal evaporator (Concentrator 5301, Eppendorf, Hamburg, Germany) until complete dryness (at 37 $^\circ\text{C}$ and 1,400 rpm for at least 1 h). For mass spectrometry, the

samples were re-dissolved in 0.2% formic acid (v/v). Further processing was performed by the group of Prof. Dr. Hartmut Schlüter at UKE Hamburg until data files were obtained for subsequent analysis.

3.6.4 LIQUID CHROMATOGRAPHY–MASS SPECTROMETRY (LC/MS)

LC/MS was conducted to detect proteins from the various conditions applied in this study. For this method, high-performance liquid chromatography (HPLC) is coupled with mass spectrometry (MS). During HPLC, the mixture is separated, and MS is applied for the analysis of peptides. This method was performed according to the protocol described by Meganathan et al. [77]. An Agilent 1100 LC/MSD-trap XCT series system was used. The Chip Cube system with a ProtID-Chip-43 (Agilent Technologies, Waldbronn, Germany) was used as the electrospray ionisation system. The flow rate was set to 4 μ L/min to load the sample onto the enrichment column. Two mobile phases at a ratio of 98:2 (mobile phase 1: 0.2% formic acid (v/v) in MS-H₂O; mobile phase 2: 100% acetonitrile) were applied. The flow rate of the LC gradient was set at 400 nL/min. Due to the use of a linear gradient of 2 - 40% in 20 min, the tryptic peptides were eluted from the reversed-phase column into the mass spectrometer. The following adjustments were applied: scan range 300-2,000 m/z, polarity positive, capillary voltage -1,800 V, and flow and temperature of the drying gas 4 L/min at 325°C. The MS/MS experiments were performed in auto MS/MS mode with a 4 Da window for precursor ion selection. Precursor ions were actively barred from fragmentation for a minimum of 1 min after 3 MS/MS spectra. The files for further database analysis were obtained by using DataAnalysis for 6300 series ion trap LC/MS, version 4.0. To select the precursor ions, a threshold of 5 S/N was set, and the absolute number of compounds was limited to 1,000 per MS/MS trial.

For peptide identification, the Mascot software (Version 2.3) was applied to identify uninterpreted MS/MS data for one or more peptides. Therefore, the following parameters were chosen: setting a taxonomy (*i.e.*, human), used enzyme (Trypsin), maximum missed cleavages (1), peptide tolerance (\pm 35 ppm), peptide charge (2+, 3+, 4+), MS/MS tolerance (0.2 Da), variable modifications (Carbamidomethyl (C), Oxidation (M)) and significance threshold ($p < 0.05$). Proteins were further identified using the UniProtKB database [78].

3.7 SAMPLE AND EXTRACT PREPARATION

Pure magnesium samples were manufactured via permanent mould indirect chill casting under a protected atmosphere in the Magnesium Innovation Center ((MagIC) Helmholtz-Zentrum Geesthacht, Germany). High-purity Mg (99.94%) was received from Magnesium Elektron (Manchester, UK). Magnesium was melted under a protective atmosphere (Ar + 2% SF₆,

Linde, Hamburg, Germany) at 750 °C and stirred at 220 rpm. Molten magnesium was spilled in a preheated form (550 °C). To ensure the purity of the ingots, a filter (Foseco SIVEX FC, Foseco, London, UK) was applied. The ingots had dimensions of 12 x 20 cm and a cylindrical appearance. Then, the ingots were extruded to rods (12 mm diameter, Strangpresszentrum Berlin, Germany; extrusion parameters: rate 1:84, speed 0.7 mm/s, extrusion and billet temperature 300 °C). These rods were further processed to discs (10 x 1.5 mm (at the workshop at Helmholtz-Zentrum Geesthacht, Germany)) and used for cell incubation directly on the materials. Because of the higher corrosion rate and the resulting higher Mg concentrations, which are interesting for the analysis, as-cast samples were used for extract preparation. The specimens had a weight of approximately 0.2 g. No further surface treatment was performed.

Titanium (Ti) discs, which were used as a control, were cut from a rod (10 x 1 mm, F. W. Hempel, Oberhausen, Germany). The surface was polished using 30 µm (P500 SiC), 18 µm (P1000 SiC), and 10 µm (P2500 SiC) particle size grinding papers and a 1.0 µm diamond paste. To obtain a mirror-polished surface, the final polishing step was conducted by applying a 0.05 µm SiO₂ paste. Cleaning of the specimens was performed in an ultrasonic bath. The samples were incubated for 30 min in HELLMANEX-solution (1% (v/v) in H₂O, Hellma GmbH & Co KG, Mühlheim, Germany), followed by washing with ddH₂O (Merck Millipore, Darmstadt, Germany). Then, the samples were treated ultrasonically for 30 min in 100% ethanol. Additionally, the discs were treated with a 1 mM methanol/chloroform (20:80; Merck Millipore, Darmstadt, Germany) solution to remove potential lipid contaminations. After the samples were dried, they were packed in sterile packages and autoclaved at 121 °C and 1 bar gauge pressure.

The extruded magnesium samples that were used for cell culture were gamma-sterilised (< 27 kGy irradiation dose, BBF Sterilisations service GmbH, Kernen, Germany).

For extract preparation, the as-cast magnesium samples were sterilised ultrasonically for 30 min in 100% ethanol. Afterwards, the samples were dried under sterile conditions and then incubated for 3 days under cell culture conditions (*i.e.*, 37 °C, 5% CO₂, 21% O₂, and 95% relative humidity) at a concentration of 0.2 g/mL in the corresponding cell culture medium. The supernatant was taken and centrifuged to remove large precipitates. The supernatant was then sterilised through a filter, and the flow-through was applied for further investigations. The extracts were diluted 1:10 in the corresponding medium.

3.7.1 ANALYTIC TESTS FOR THE EXAMINATION OF EXTRACT CONSTITUTION (OSMOLALITY, pH, AND MAGNESIUM CONCENTRATION)

Osmolality was examined with a freezing point osmometer (Osmomat 030-D; Gonotec, Berlin, Germany). Osmolality is analysed by comparative measurements of the freezing points of aqueous solutions. The freezing point decreases with increased osmolality. 60 µL of each sample were examined. The pH values of the media and extracts were analysed with a pH meter (Sentron Europe BV, Roden, Netherlands).

Xylidyl blue (Sigma-Aldrich, Taufkirchen, Germany) was used as a colorimetric reagent to analyse the magnesium concentrations in the produced extracts. If free magnesium ions react with Xylidyl blue, a coloured chelate complex is formed in alkaline solution. The magnesium concentration and the intensity of the staining are proportional to each other. An MgCl₂ calibration solution was diluted several times, and numerous dilutions of magnesium-based extracts were produced. Afterwards, the dilutions were mixed with the Xylidyl blue reagent according to the manufacturer's instructions (Futura System Srl, Formello, Italy). The absorbance of the obtained complex was determined at 520 nm with an Elisa Plate Reader (Tecan Group AG, Männedorf, Switzerland). The final results of magnesium concentrations were obtained via calculation using the equation from the linear part of the calibration curve.

3.9 STATISTICAL ANALYSIS

To verify the statistical significance of the experiments, the SigmaStat package (Systat software GmbH, Erkrath, Germany) was used. Applying one-way analysis of variance (ANOVA), a standard analysis comparing more than two treatments was conducted. Either a one-way ANOVA or an ANOVA on ranks was carried out, depending on the data distribution. The employed post-hoc tests were Dunn's test or the Holm-Sidak test versus the control group. For relevant experiments, the statistical values are displayed.

4. RESULTS

4.1 INFLUENCE OF MAGNESIUM CHLORIDE ON OSTEOINDUCTIVE FEATURES

The influence of magnesium on different types of bone cells (the osteosarcoma-derived cell lines U2OS, MG63, and SaoS2 and primary human osteoblasts) was analysed. Thus, salt was investigated as the simplest form in the first step. Therefore, MgCl_2 was chosen as the initial model, as the Mg^{2+} ions from the salt should behave similarly to any other dissolved Mg^{2+} ions.

Osmolality of the media

The osmolality and pH were determined to confirm that the cells were not dying of osmotic shock or pH changes caused by enhanced MgCl_2 concentrations in the environment (Fig. 5). An increase in osmolality of 0.05 osmol/kg was recorded for DMEM and DMEM GlutaMAX I. The osmolality of McCoy's 5A medium increased approximately 0.06 osmol/kg. All gradients were linear. The addition of MgCl_2 had no effect on the pH values (data not shown).

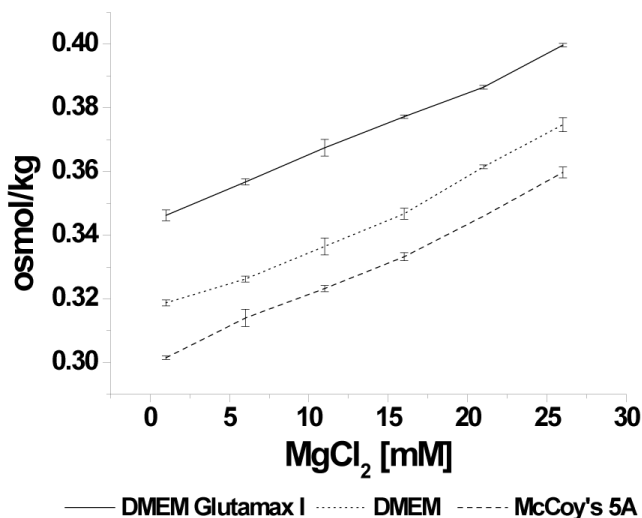


Figure 5. Influence of increased MgCl_2 concentrations on the osmolality of the media.

The effect of increased MgCl_2 concentrations on osmolality in DMEM GlutaMAX I is presented by the solid line, DMEM is presented by the dotted line and McCoy's 5A is presented by the dashed line [79].

4.1.1 PROLIFERATING CELLS

Cell proliferation and cell viability

The effects of the addition of extracellular MgCl_2 were initially investigated by analysing the cell count and viability of proliferating cells. Supplying MgCl_2 resulted in a change in the cell count (Fig. 6 A). The cell count of the SaoS2 cells was significantly reduced (14%) by the addition of 10 mM MgCl_2 . In total, the cell count of the SaoS2 cells was reduced by approximately 60% after the addition of 25 mM MgCl_2 . Interestingly, only 5 mM MgCl_2 caused a significant reduction (7%) in primary human osteoblasts. The supply of 25 mM

4. Results

MgCl₂ led to a 75% cell count reduction. On the other hand, supplying 20 mM MgCl₂ resulted in significant reductions of 50% in U2OS cells and 40% in MG63 cells. The total reduction was 75% in U2OS cells and 53% in MG63 cells after the addition of 25 mM MgCl₂.

Additionally, an analysis of the cell viability of primary human osteoblasts revealed behaviour that differed from that of the examined cell lines. The viability of the cell lines was not influenced by the presence of increased MgCl₂ in the environment (Fig. 6 B) and remained above 90%. However, the viability of the primary human osteoblasts was reduced significantly (approximately 25%) by increasing extracellular MgCl₂ concentrations.

Both the division and proliferation rates were reduced by increasing MgCl₂ concentrations in the environment (Fig. 6 C). The latter factor was reduced by approximately 10%.

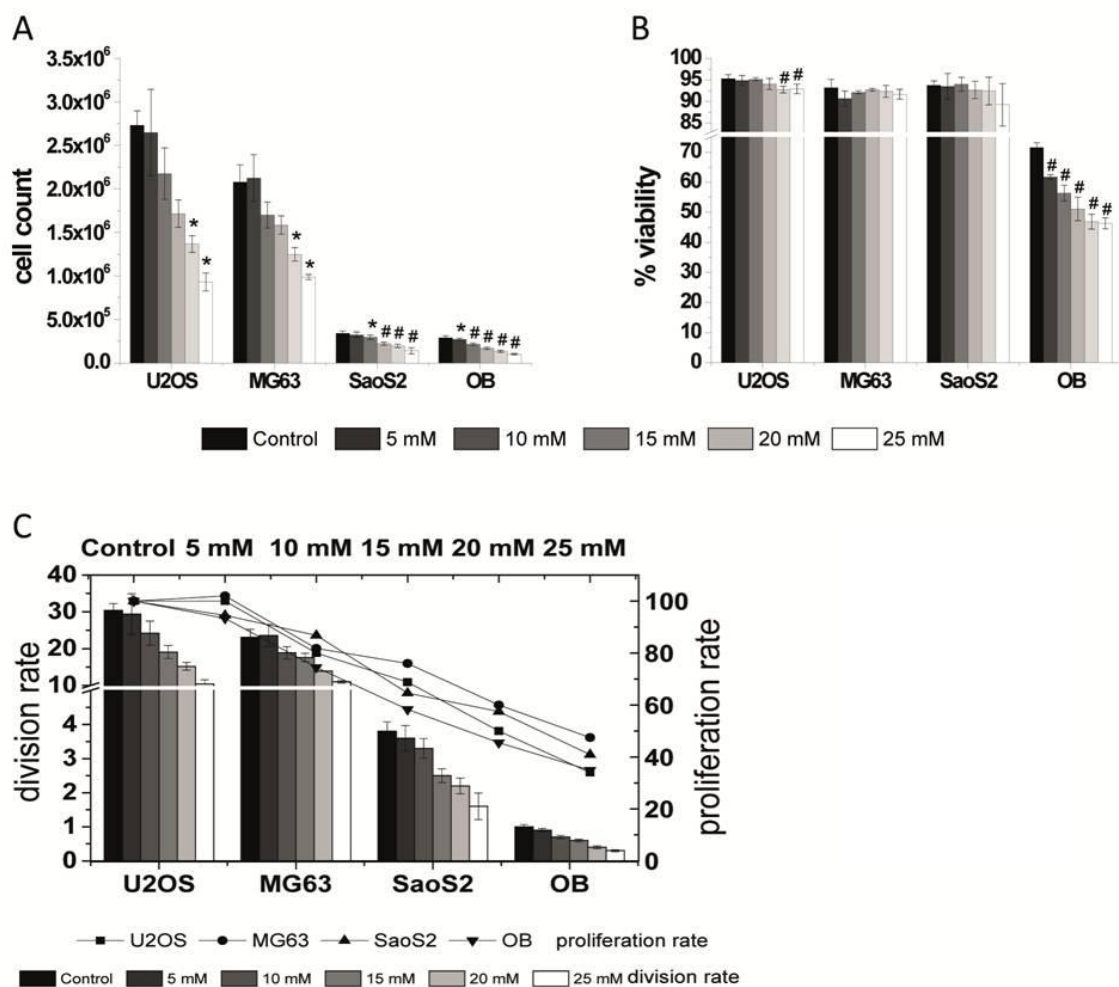


Figure 6. Cell count, viability, division and proliferation rates of osteoblastic cells after MgCl₂ addition.

Cell count (A), viability (B) and division and proliferation rates (C) of osteoblastic cells. The osteosarcoma-derived cell lines U2OS, MG63 and SaoS2 and primary human osteoblasts (OB) were incubated with increasing concentrations of MgCl₂ (0-25 mM). Significant differences between the control and the indicated conditions are shown by asterisks or hash tags ($p < 0.05 = *$, $p < 0.001 = \#$). The viability was normalised to the total number of cells measured in (A) [79].

Cell size

Throughout the preceding analysis, it could be determined that the cell size increased with enhanced MgCl_2 concentrations. As it is known that the cell spreading area has an essential impact on entry into the differentiation phase [80], the sizes of both trypsinised cells in suspension and adherent cells were investigated.

Supplementation with MgCl_2 had no effect on the sizes of trypsinised MG63 and SaoS2 cells (Fig. 7 A). The addition of 15 mM MgCl_2 led to a significant size reduction of 2.5% in trypsinised U2OS cells. In contrast, supplying 25 mM MgCl_2 resulted in a significant augmentation of cell size (approximately 18%) in primary human osteoblasts. The length and width of SaoS2 cells and primary human osteoblasts increased with increasing concentrations of MgCl_2 available in the medium (Fig. 7 B).

These observations were made for spherical-shaped cells in suspension. However, adhered cells presented another response to enhanced MgCl_2 concentrations in the environment.

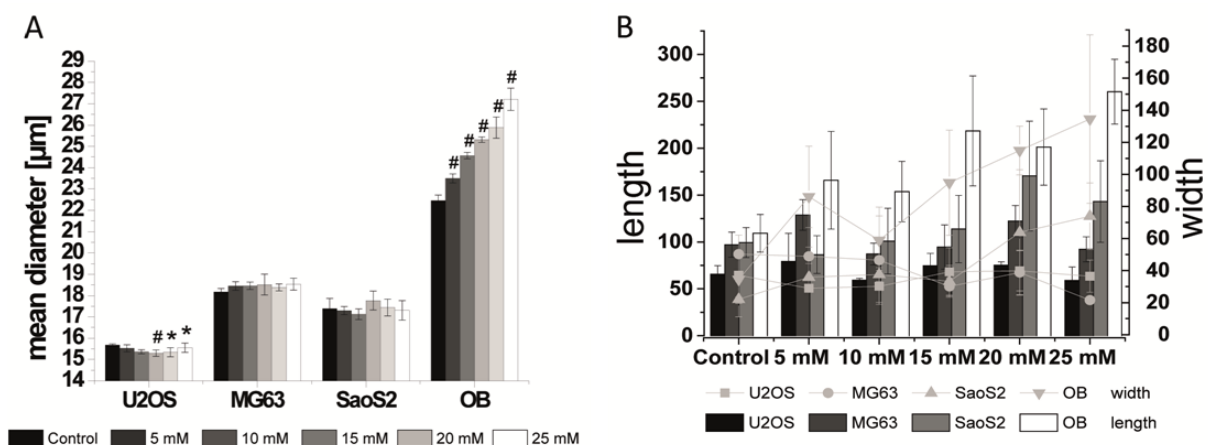


Figure 7. Size of cells from the bone system in suspension and adherent cells.

Cell size of trypsinised cells in suspension (A) and adherent cells (B) of the osteosarcoma-derived cell lines U2OS, MG63 and SaoS2 and primary human osteoblasts (OB) after incubation with increasing extracellular MgCl_2 concentrations (0-25 mM). Significant differences between the control and the indicated conditions are shown by asterisks or hash tags ($p < 0.05 = *$, $p < 0.001 = \#$) [79].

To verify whether the addition of increased concentrations of MgCl_2 had an effect on the size of adhered cells, cytoskeletal staining was conducted. Therefore, actin filaments (green) and nuclei (blue) were visualized. U2OS and MG63 cells revealed no changes in cell shape in response to MgCl_2 addition (Fig. 8 A + B, Table 9). It was difficult to identify single cells because the U2OS cells grew in "islands."

However, the SaoS2 cells increased their adherent shape by approximately 69% after the addition of 25 mM MgCl_2 (Fig. 8 E + F, Table 9). The cells exhibited a more large-scale form in comparison to the control. The influence of MgCl_2 addition was even more obvious in primary human osteoblasts. The addition of 25 mM resulted in an increase in size of

approximately 240%. The nucleus also increased relative to the cell size (Fig. 8 G + H, Table 9).

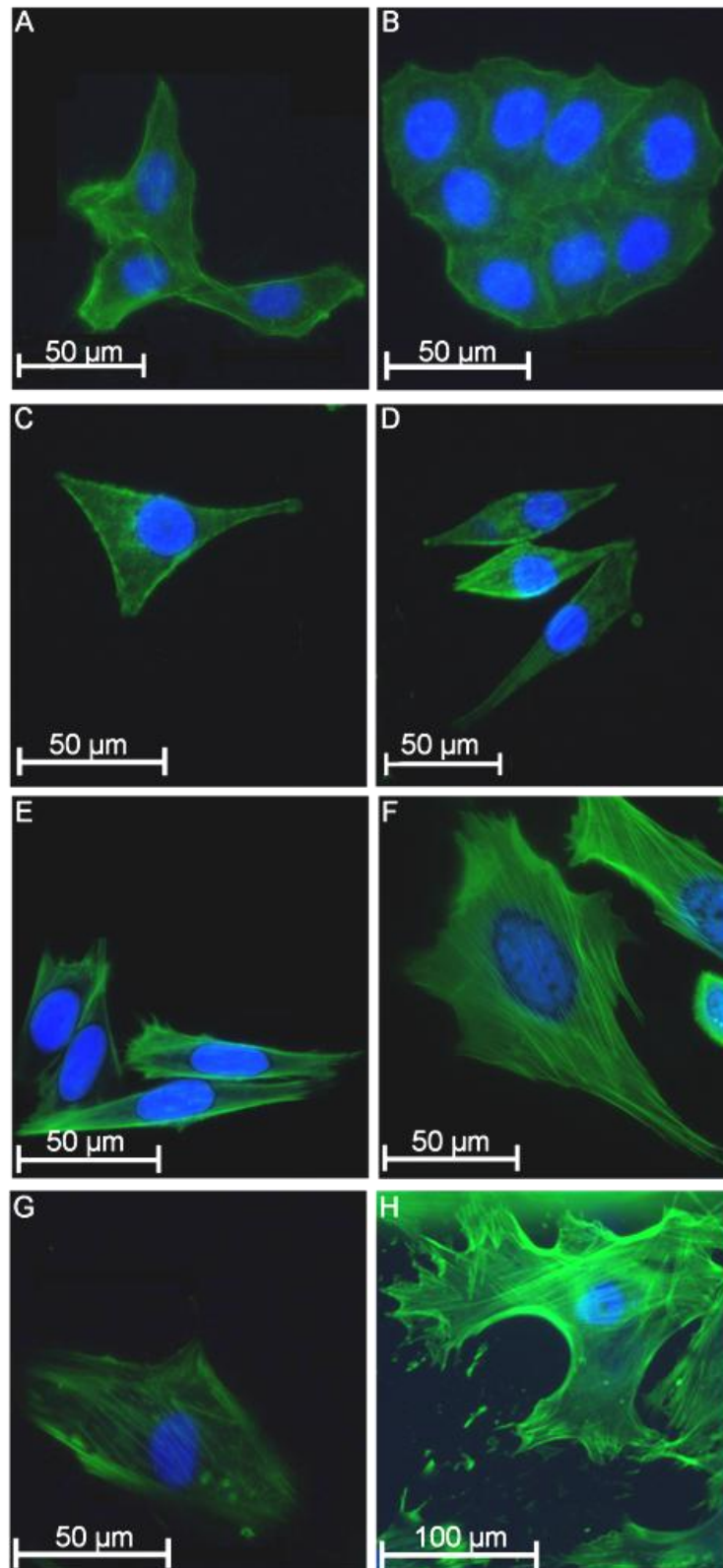


Figure 8. Cell size of adherent cells from the bone system after the addition of MgCl₂.

Fluorescent microscopy images of adherent U2OS cells grown under cell culture conditions (A) and after the addition of 25 mM MgCl₂ (B), as well as MG63 cells (C and D), SaoS2 cells (E and F) and primary human osteoblasts (G and H). Actin filaments were stained green, and nuclei were stained blue [79].

Table 9. Cell dimensions in μm of adherent cells (length (\leftrightarrow) and width (\downarrow)) under control conditions and proliferating cells supplemented with MgCl_2 . The mean values and standard deviations are presented [79].

		Control	5 mM	10 mM	15 mM	20 mM	25 mM
U2OS	\leftrightarrow	66 ± 9	79 ± 30	59 ± 2	75 ± 13	75 ± 4	59 ± 14
	\downarrow	37 ± 14	29 ± 2	30 ± 10	39 ± 15	40 ± 13	37 ± 10
MG63	\leftrightarrow	97 ± 13	129 ± 16	87 ± 12	95 ± 24	122 ± 16	92 ± 13
	\downarrow	50 ± 12	49 ± 18	47 ± 28	30 ± 5	39 ± 14	22 ± 2
SaoS2	\leftrightarrow	99 ± 16	87 ± 20	101 ± 35	114 ± 36	170 ± 59	143 ± 43
	\downarrow	22 ± 11	36 ± 9	38 ± 4	33 ± 10	64 ± 39	74 ± 21
OB	\leftrightarrow	109 ± 20	166 ± 52	154 ± 32	218 ± 59	201 ± 41	260 ± 35
	\downarrow	35 ± 15	86 ± 32	59 ± 21	95 ± 33	115 ± 15	135 ± 53

*Gene expression**RT-PCR*

A balance between bone resorption and formation is important for healthy bone. However, after a trauma, bone formation must come to the fore. Thus, osteoclast differentiation should be inhibited (Fig. 2). To examine whether the addition of enhanced MgCl_2 concentrations impacts these processes, gene expression was analysed. In a first step, a qualitative analysis was conducted using RT-PCR. Although slight negative effects were measured, an analysis of control cells and cells after the addition of 25 mM MgCl_2 was performed.

The gene expression patterns of the various cell types examined were diverse. SaoS2 cells revealed the most comparable gene expression pattern in comparison to primary human osteoblasts (Fig. 9 A). The addition of 25 mM MgCl_2 led to reduced expression of OC and osteopontin (OPN).

MG63 cells exhibited a gene expression pattern that was notably different from that of primary human osteoblasts. For MG63 cells, no OPN and bone sialoprotein (BSP) expression was detected. The expression of alkaline phosphatase (ALP) was only slight. The addition of 25 mM MgCl_2 resulted in enhanced ALP expression, but OPG expression was not reduced.

In comparison to primary human osteoblasts, U2OS cells expressed no BSP and only weakly expressed OC and OPN under control conditions. After supplementation with 25 mM MgCl_2 , the expression of BSP was slightly enhanced, whereas no OC expression was detected in U2OS cells (Fig. 9 B).

The addition of 25 mM MgCl_2 had no significant influence on the gene expression pattern in primary human osteoblasts.

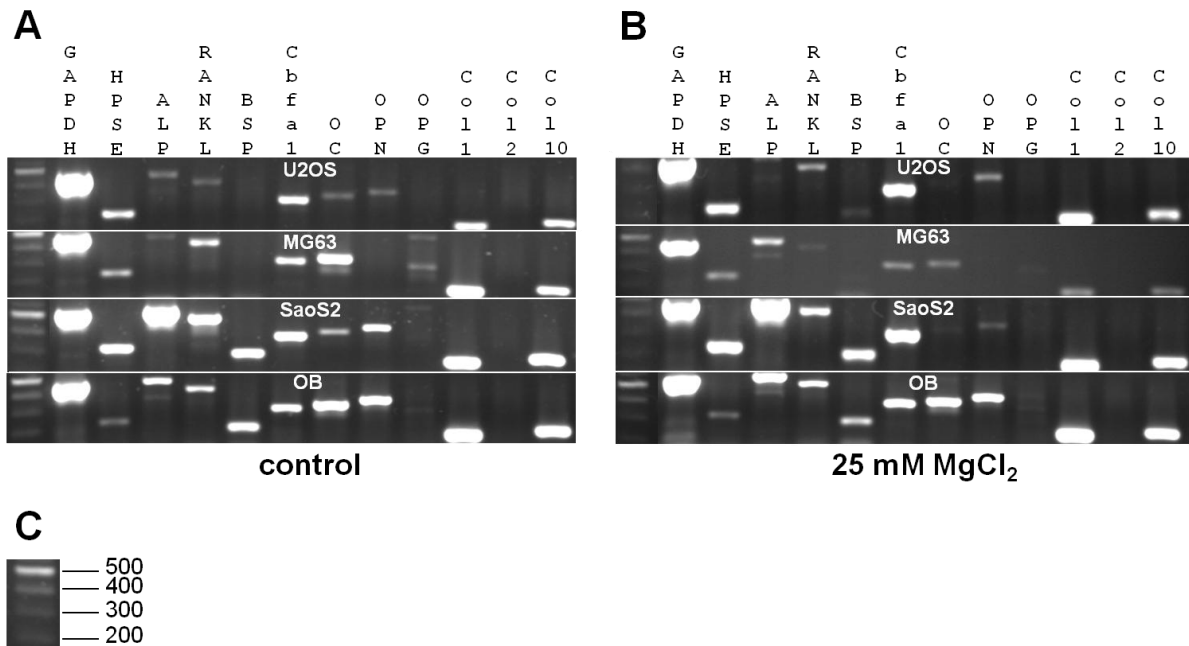


Figure 9. Comparison of the gene expression of various genes involved in bone formation.

Evaluation of the expression of various genes involved in bone and matrix formation in primary human osteoblasts (OB) and the osteosarcoma cell lines MG63, SaoS2, and U2OS under cell culture conditions (A) and after the addition of 25 mM MgCl₂ (B). The sizes of the DNA ladder are indicated in C. GAPDH: glyceraldehyde-3-phosphate dehydrogenase; HPSE: heparanase; ALP: alkaline phosphatase; RANKL: RANK ligand; BSP: bone sialoprotein; Cbfa1: runt-related transcription factor 2; OC: osteocalcin, OPN: osteopontin; OPG: osteoprotegerin; and Col: Collagen [79].

Moreover, the relative densities (% of control) of the gene expression patterns were investigated (Table 10). MG63 cells were most affected by enhanced MgCl₂ concentrations in the environment. Except for heparanase (HPSE), all other analysed markers of bone formation were reduced. HPSE was the only marker that could be compared to primary human osteoblasts.

The addition of MgCl₂ influenced only two genes in primary human osteoblasts: ALP (~150% upregulated) and BSP (~45% downregulated). After the addition of MgCl₂, five genes were upregulated in SaoS2 cells (HPSE ~140%, ALP ~127%, Cbfa1 (~139%), OPG (~130%), and Col19 (~140%). Supplementation with MgCl₂ resulted in the upregulation of HPSE (~169%), RANKL (~300%), Cbfa1(~957%), OPG (~210%), and Col1 (~169%) in U2OS cells. The other genes were downregulated. In MG63 the expression of all genes is downregulated except HPSE and Col1.

Table 10. Changes in relative density (% of control) after exposure to 25 mM MgCl₂ [79].

	U2OS	MG63	SaoS2	Osteoblasts
GAPDH	100	100	100	100
HPSE	169.71	111.45	140.14	82.56
ALP	69.87	29.63	127.97	152.46
RANKL	304.56	0.01	89.23	108.45
BSP	0.011	49.93	115.67	55.29
Cbfa1	957.25	29.17	139.36	111.50
OC	0.015	0.019	0.01	87.63
OPN	33.32	37.64	0.02	84.23
OPG	210.18	46.22	128.98	29.27
Col 1	169.71	111.45	101.19	98.92
Col 10	69.87	29.63	140.14	92.15

qPCR

By applying qPCR, gene expression for the most interesting genes was examined quantitatively in response to increasing MgCl₂ concentrations.

The opposite of the results obtained for the cell count and cell size was observed, in which a direct correlation with enhanced MgCl₂ concentrations was detected (Fig. 6 + 7). The results were more diverse when investigating gene expression (Fig. 10).

Regarding the investigated cell lines, the gene expression of U2OS cells was substantially different from that of MG63 and SaoS2 cells. In U2OS cells, the addition of MgCl₂ resulted in a 2- to 5-fold increase in gene expression for nearly all genes, except for 25 mM MgCl₂, for which gene expression dropped to the control level, except for OPG (Fig. 10 A).

The addition of MgCl₂ caused only minor variations in MG63 gene expression. BSP and OPG expression was increased 2-fold. OPN and RANKL gene expression exhibited a negative bell-shaped response to enhanced MgCl₂ concentrations (Fig. 10 B). This pattern could also be observed in SaoS2 cells (Fig. 10 C). SaoS2 cells were less affected by the MgCl₂ supply, as gene expression was increased by less than 2-fold.

For all investigated cell types, the addition of MgCl₂ had no influence on OC gene expression. However, OPG gene expression was increased in all cell types. The maximum increase was detected in U2OS cells for OPG, for which the expression increased by a factor of 4.5.

The maximum effect of MgCl₂ addition was detected in primary human osteoblasts. The gene expression levels of BSP, OPG, OPN and RANKL were increased up to 7-fold (Fig. 10 D).

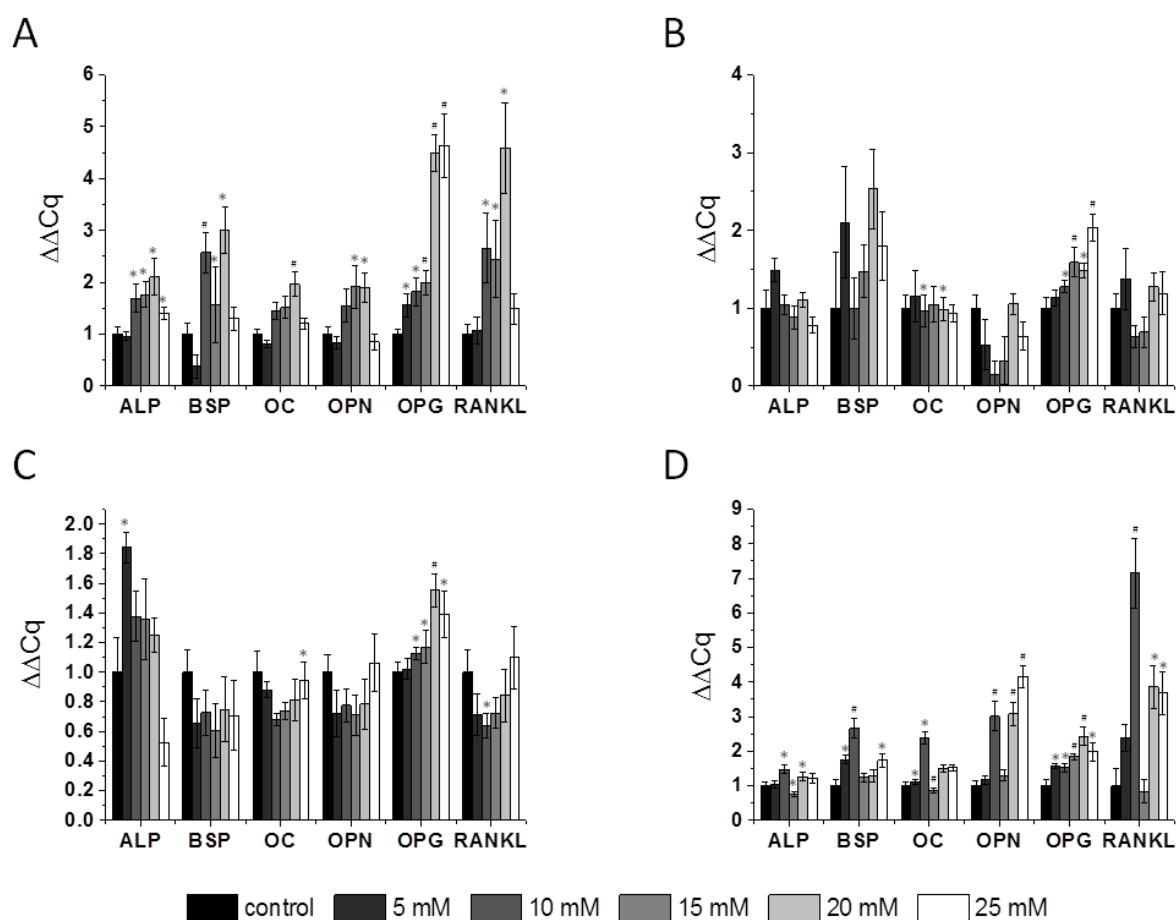


Figure 10. Gene expression of genes involved in bone metabolism after the addition of $MgCl_2$.

Investigation of the expression of genes involved in bone metabolism in the osteosarcoma-derived cell lines U2OS (A), MG63 (B), SaoS2 (C), and primary human osteoblasts (D) after the addition of a range of $MgCl_2$ concentrations (0-25 mM). Gene expression was normalised to the expression of GAPDH and β -Actin and additionally to the control condition ($\Delta\Delta Cq$). The expression level in the presence of 0 mM $MgCl_2$ was set as the control (= 1). GAPDH: glyceraldehydes-3-phosphate dehydrogenase; ALP: alkaline phosphatase; BSP: bone sialoprotein; OPN: osteopontin; OPG: osteoprotegerin; and RANKL: RANK ligand. Significant differences between the control and the indicated conditions are shown by asterisks or hash tags ($p < 0.05 = *$, $p < 0.001 = \#$) [79].

The OPG/RANKL ratios, which were calculated from the qPCR results, were very inconsistent in U2OS cells (Table 11). After the addition of 5 mM $MgCl_2$, the ratio was 1.5. The ratio decreased after the addition of 10-20 mM $MgCl_2$ but increased to 3.1 when 25 mM $MgCl_2$ was added to the medium. In MG63 cells, the OPG/RANKL ratio increased 2.3-fold following the addition of 15 mM $MgCl_2$. The ratio showed only slight alterations in SaoS2 cells and was always > 1 (1.3 - 1.8). In primary human osteoblasts, the OPG/RANKL ratio increased to 2.2 after exposure to 15 mM $MgCl_2$. However, at all other concentrations tested, the ratio was < 1 .

Table 11. OPG/RANKL gene expression ratios examined by qPCR at different MgCl₂ concentrations [79].

	U2OS	MG63	SaoS2	Osteoblasts
5 mM MgCl ₂	1.5	0.8	1.4	0.7
10 mM MgCl ₂	0.7	2.0	1.8	0.2
15 mM MgCl ₂	0.8	2.3	1.6	2.2
20 mM MgCl ₂	1.0	1.2	1.8	0.6
25 mM MgCl ₂	3.1	1.7	1.3	0.5

4.1.2 DIFFERENTIATING CELLS

In addition to proliferating cells, it is also important that differentiating cells are available to keep the bone environment and metabolism in balance and prevent the generation of a bone callus. Therefore, in the next step, the influence of magnesium salt on differentiating cells was examined.

Cell proliferation and cell viability

The influence of increased MgCl₂ concentrations (0-25 mM) was determined by measuring the cell count and viability of differentiating cells. The cell count was reduced by the addition of differentiation medium to the cells (44% for SaoS2 cells up to 83% for U2OS cells) and was further reduced by the addition of MgCl₂ (78% for primary human osteoblasts up to 89% for U2OS cells; Fig. 11 A). The viability of differentiating U2OS cells was not influenced significantly, whereas the viability of MG63 cells was increased in comparison to the control (+ 17%). SaoS2 cell viability was reduced by approximately 23% after the addition of 25 mM MgCl₂, and the viability of primary human osteoblasts was also reduced (reduction of 34% with 25 mM MgCl₂; Fig. 11 B).

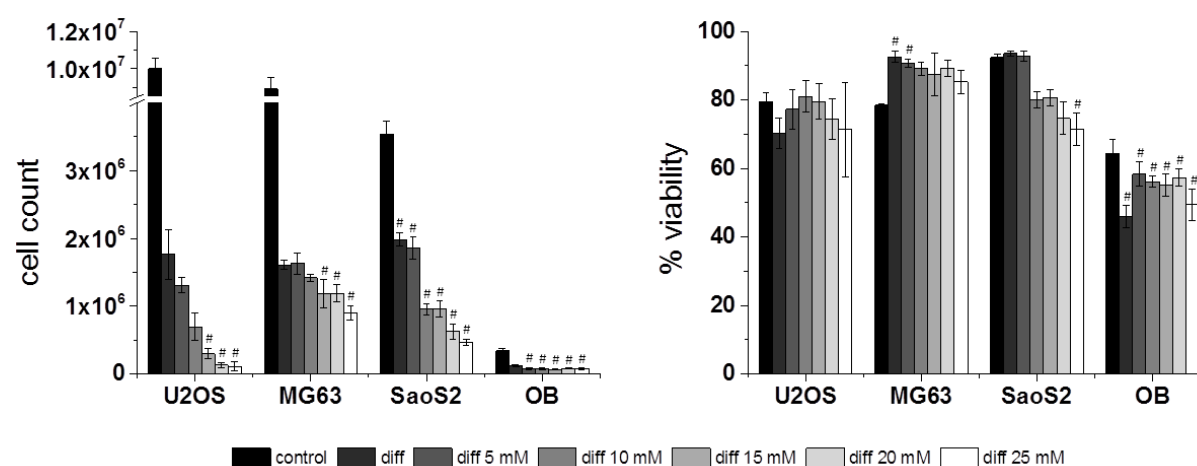


Figure 11. Cell counts and viability of differentiating cells from the bone system incubated with MgCl₂.

Cell counts (A) and viability (B) of trypsinised cells of the osteosarcoma-derived cell lines U2OS, MG63, SaoS2, and primary human osteoblasts (OB) after incubation with increasing concentrations of MgCl₂ and additional supplementation with differentiation medium (diff). The viability was normalised to the total number of cells measured in (A). Significant differences between the control and the indicated conditions are shown by hash tags (# = p < 0.05).

Cell size

The cell size was determined for trypsinised cells in suspension and adherent cells. The diameter of cells in suspension was increased for all cell types after the addition of differentiation medium and MgCl₂ (Fig. 12). U2OS cells increased their size by approximately 30% after the addition of 25 mM MgCl₂. MG63 cells increased their size by approximately 17% after supplementation with differentiation medium and remained at that value. The addition of 25 mM MgCl₂ led to increases in cell size of 23% in SaoS2 cells and 34% in primary human osteoblasts.

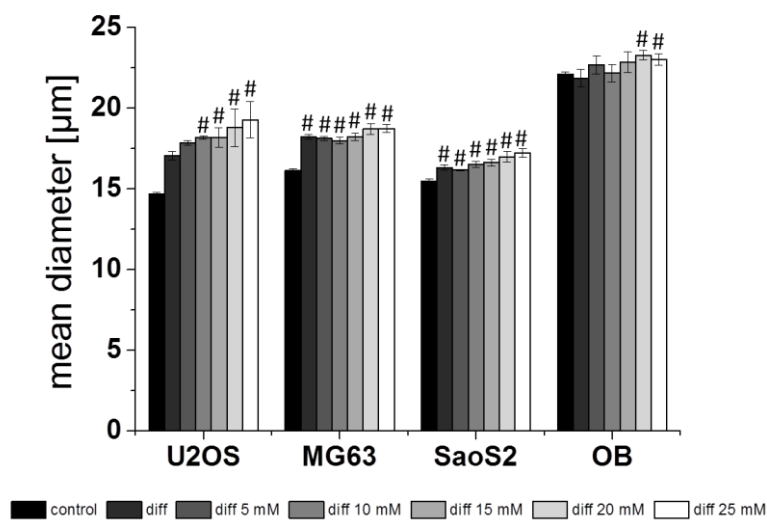


Figure 12. Cell size of differentiating cells from the bone system incubated with MgCl₂.

The sizes of trypsinised cells of the osteosarcoma-derived cell lines U2OS, MG63, SaoS2, and primary human osteoblasts (OB) after incubation with increasing concentrations of MgCl₂ and additional supplementation with differentiation medium. Significant differences between the control and the indicated conditions are shown by hash tags (# = $p < 0.05$).

The cell size of adhered U2OS and MG63 cells was not influenced by supplementation with differentiation medium (Fig. 13, Table 12). With increasing MgCl₂ (25 mM) concentrations, MG63 cells became larger in comparison to the control.

The same trend was observed for SaoS2 cells. These cells were up to three times larger after the addition of 25 mM MgCl₂ in comparison to the control.

Primary human osteoblasts were already enlarged by supplementation with differentiation medium and further increased their size with MgCl₂ addition.

In comparison to undifferentiated cells, U2OS and MG63 cells were approximately 2-fold smaller until they reached the same size after the addition of 20 mM MgCl₂ (Table 12). In contrast, SaoS2 cells and primary human osteoblasts nearly doubled in size when differentiation medium and MgCl₂ were added in comparison to undifferentiated cells (Table 12).

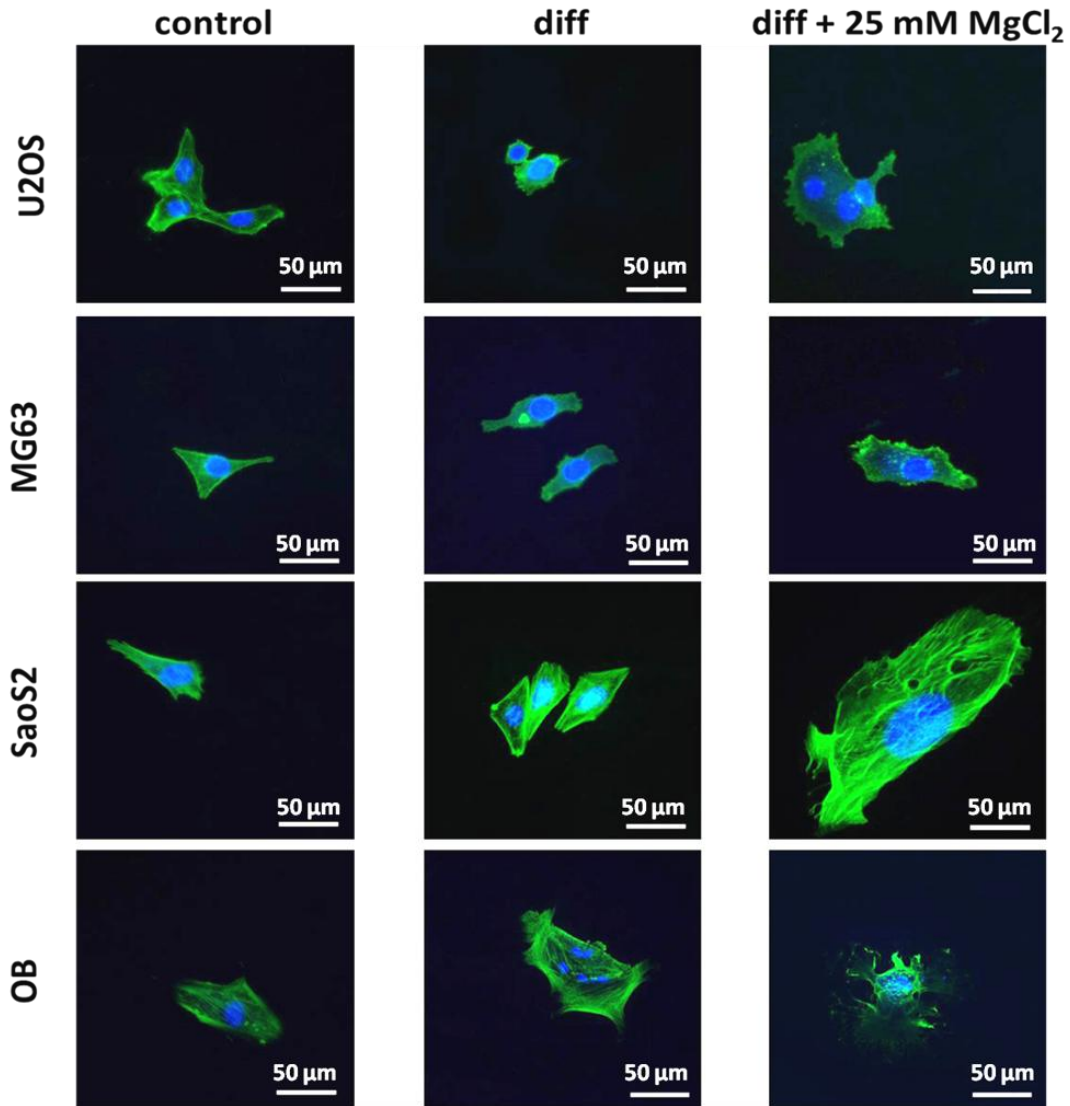


Figure 13. Cell size of adherent differentiating cells from the bone system incubated with MgCl₂.

Fluorescent microscopy images of U2OS cells under cell culture conditions, after incubation with differentiation medium, and after supplementation with differentiation medium and the addition of MgCl₂, as well as MG63, SaoS2, and primary human osteoblasts (OB). Actin filaments were stained green, and nuclei were stained blue.

Table 12. Cell dimensions in μm of adherent cells (length (↔) and width (↓)) under control conditions and differentiating cells (diff) supplemented with MgCl₂ (0 - 25 mM). The mean values and standard deviations are presented.

		Control	diff	5 mM diff	10 mM diff	15 mM diff	20 mM diff	25 mM diff
U2OS	↔	44 ± 5	30 ± 11	28 ± 12	31 ± 16	47 ± 7	64 ± 15	52 ± 14
	↓	33 ± 6	21 ± 6	17 ± 3	16 ± 4	20 ± 5	21 ± 5	20 ± 2
MG63	↔	60 ± 14	69 ± 13	75 ± 18	40 ± 11	67 ± 5	69 ± 15	98 ± 8
	↓	32 ± 4	31 ± 7	31 ± 6	23 ± 8	21 ± 7	35 ± 3	30 ± 14
SaoS2	↔	67 ± 7	72 ± 3	141 ± 47	107 ± 29	82 ± 75	159 ± 21	194 ± 56
	↓	26 ± 8	30 ± 3	83 ± 11	32 ± 10	31 ± 24	125 ± 25	111 ± 13
OB	↔	112 ± 17	144 ± 54	143 ± 51	109 ± 4	146 ± 48	141 ± 44	217 ± 42
	↓	43 ± 17	79 ± 45	89 ± 23	51 ± 12	81 ± 34	106 ± 35	156 ± 64

Gene expression

To examine whether MgCl₂ influences the initiation of primary human osteoblast maturation in differentiating cells, genes involved in bone and matrix formation were analysed by qPCR. The gene expression pattern was specific for each cell type. In U2OS cells, significant changes in gene expression were detected. The most obvious change occurred after the addition of 10 mM MgCl₂. Gene expression was upregulated for all examined genes (Fig. 14 A).

Regarding MG63 cells, the gene expression level was generally lower but increased with ascending MgCl₂ concentrations (Fig. 14 B). However, for BSP, the gene expression level remained nearly unchanged.

Decreased gene expression was detected for ALP in SaoS2 cells with increasing MgCl₂ concentrations. The expression of genes such as OPN, OPG and RANKL increased with increasing MgCl₂ concentrations. The expression of BSP was slightly different and can be described by a Gauss distribution, with upregulation at lower MgCl₂ concentrations and downregulation at higher MgCl₂ concentrations (Fig. 14 C).

In primary human osteoblasts, the addition of MgCl₂ led to increased gene expression for all analysed genes except OPN. OPN gene expression first increased and then decreased starting at 15 mM MgCl₂ (Fig. 14 D).

Except for U2OS cells, all conditions had a strong influence on OC gene expression (Fig. 14). In U2OS cells, most of the OPG/RANKL ratios were < 1 (0.03 - 0.8). Only after the addition of 15 mM MgCl₂ was the gene expression ratio 6.6. For MG63 cells, all OPG/RANKL ratios were > 1 (1.3 - 2.1). SaoS2 cells and primary human osteoblasts showed values < 1 (0.3 - 0.6) for all calculated OPG/RANKL ratios. The values for each condition and cell type are presented in Table 13.

Table 13. OPG/RANKL gene expression ratios examined by qPCR at different MgCl₂ concentrations for differentiating cells.

	U2OS	MG63	SaoS2	Osteoblasts
0 mM MgCl ₂	0.6	1.7	0.7	0.6
5 mM MgCl ₂	0.8	1.3	0.6	0.4
10 mM MgCl ₂	0.3	1.5	0.7	0.4
15 mM MgCl ₂	6.6	2.1	0.4	0.3
20 mM MgCl ₂	0.03	1.3	0.2	0.4
25 mM MgCl ₂	0.1	1.5	0.7	0.4

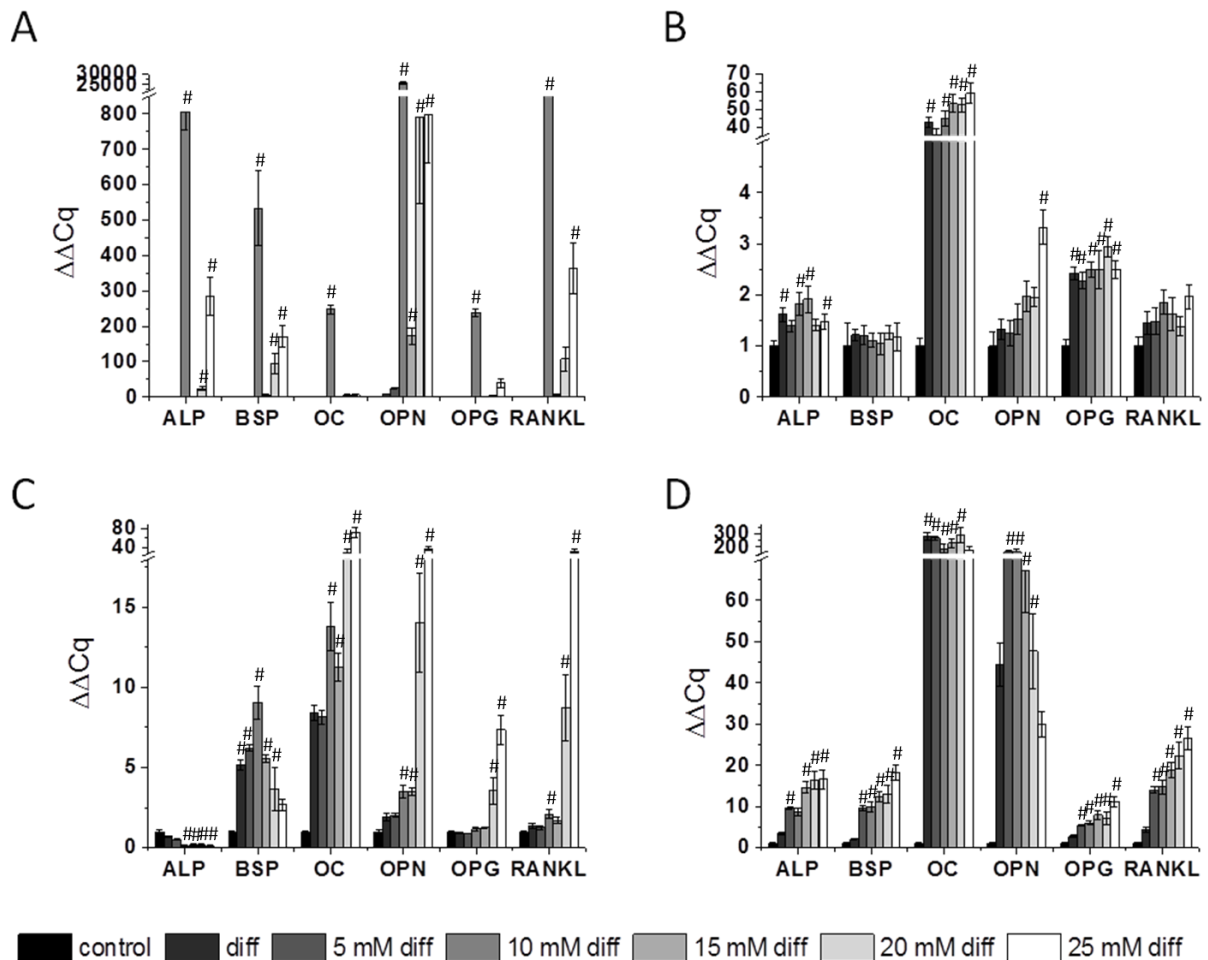


Figure 14. Gene expression of genes involved in bone metabolism in differentiating cells incubated with MgCl₂.

Investigation of the expression of genes involved in bone and matrix formation in the osteosarcoma-derived cell lines U2OS (A), MG63 (B), SaoS2 (C), and primary human osteoblasts (D) after incubation with increasing concentrations of MgCl₂ and supplementation with differentiation medium. Gene expression was normalised to the expression of GAPDH and β -Actin and additionally to the control condition ($\Delta\Delta Cq$). GAPDH: glyceraldehyde-3-phosphate dehydrogenase; ALP: alkaline phosphatase; BSP: bone sialoprotein; OC: osteocalcin; OPN: osteopontin; OPG: osteoprotegerin; and RANKL: RANK ligand. Significant differences between the control and the indicated conditions are shown by hash tags ($\# = p < 0.05$).

4.2 INFLUENCE OF MAGNESIUM-BASED EXTRACTS ON OSTEOINDUCTIVE FEATURES

Due to the heterogeneous results obtained with magnesium salt, it was necessary to find more reliable experimental environments. Thus, extracts of pure magnesium samples were investigated in the next step. The experiments were performed on the one hand to simulate corrosion and physiological conditions and on the other hand to keep the test system as simple as possible. In comparison to the previous approach with MgCl₂, additional degradation-induced factors, such as an alkaline pH and precipitation, occurred. This kind of precipitation was observed in preceding studies as well [81].

4.2.1 MEDIA AND EXTRACT CHARACTERISATION

To determine the influence of magnesium corrosion on the osmolality, pH and magnesium concentration, the composition of the media and extracts were analysed. The results are presented in Table 14.

The osmolality was enhanced by magnesium corrosion (0.09 - 0.1 osmol/kg). The same trend was observed for the pH, which increased 10-15%. Moreover, magnesium concentrations were increased by factors of 31.6 (DMEM GlutaMAX I), 32.9 (DMEM) and 35.6 (McCoy's 5A).

Table 14. Cell culture media and corresponding extract compositions (osmolality, pH and amount of Mg in the extract) for DMEM GlutaMAX I, DMEM and McCoy's 5A. The mean values and standard deviations are presented [82].

Media	DMEM GlutaMAX I	DMEM	McCoy's 5A
media osmolality [osmol/kg]	0.346 ± 0.002	0.319 ± 0.001	0.302 ± 0.001
media pH	7.325 ± 0.05	7.275 ± 0.05	7.225 ± 0.05
extract osmolality [osmol/kg]	0.433 ± 0.01	0.413 ± 0.01	0.410 ± 0.01
extract pH	8.1 ± 0.29	8.2 ± 0.04	8.3 ± 0.13
Mg [mM] in the extract	25.3 ± 10.0	26.3 ± 5.3	28.5 ± 1.1

Furthermore, the osmolality and pH of the magnesium-based extracts and titanium-based extracts (as a control) were examined in the presence or absence of cells for a period of 10 d (17 d for differentiating primary human osteoblasts).

The osmolality of the supernatants of titanium-based extracts was reduced or comparable to that of the control with respect to proliferating cells (Fig. 15 A-D). Regardless of whether or not cells were present, the osmolality was enhanced in the supernatants of magnesium-based extracts. The osmolality of magnesium-based extracts was decreased in the presence of differentiating primary human osteoblasts in comparison to the values obtained in the absence of cells (Fig. 15 E).

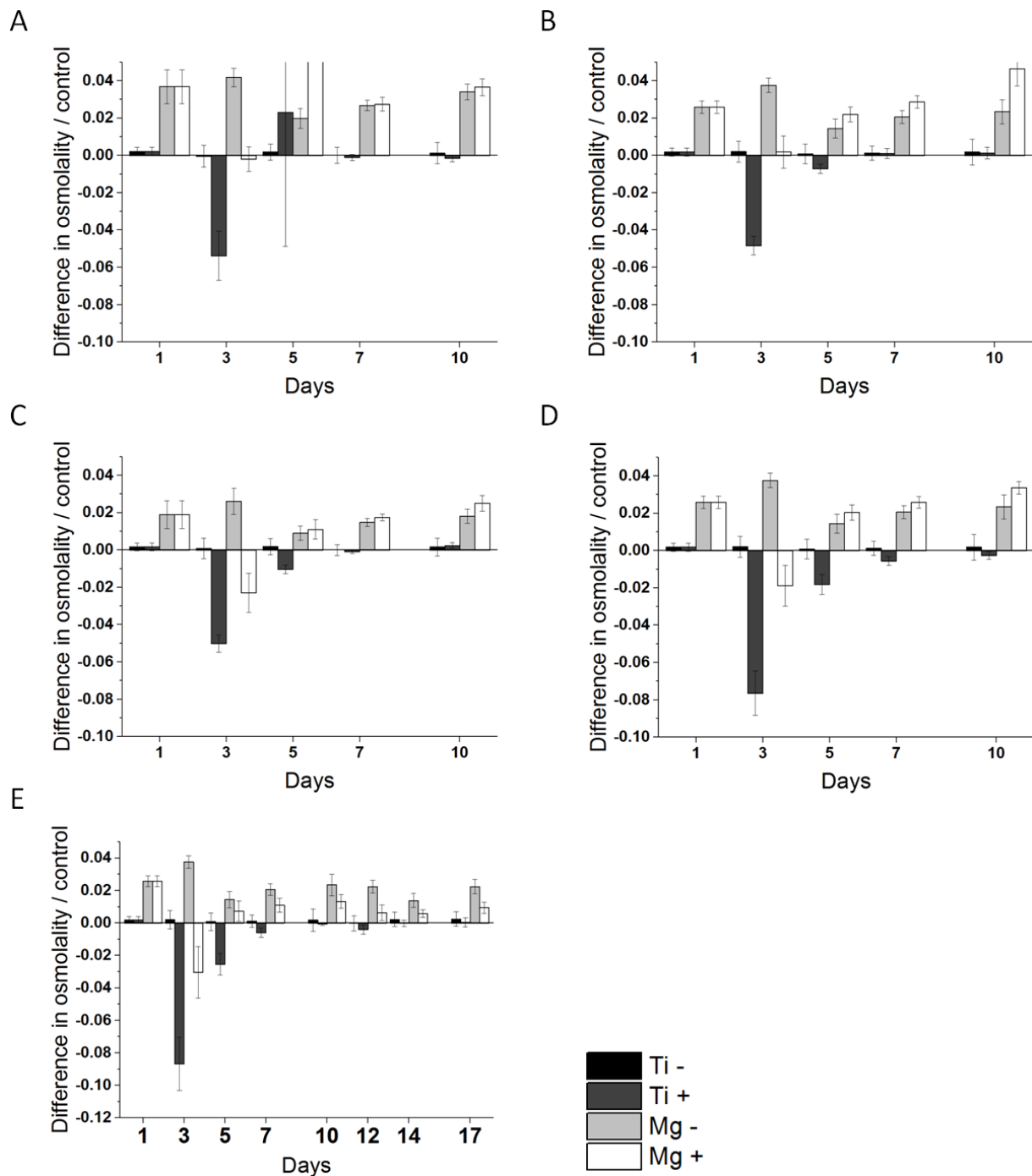


Figure 15. Differences in extract osmolalities vs. the control.

Differences in extract osmolalities vs. the control (corresponding cell culture medium) were measured in the absence (-) and presence (+) of cells for titanium (Ti) and magnesium (Mg) samples during a 10 d exposure (up to 17 d for differentiating primary human osteoblasts). U2OS (A), MG63 (B), and SaoS2 cells (C), proliferating primary human osteoblasts (D), and differentiating primary human osteoblasts (E) are presented [82].

The pH was enhanced in all titanium- and magnesium-based extracts (Fig. 16). Differentiating primary human osteoblasts decreased the pH with increasing time of exposure (Fig. 16 E; up to day 17).

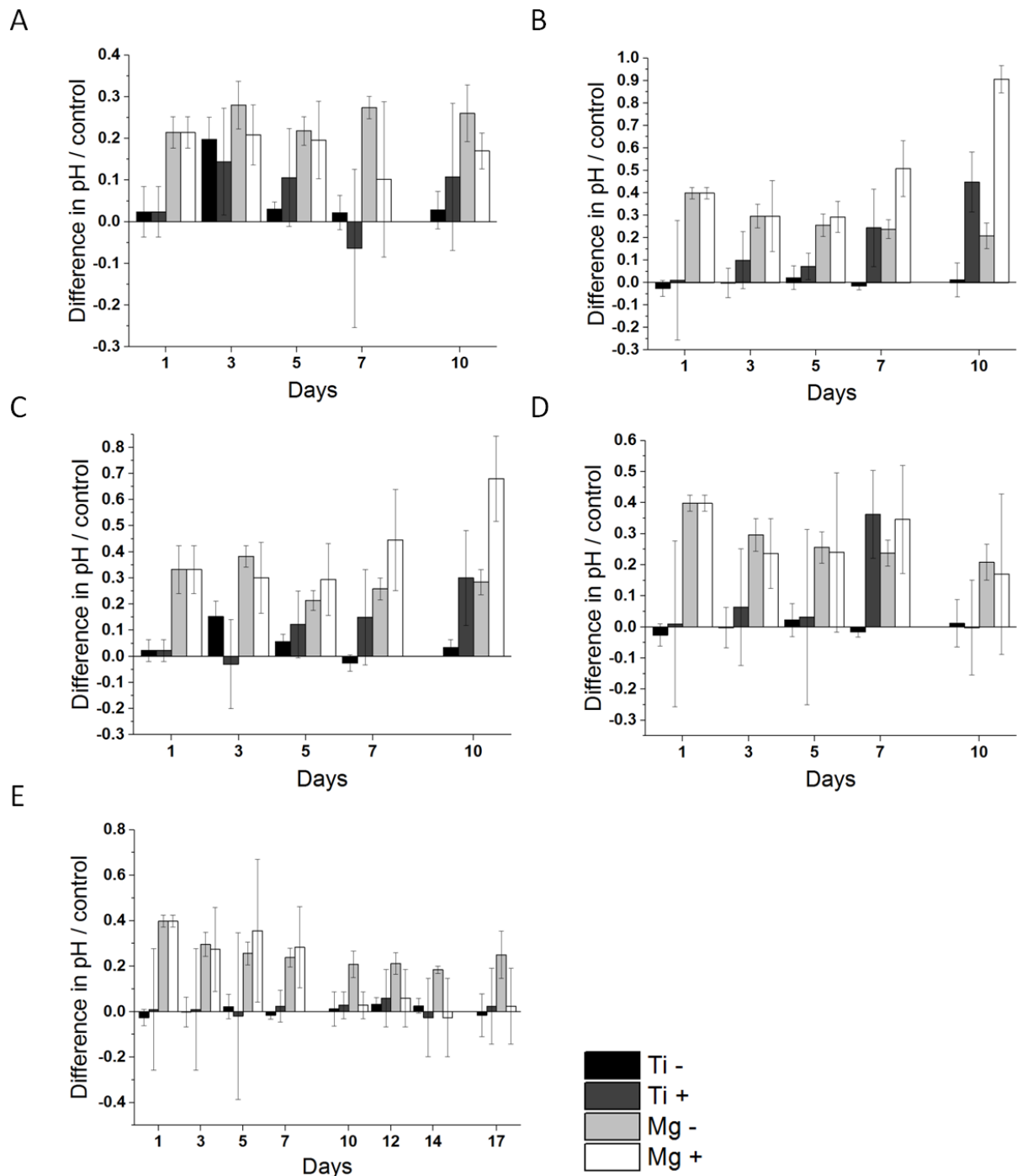


Figure 16. Differences in extract pH values vs. the control.

Differences in extract pH values vs. the control (corresponding cell culture medium) were measured in the absence (-) and presence (+) of cells for titanium (Ti) and magnesium (Mg) samples during a 10 d exposure (up to 17 d for differentiating primary human osteoblasts). U2OS (A), MG63 (B), and SaoS2 cells (C), proliferating primary human osteoblasts (D), and differentiating primary human osteoblasts (E) are presented [82].

4.2.2 PROLIFERATING CELLS

Cell proliferation and cell viability

The influence of magnesium-based extracts was examined by verifying the cell count and viability of proliferating cells. The cell counts of the U2OS and MG63 cell lines were not significantly influenced after the addition of extracts (Fig. 17 A). However, the U2OS cell

count was reduced by approximately 28%, and the MG63 cell count was reduced by approximately 13%. For SaoS2 cells, the cell count decreased significantly (25% reduction). In contrast, the cell count increased significantly by approximately 64% for primary human osteoblasts (Fig. 17 A). The viability was not affected significantly in any case (Fig. 17 B).

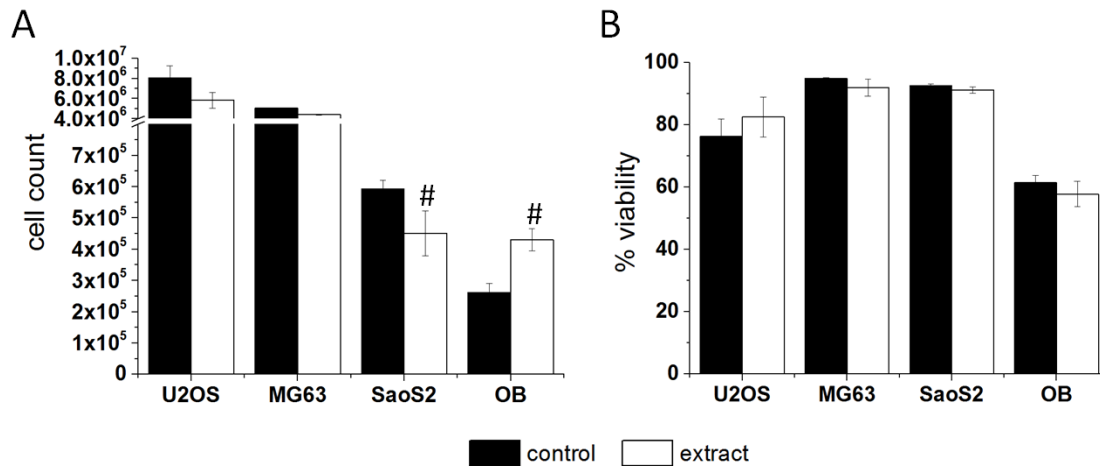


Figure 17. Cell count and viability of cells from the bone system after the addition of magnesium-based extracts.

Cell counts (A) and viability (B) of the osteosarcoma-derived cell lines U2OS, MG63, and SaoS2 as well as primary human osteoblasts (OB). Cells were incubated under cell culture conditions (control) and supplemented with magnesium-based extracts (cell lines 1 week, primary human osteoblasts 4 weeks). Significant differences between the control and the indicated condition are shown by hash tags (# = $p < 0.05$). The viability is normalised to the total number of cells measured in (A) [82].

Cell size

The size of the cells was examined for trypsinised cells in suspension and adherent cells. The diameter of proliferating cells in suspension increased significantly for U2OS cells (4%), MG63 cells (2%), and primary human osteoblasts (5%), whereas SaoS2 cells were unaffected (Fig. 18).

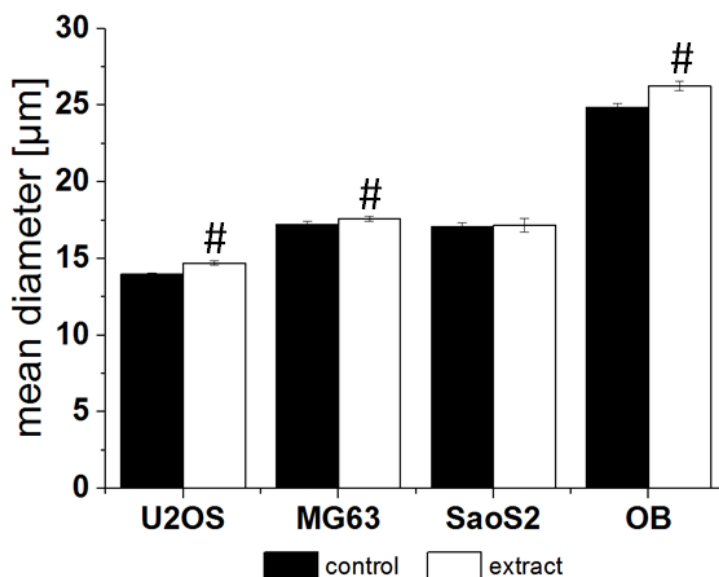


Figure 18. Size of cells from the bone system after the addition of magnesium-based extract.

Cell size of trypsinised cells of the osteosarcoma-derived cell lines U2OS, MG63, SaoS2 and primary human osteoblasts (OB) after exposure (cell lines 1 week, primary human osteoblasts 4 weeks) to cell culture conditions (control) and magnesium-based extracts. Significant differences between the control and the indicated conditions are shown by hash tags (# = $p < 0.05$) [82].

Regarding adhered cells, proliferating U2OS cells became slightly smaller after the addition of the extract (Fig. 19, Table 15). Adherent MG63 cells increased slightly in size. The cell size of SaoS2 cells increased by a factor of 2.5 after the addition of the magnesium-based extract. The same trend was observed for primary human osteoblasts. Primary human osteoblasts enhanced their size by approximately 3-fold.

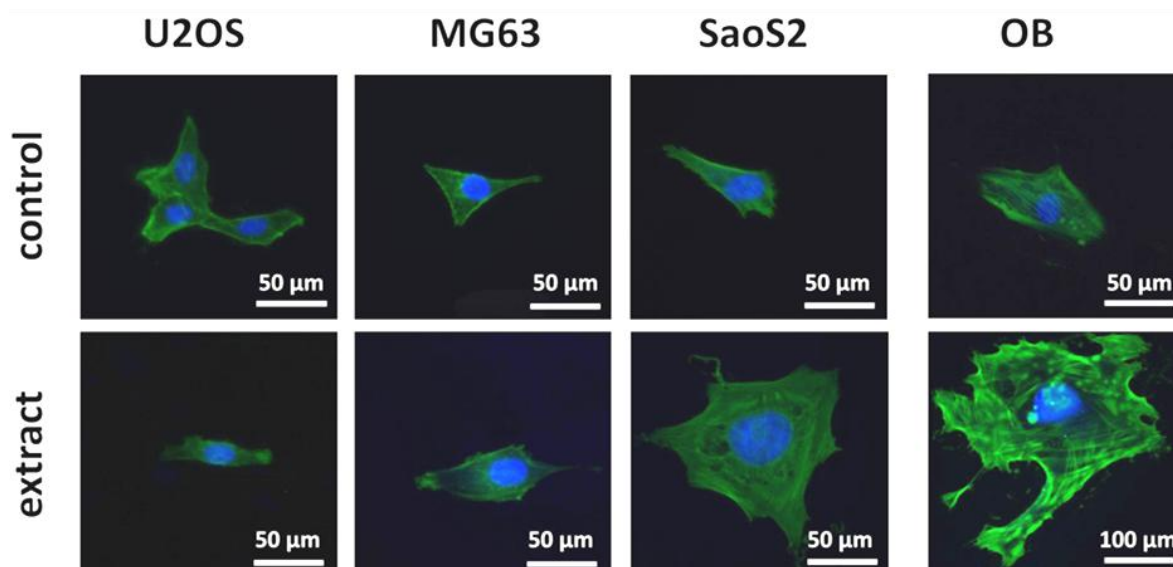


Figure 19. Size of adherent cells from the bone system after the addition of magnesium-based extract. Fluorescent microscopy images of U2OS cells under cell culture conditions and after the addition of magnesium-based extracts, as well as MG63, SaoS2 and primary human osteoblasts (OB). Actin filaments were stained green, and nuclei were stained blue [82].

Table 15. Cell dimensions in μm of adherent cells (length (↔) and width (↓)) under cell control conditions and after magnesium-based extract addition. The mean values and standard deviations are presented [82].

		Control	Extract
U2OS	↔	58 ± 14	56 ± 19
	↓	35 ± 16	22 ± 12
MG63	↔	77 ± 39	84 ± 23
	↓	39 ± 10	43 ± 9
SaoS2	↔	65 ± 17	170 ± 65
	↓	19 ± 7	165 ± 65
OB	↔	108 ± 21	331 ± 76
	↓	35 ± 17	174 ± 122

Gene expression

It was also examined whether magnesium-based extracts influence the genes involved in bone and matrix formation at different time points (1 and 2 weeks for cell lines and 1 and 4 weeks for primary human osteoblasts). In U2OS cells, a longer exposure to the extract had a stronger influence on gene expression (Fig. 20 A). ALP, OPN and OPG expression levels were significantly increased by a factor of 2 after 2 weeks.

4. Results

For MG63 cells, the results were more variable after exposure to the magnesium-based extract for 1 or 2 weeks (Fig. 20 B). No clear trend was observed.

For SaoS2 cells, an inhibitory effect was observed after 1 week of extract addition for BSP, OC, OPN and RANKL (Fig. 20 C). The expression levels decreased by nearly a factor of 5. Increases were recorded for ALP (not significant) and OPG (significant). After 2 weeks, the gene expression was comparable to that of the control (except for ALP, which was reduced significantly).

In primary human osteoblasts, supplementation with magnesium-based extracts for 1 week resulted in increased gene expression by a factor of at least 3 for almost all analysed genes (except OC and OPG) (Fig 20 D). This gene expression pattern is typical for bone formation. After 4 weeks, gene expression dropped to the level of the control or below (for ALP, OC and RANKL).

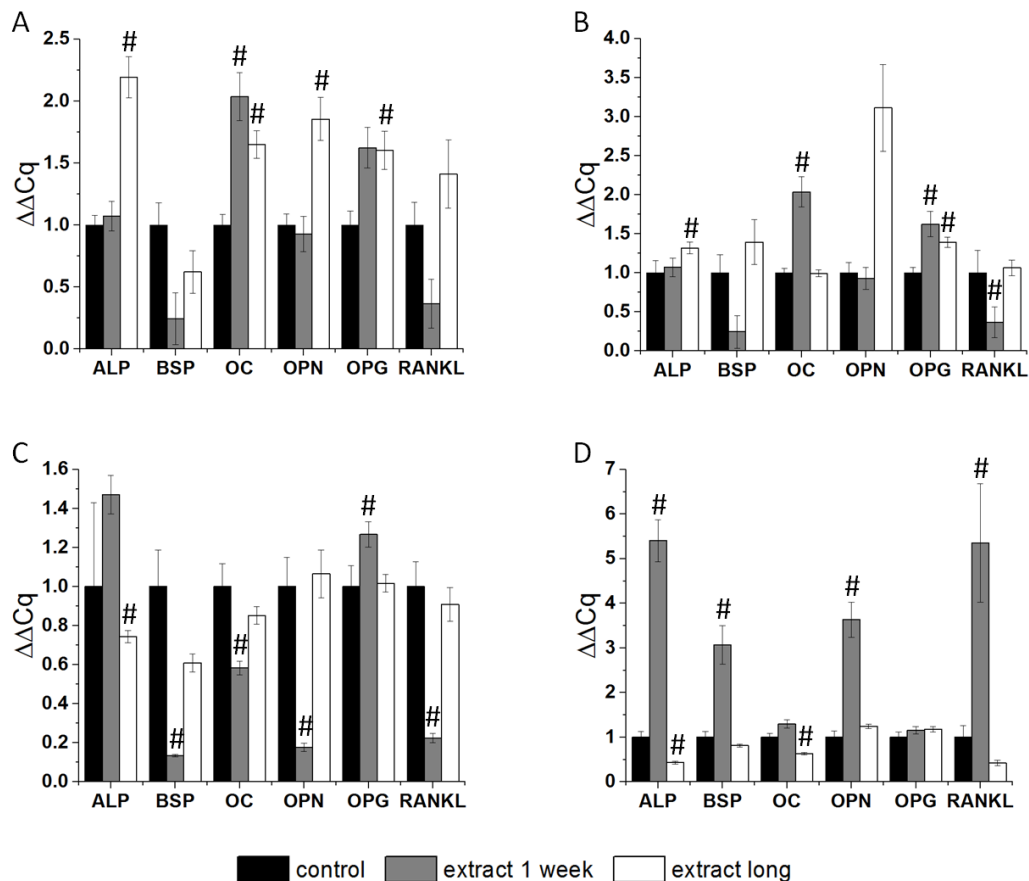


Figure 20. Gene expression of genes involved in bone metabolism after the addition of magnesium-based extract.

Gene expression of genes involved in bone metabolism in the osteosarcoma-derived cell lines U2OS (A), MG63 (B), SaoS2 (C), and primary human osteoblasts (D) after incubation with magnesium extracts for 1 week, 2 weeks (cell lines) or 4 weeks (OB). Gene expression was normalised to the expression of GAPDH and β -Actin and additionally to the control condition ($\Delta\Delta Cq$). Expression under cell culture conditions was set as the control (= 1). GAPDH: glyceraldehyde-3-phosphate dehydrogenase; ALP: alkaline phosphatase; BSP: bone sialoprotein; OC: osteocalcin; OPN: osteopontin; OPG: osteoprotegerin; and RANKL: RANK ligand. Significant differences between the control and the indicated conditions are shown by hash tags (# = $p < 0.05$) [82].

The OPG/RANKL ratios that were calculated from the qPCR results were > 1 for almost all cell types (1.47 - 5.65), except for primary human osteoblasts (0.22) after 1 week of extract exposure. The ratios of the cell lines decreased after longer extract addition but increased for primary human osteoblasts. The ratios are presented in Table 16.

Table 16. OPG/RANKL gene expression ratios determined by qPCR after exposure to magnesium-based extract for 1 and 2 weeks (OB 4 weeks) [82].

	U2OS	MG63	SaoS2	OB
extract 1 week	1.47	4.43	5.65	0.22
extract 2 weeks (OB 4 weeks)	1.13	1.31	1.12	2.75

4.2.3 DIFFERENTIATING CELLS

After the experiments with $MgCl_2$, it became obvious that differentiating cells behave differently than proliferating cells. For this reason, magnesium-based extracts were added to differentiating cells, and common parameters were analysed.

Cell proliferation and cell viability

Cell counts and viability were also measured after the addition of differentiating medium to the magnesium-based extracts. The cell numbers decreased significantly in all cases (Fig. 21 A). The reduction was approximately 45% in U2OS cells and primary human osteoblasts but 95% or higher in MG63 and Saos2 cells. Viability was influenced positively for U2OS and MG63 cells (+ 10%) but negatively for Saos2 cells (40% reduction) and primary human osteoblasts (15% reduction; Fig. 21 B).

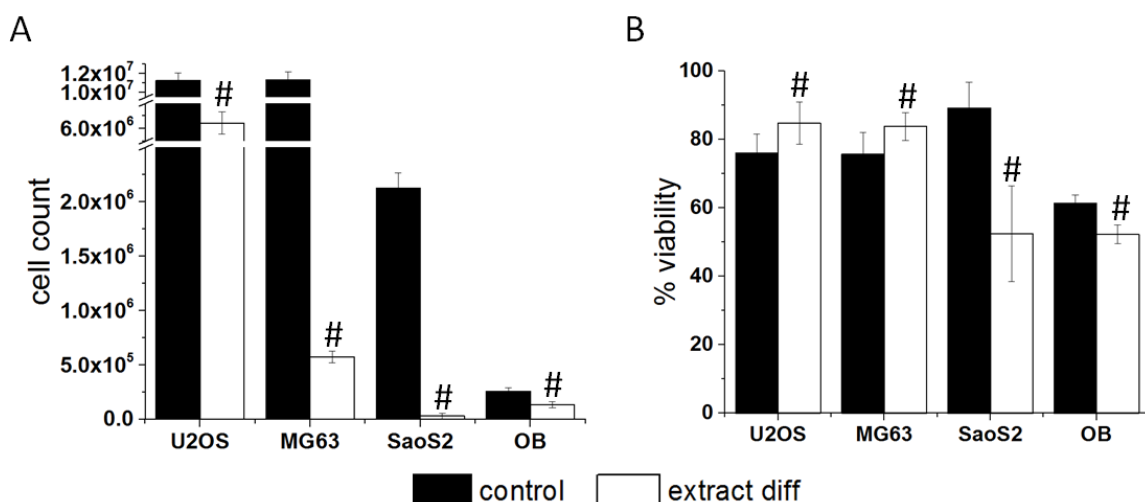


Figure 21. Cell counts and viability of differentiating cells from the bone system after the addition of magnesium-based extract.

Cell counts (A) and viability (B) of trypsinised cells of the osteosarcoma-derived cell lines U2OS, MG63, and SaoS2 as well as primary human osteoblasts (OB) after incubation (cell lines 2 weeks, primary human osteoblasts 4 weeks) under cell culture conditions (control) and with magnesium-based extracts supplemented with differentiation medium. Significant differences between the control and the indicated conditions are shown by hash tags ($\# = p < 0.05$). The viability was normalised to the total number of cells measured in (A) [82].

Cell size

Cell size was determined for trypsinised and adherent cells. The size of trypsinised cells increased significantly for all cell lines (17 - 22%). In case of primary human osteoblasts (Fig. 22) a significant decrease of 11% was recorded.

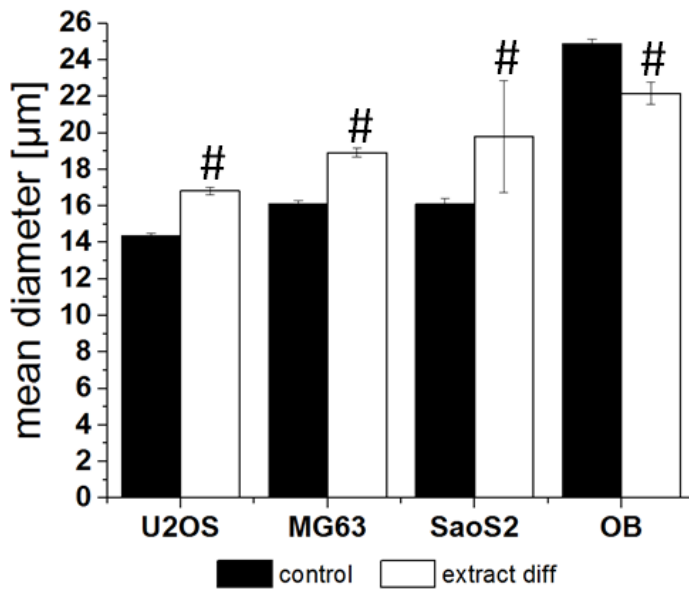


Figure 22. Cell size of differentiating cells from the bone system after the addition of magnesium-based extract.

Cell sizes of trypsinised cells of the osteosarcoma-derived cell lines U2OS, MG63, and SaoS2 as well as primary human osteoblasts (OB) under cell culture conditions (control) and after incubation (cell lines 2 weeks, primary human osteoblast 4 weeks) with magnesium-based extracts supplemented with differentiation medium. Significant differences between the control and the indicated conditions are shown by hash tags (# = $p < 0.05$) [82].

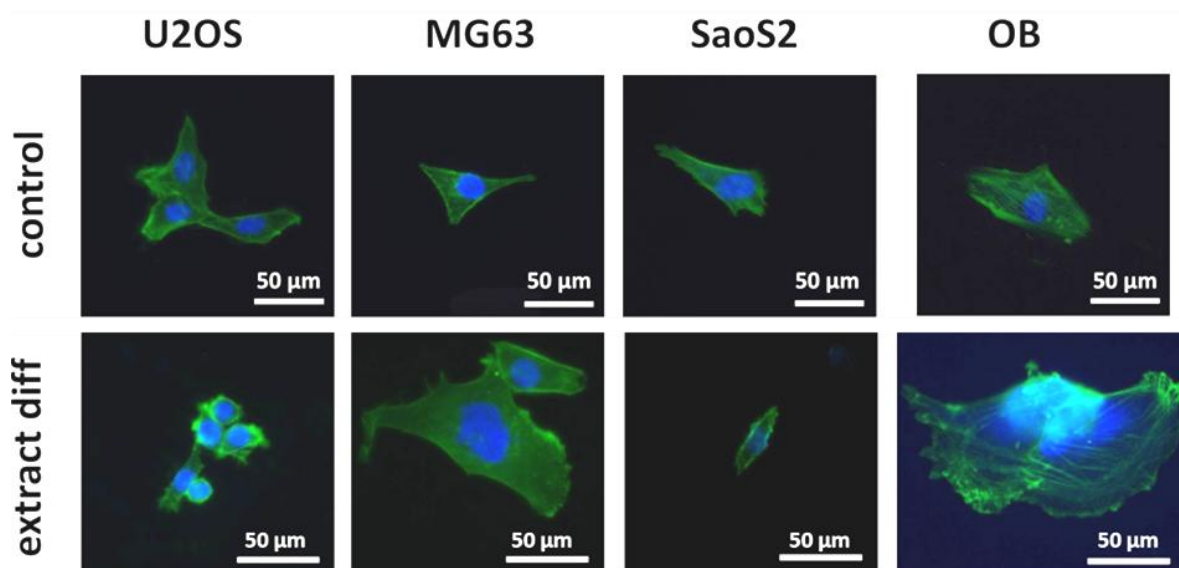


Figure 23. Size of adherent differentiating cells from the bone system after the addition of magnesium-based extract.

Fluorescence microscopy images of U2OS cells under cell culture conditions and after the addition of extract with differentiation medium, as well as MG63, SaoS2 and primary human osteoblasts (OB). Actin filaments were stained green, and nuclei were stained blue [82].

If the cells were adhered to tissue culture plastic, U2OS and SaoS2 cells decreased in size and MG63 and primary human osteoblasts increased in size after exposure to magnesium-based extracts supplemented with differentiation medium (Fig. 23, Table 17).

Table 17. Cell dimensions in μm of adherent cells (length (\leftrightarrow) and width (\updownarrow)) under cell control conditions and after extract addition supplemented with differentiating medium (extract diff). The mean values and standard deviations are presented [82].

		Control	Extract diff
U2OS	\leftrightarrow	58 ± 14	25 ± 3
	\updownarrow	35 ± 16	12 ± 1
MG63	\leftrightarrow	77 ± 39	119 ± 69
	\updownarrow	39 ± 10	45 ± 42
SaoS2	\leftrightarrow	65 ± 17	52 ± 10
	\updownarrow	19 ± 7	19 ± 5
OB	\leftrightarrow	108 ± 21	106 ± 31
	\updownarrow	35 ± 17	59 ± 26

Gene expression

The gene expression of ALP, OPN and OPG increased significantly after exposure to magnesium-based extracts and differentiating medium in U2OS cells. The expression of BSP, OC and RANKL remained unchanged in comparison to the control (Fig. 24 A).

In MG63 cells, the expression of all examined genes increased significantly by a factor of 2 (Fig. 24 B). The largest increases in gene expression were recorded for OC (factor of 30) and OPN (factor of 12).

When differentiating SaoS2 cells were exposed to magnesium-based extracts, the expression of nearly all genes increased significantly by several 100-fold. Only OPN and BSP remained unchanged in comparison to the control (Fig. 24 C).

For differentiating primary human osteoblasts, the gene expression levels of ALP and BSP were not significantly increased. For OC, OPN, OPG and RANKL, a significant increase in gene expression of up to 160-fold was recorded after exposure to the magnesium extract (Fig. 24 D).

The OPG/RANKL ratios were calculated from the qPCR results. Only for U2OS cells was a ratio > 1 determined (1.56). For all other cell types, a ratio of < 1 was observed (MG63: 0.84; SaoS2: 0.18 and OB: 0.13).

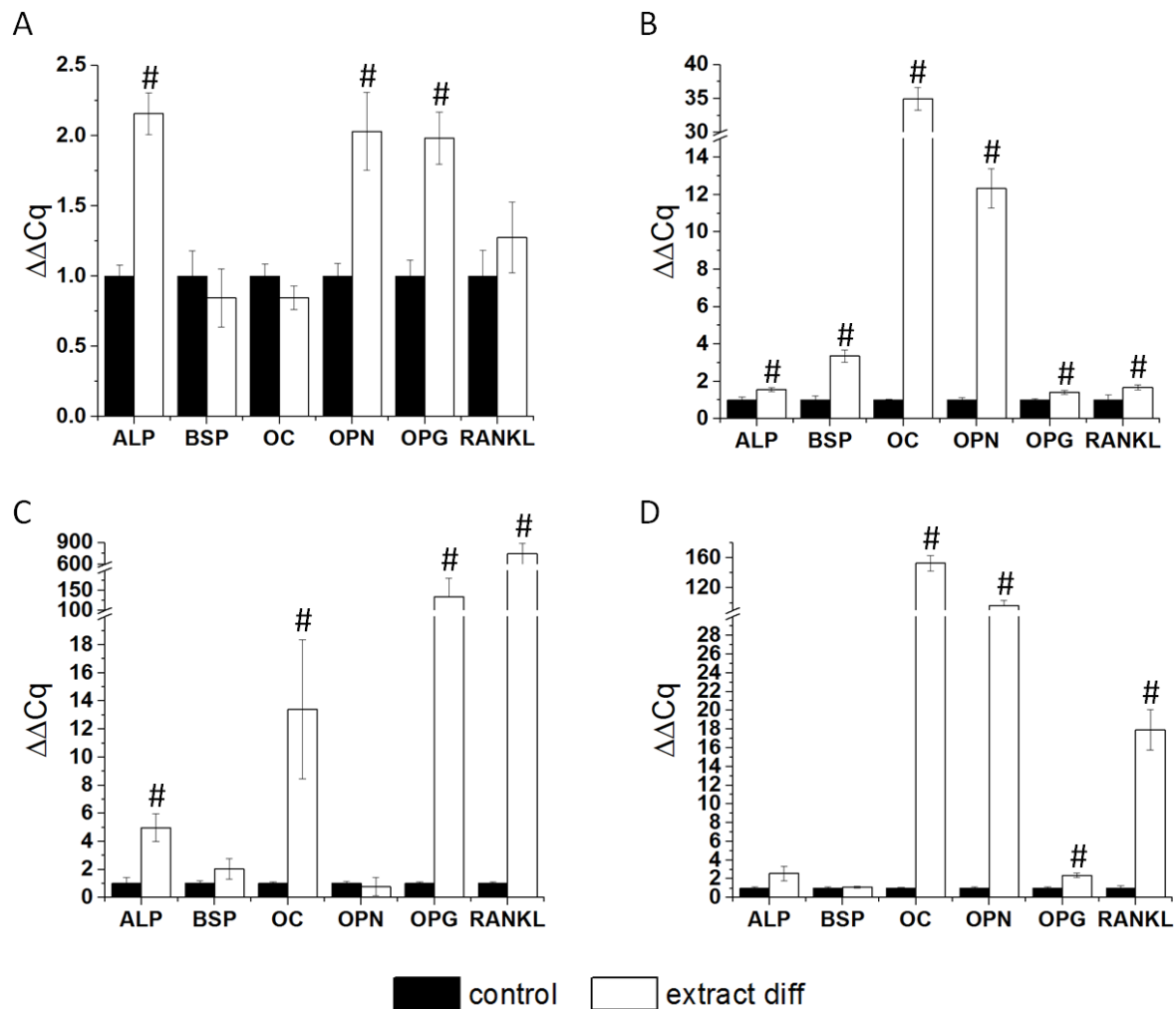


Figure 24. Gene expression of genes involved in bone metabolism in differentiating cells after the addition of magnesium-based extract.

Gene expression of genes involved in bone metabolism in the osteosarcoma-derived cell lines U2OS (A), MG63 (B), SaoS2 (C), and primary human osteoblasts (D) after incubation (cell lines 2 weeks, primary human osteoblast 4 weeks) with magnesium extracts supplemented with differentiation medium. Gene expression was normalised to the expression of GAPDH and β -Actin and additionally to the control condition ($\Delta\Delta Cq$). The expression under cell culture conditions was set as the control (= 1). GAPDH: glyceraldehyde-3-phosphate dehydrogenase; ALP: alkaline phosphatase; BSP: bone sialoprotein; OC: osteocalcin; OPN: osteopontin; OPG: osteoprotegerin; and RANKL: RANK ligand. Significant differences between the control and the indicated conditions are shown by hash tags (# = $p < 0.05$) [82].

4.3 DIRECT CONTACT WITH THE MATERIAL AND ITS INFLUENCE ON OSTEOINDUCTION

Magnesium-based extracts revealed very promising results regarding osteoinductive effects. For further investigations, direct contact with simultaneously degrading magnesium material was analysed. Therefore, the cells were grown on titanium (Ti), which is a commonly used implant material (as a further control), and on pure magnesium.

Cell proliferation and cell viability

Live/Dead image examination was conducted with cells grown on metal samples. Trypsinisation was not feasible with the cells; therefore, counting of the cells with a common

cell counter was also technically not practicable. The cell count was negatively influenced in U2OS cells, MG63 cells, and primary human osteoblasts if the cells were incubated on titanium samples (Fig. 25 A). The cell count was further reduced on magnesium samples when using SaoS2 cells.

The viability of the cell lines was not influenced by the implant materials (Fig. 25 B). Only the viability of primary human osteoblasts was reduced when the cells were incubated on titanium samples.

Only a few dead cells (red) were detected under cell culture conditions for primary human osteoblasts (Fig. 25 C; control). An increase in dead cells was observed when the cells were incubated on titanium plates (Fig 25 C; Ti). On pure extruded magnesium samples, the quantity of dead cells in comparison to living cells (green) was smaller than that observed for the titanium control (Fig 25 C; pure Mg). The same tendency was recorded for the cell lines (Appendix 6). To ensure that the cells in this layer were responsible for the observed green staining, it was verified whether there was a possible cross reaction between the material and the enzymes in the experiment. The corroded magnesium surfaces were tested without cells, but no green staining was observed (data not shown). This phenomenon was observed in other experiments within the laboratory in which the metabolism of the cells and the corrosion of the material were examined.

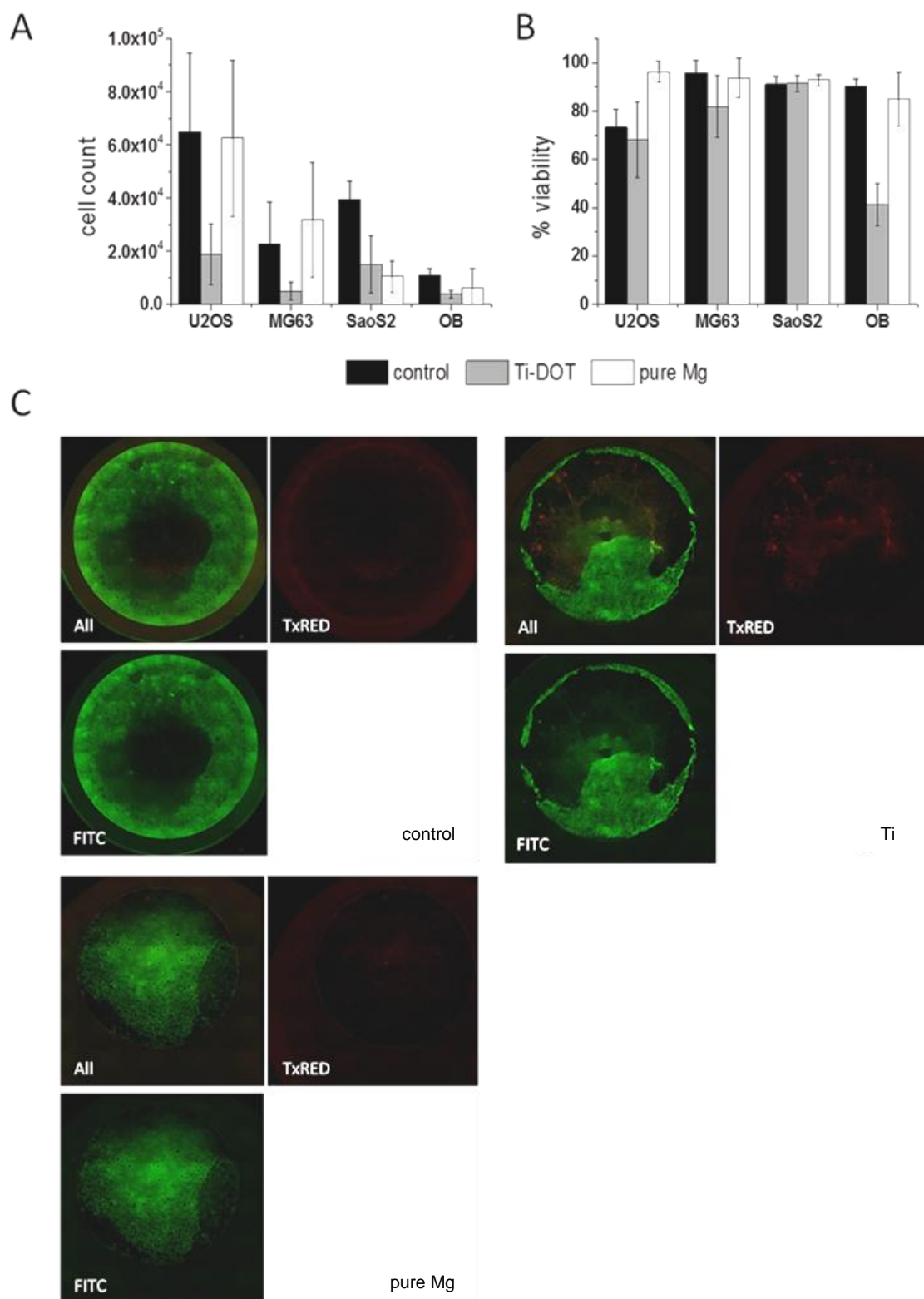


Figure 25. Cell counts and viability of cells from the bone system in direct contact with the material.

Live/Dead staining of cells cultured directly on different materials. Calculated total cell number of living cells (A), viability as a percentage of living and dead cells (B), and example images of stained primary human osteoblasts on different materials (C). Living cells were stained green (FITC), and dead cells appeared red (TexasRED); All: merged image [82].

Cell size

U2OS cells were smaller on the titanium and magnesium materials in comparison to the control (Fig. 26, Table 18). MG63 and SaoS2 cells exhibited a reduced size on titanium and were even smaller on magnesium. Primary human osteoblasts exhibited an increased size on magnesium samples in comparison to control conditions.

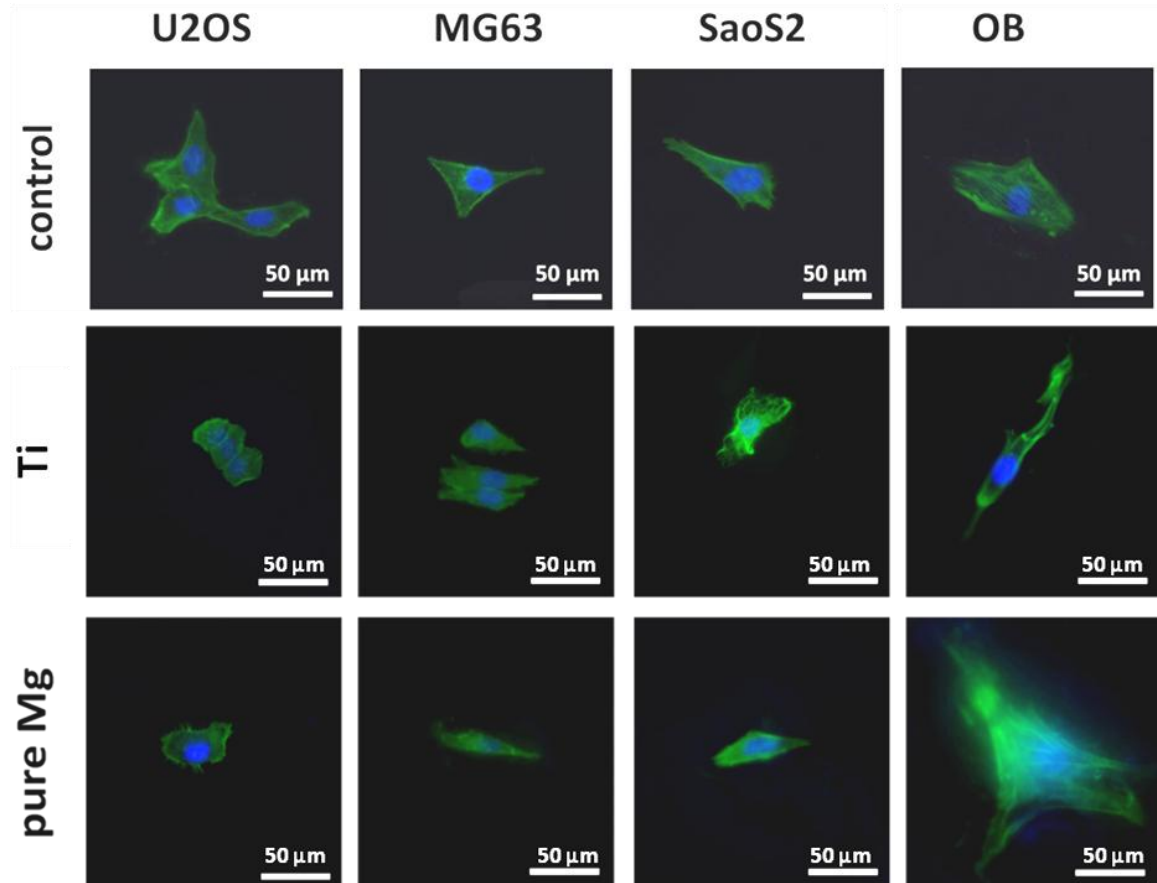


Figure 26. Size of adherent cells from the bone system after direct contact with the material.

Fluorescence microscopy images of U2OS cells under cell culture conditions, after incubation on mirror-polished titanium (Ti) samples, and after incubation on degrading pure magnesium samples (pure Mg), as well as MG63, SaoS2, and primary human osteoblasts (OB). Actin filaments were stained green, and nuclei were stained blue [82].

Table 18. Cell dimensions in μm of adherent cells (length (↔) and width (↓)) under cell control conditions and on titanium and pure magnesium samples. The mean values and standard deviations are presented [82].

		Control	Ti	Pure Mg
U2OS	↔	58 ± 14	24 ± 2	43 ± 2
	↓	35 ± 16	16 ± 3	23 ± 3
MG63	↔	77 ± 39	58 ± 21	49 ± 17
	↓	39 ± 10	20 ± 3	12.2 ± 1
SaoS2	↔	65 ± 17	59 ± 9	64 ± 11
	↓	19 ± 7	31 ± 2	20 ± 2
OB	↔	108 ± 21	108 ± 9	136 ± 36
	↓	35 ± 17	24 ± 5	59 ± 39

Focal adhesion

As magnesium is known to influence the adhesion strength of cells [47, 83], the impact on FAs was determined for primary human osteoblasts. Two controls (cell culture plastic and titanium) were used to show the possible influence of the different materials. Many FAs were observed from the first day for cells grown on cell culture plastic (Fig. 27). The FAs were spread throughout the cell area. In addition, the cells exhibited a smooth surface. On mirror-polished titanium samples, the FAs were arranged more on the border and around the nuclei of the cells. Moreover, the cells appeared to be exerted, especially after one week. The cells exposed to pure magnesium samples also exhibited many FAs all over the surface. A count of green particles, which represented vinculin in the focal adhesion complex, showed that FAs were reduced with longer incubation times. On tissue culture plastic, the reduction of vinculin was more than 95%, on titanium, the reduction was 75% and on pure magnesium, the reduction was 80%. The vinculin particle counts are presented in Table 19. However, on magnesium samples, it was not easy to identify single vinculin spots due to the rough surface.

Table 19. Vinculin particle counts for the control, titanium and pure magnesium samples after exposure of primary human osteoblasts for 1 day, 3 days, 1 week and 2 weeks [82].

	1 day	3 days	1 week	2 weeks
control	615 ± 439	71 ± 19	47 ± 20	25 ± 6
Ti	110 ± 33	67 ± 40	40 ± 12	28 ± 25
pure Mg	91 ± 61	11 ± 14	20 ± 11	18 ± 16

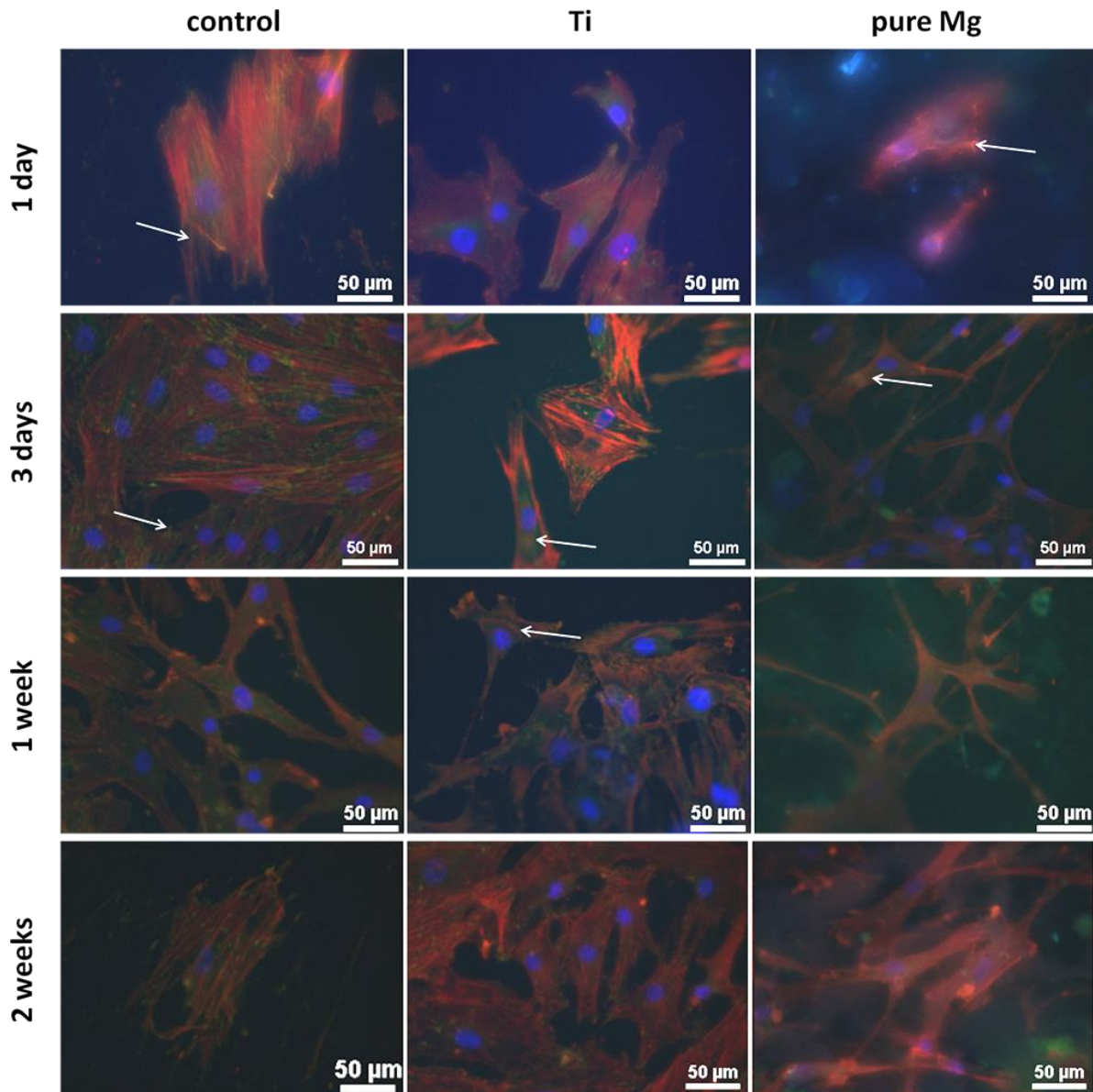


Figure 27. Focal adhesions of primary human osteoblasts.

Focal adhesions of primary human osteoblasts were analysed on different materials and at different time points. Actin filaments were stained red, vinculin was stained green, and nuclei were stained blue. Interesting parts are highlighted with arrows [82].

Gene expression

The gene expression of all analysed genes increased significantly when U2OS and MG63 cells were exposed to a commonly used titanium implant material in comparison to cell culture conditions (Fig. 28 A + B). This effect was even more distinct when the cells were exposed to pure magnesium samples, with gene expression levels increased by factors of 120. In SaoS2 cells, the examined gene expression pattern was different than those observed for U2OS and MG63 cells. The expression of nearly all genes increased significantly after contact with titanium (Fig. 28 C). However, the maximum factor was only 30. Only for OC

4. Results

was a significant decrease detected. The same trend was observed after exposure to pure magnesium. The increase was not so great for ALP and BSP in comparison to titanium. In contrast to titanium, RANKL expression was increased significantly by 2-fold.

The gene expression of primary human osteoblasts was not comparable to that of the other investigated cell lines (Fig. 28 D). Contact with titanium led to significantly increased gene expression (by a factor of 8 for BSP, OC, OPN and RANKL). After exposure to magnesium, the gene expression of OC, OPN and RANKL was even higher (factor of 40). For ALP, a significant increase was detected, which was not observed after exposure to titanium. The expression of BSP was comparable to that observed after contact with titanium, whereas OPG expression decreased significantly after contact with magnesium.

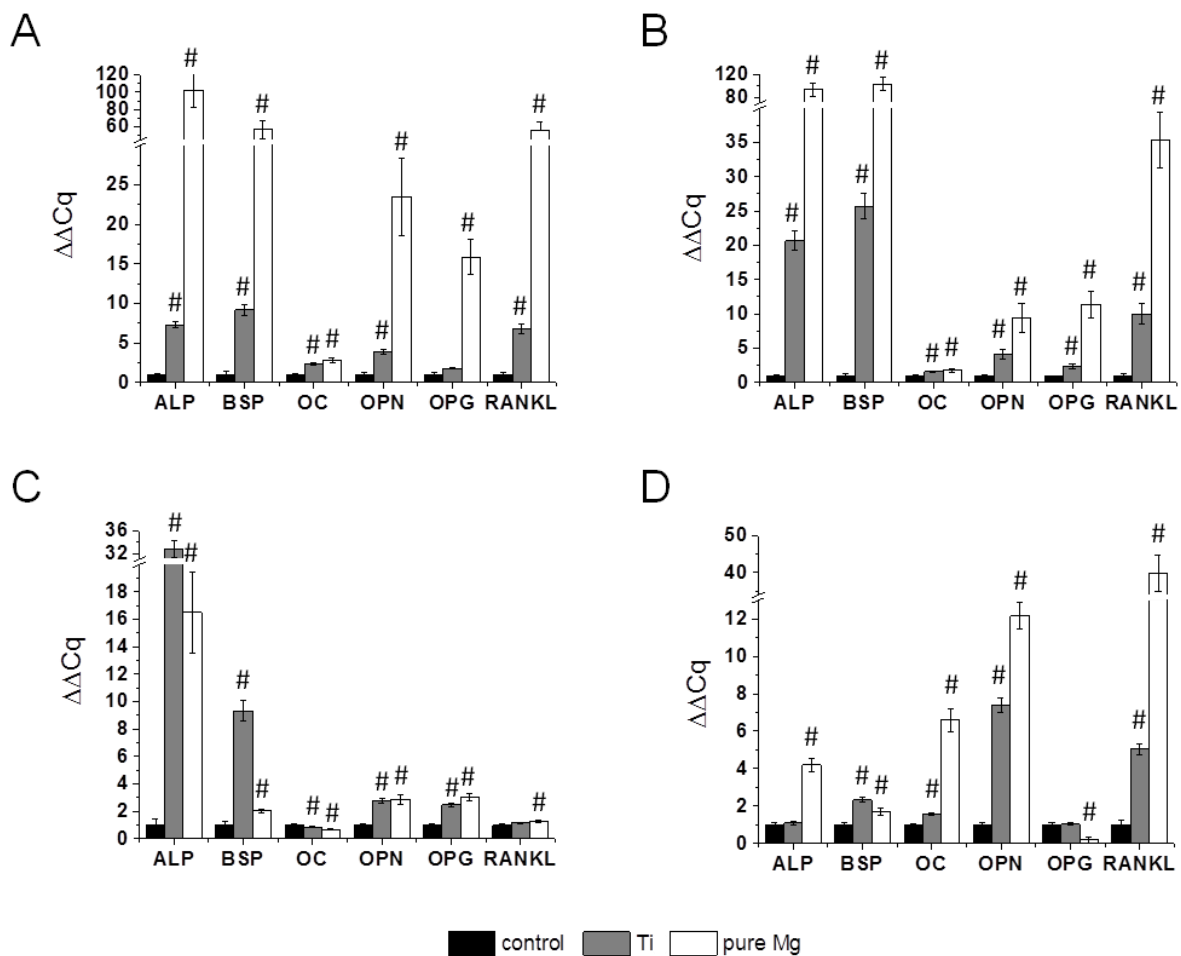


Figure 28. Expression of genes involved in bone metabolism in cells after direct contact with the materials. Expression of genes involved in bone metabolism in the osteosarcoma-derived cell lines U2OS (A), MG63 (B), SaoS2 (C), and primary human osteoblasts (D) after incubation under cell culture conditions (control) or on metal samples (1 week). Gene expression was normalised to the expression of GAPDH and β -Actin and additionally to the control condition ($\Delta\Delta Cq$). The expression under cell culture conditions was set as the control (= 1). GAPDH: glyceraldehyde-3-phosphate dehydrogenase; ALP: alkaline phosphatase; BSP: bone sialoprotein; OC: osteocalcin; OPN: osteopontin; OPG: osteoprotegerin; and RANKL: RANK ligand. Significant differences between the control and the indicated conditions are shown by hash tags (# = $p < 0.05$) [82].

The OPG/RANKL ratios were calculated from the qPCR results and are presented in Table 20. SaoS2 cells reacted differently than the other cells and had ratios > 2 (2.08 - 2.41). In contrast, the ratios for the other cells were < 0.5 (0.01 - 0.32).

Table 20. OPG/RANKL gene expression ratios determined by qPCR after exposure to titanium (Ti) and pure magnesium (Mg) [82].

	U2OS	MG63	SaoS2	OB
Ti	0.26	0.24	2.08	0.20
pure Mg	0.29	0.32	2.41	0.01

4.4 OSTEOINDUCTIVE EFFECTS REFLECTED IN PROTEOMICS

The investigations with extracts and direct contact with degrading material revealed promising results concerning putative bone-inducing behaviours. The next step was to determine whether a proteomics approach with primary human osteoblasts would yield similar results.

Therefore, all previously analysed conditions were investigated with proteomics. Most of the protein patterns were similar under all conditions. However, some distinct differences were observed (Fig. 29; merged image). The largest numbers of exclusive spots were observed after the addition of extract supplemented with differentiating medium (177 spots) and extract with proliferating cells (156 spots). The smallest number of differences was observed under control conditions (26 spots).

In a first approach, selected spots from 2-DE gels were analysed via tryptic in-gel digestion and mass spectrometry. Only spots that occurred under a single specific condition were cut and further analysed. A further analysis of the most interesting proteins was performed by qPCR to verify the initial proteomics results.

In the next step, all previously examined conditions were investigated by LC-MS (UKE Hamburg) directly from the samples. A large number of different proteins were identified (Appendix 1). Among those proteins, many proteins are involved in cell metabolism and cell structure. In addition, 75 proteins involved in translation (*e.g.*, 40S ribosomal protein S11, elongation factor Tu, and glycine-tRNA ligase) and 20 proteins involved in transcription were identified (*e.g.*, MICOS complex subunit MIC19 and interleukin enhancer-binding factor 3).

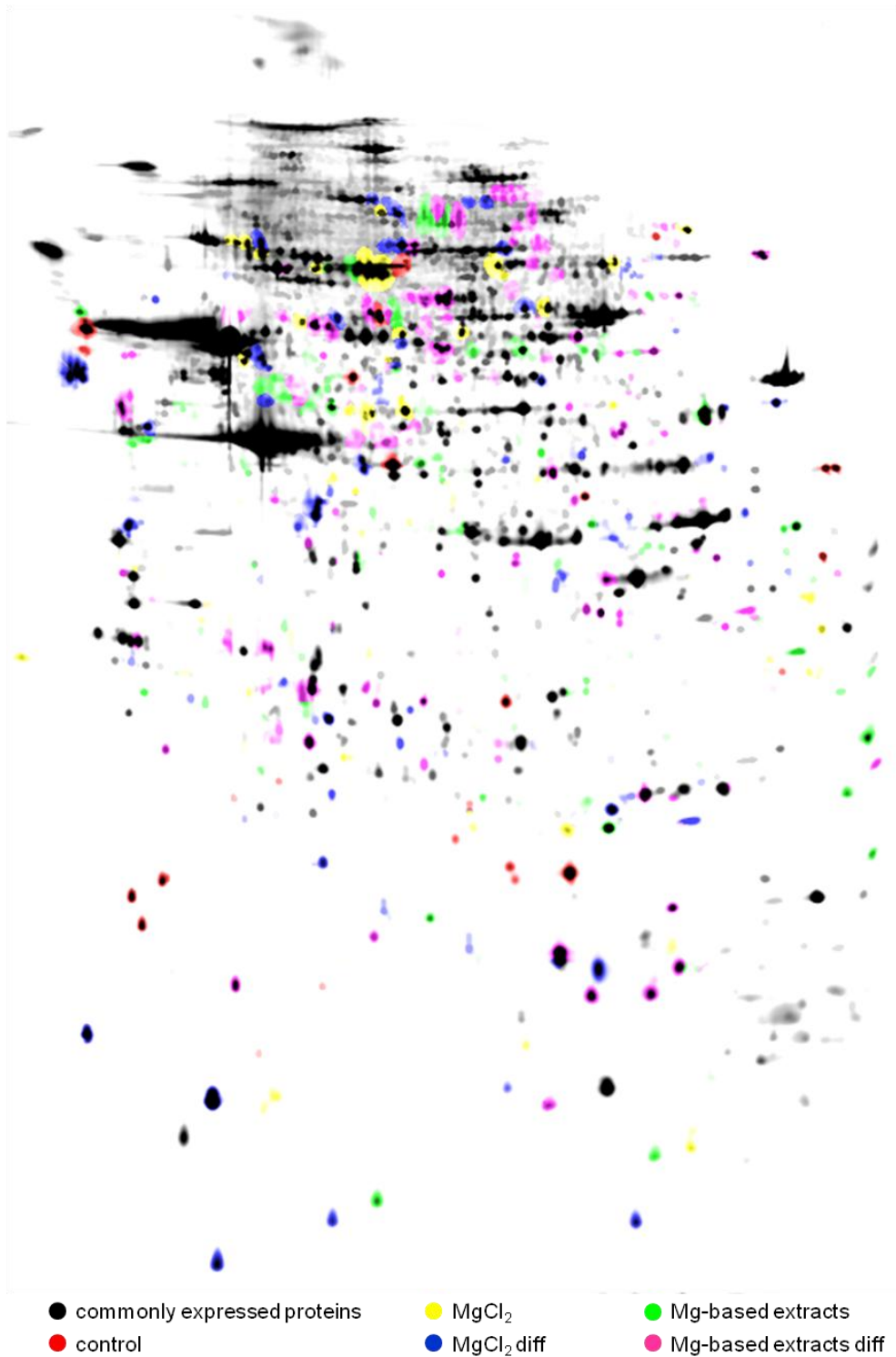


Figure 29. Merged 2-DE image of all analysed conditions with proteomics.

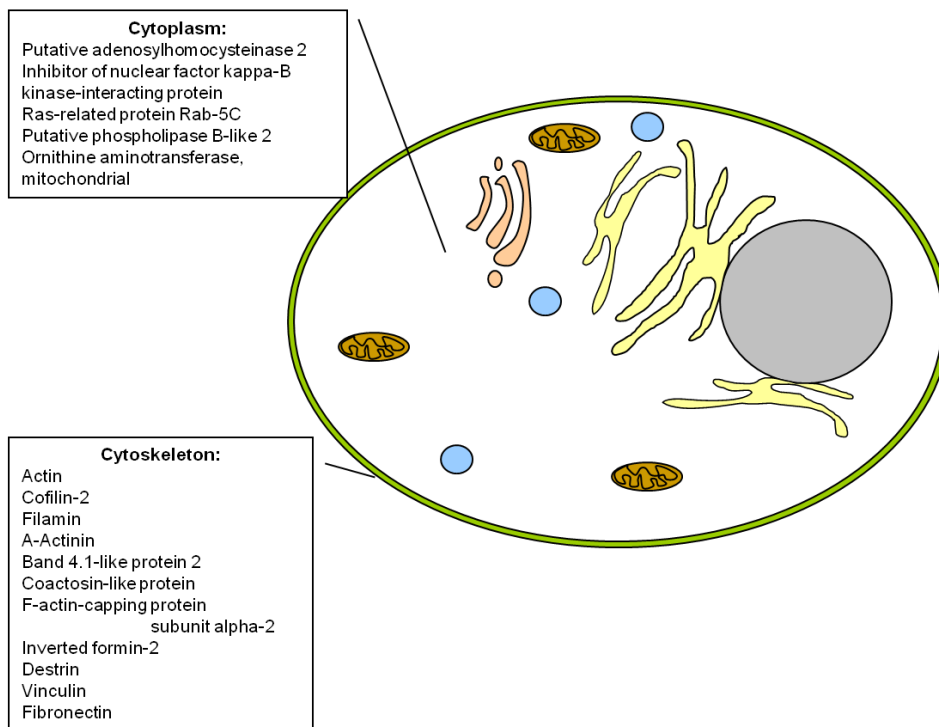
Combined image of all analysed conditions from the proteomics approach. Black dots indicate commonly expressed proteins. Solely expressed proteins and increased expression are indicated in the corresponding colours. Diff: differentiating cells.

Most of these proteins were only expressed after extract exposure in proliferating cells. 40 proteins involved in metabolic processes, such as glycolysis, were detected (*e.g.*, 6-phosphofruktokinase type C and phosphoglucomutase-1). Most of these proteins were expressed after extract exposure in proliferating cells, as shown in previous experiments (Fig.

4. Results

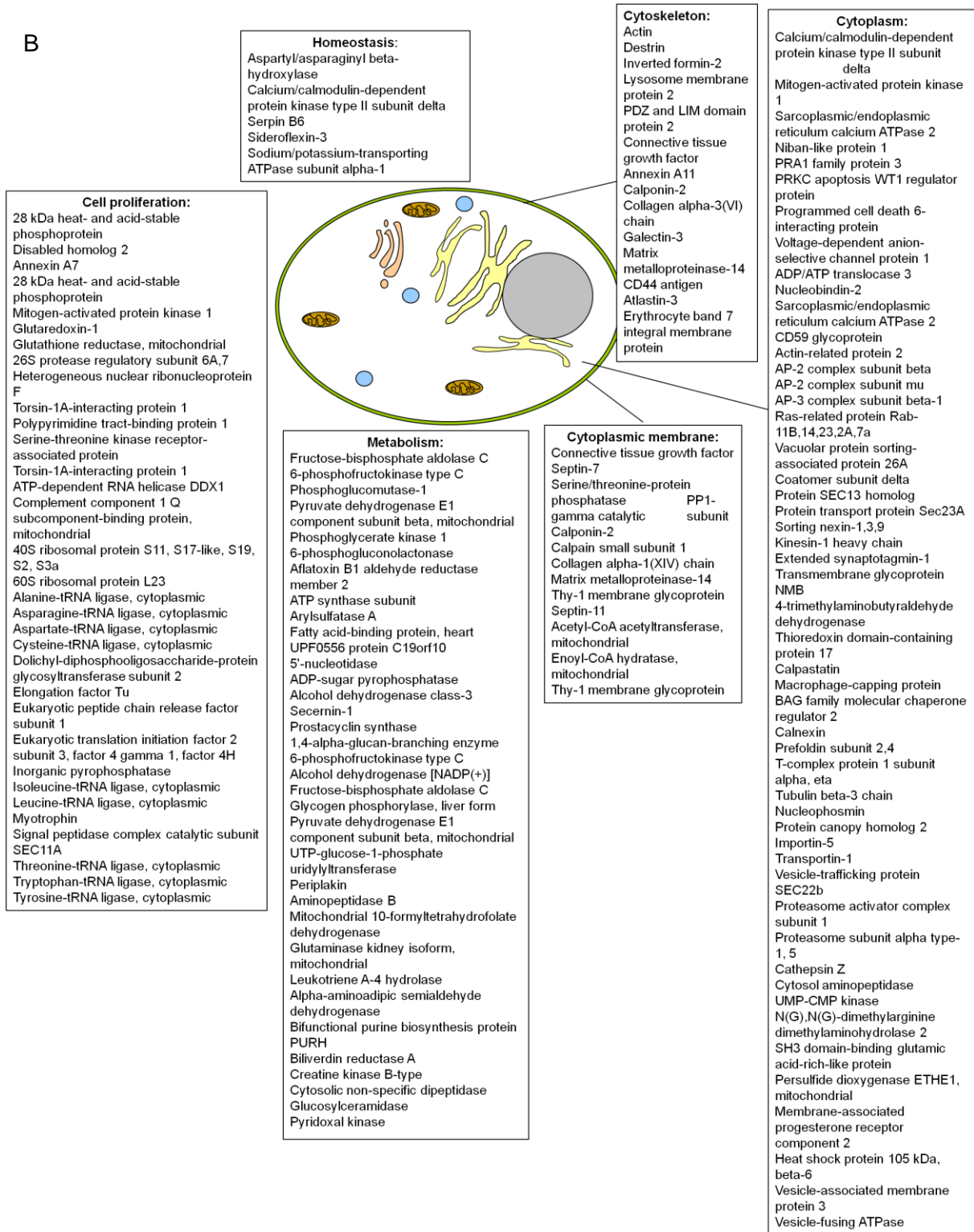
30). Moreover, > 50 proteins involved in the cytoskeleton and cell structure (e.g., drebrin, galectin-3, and mitochondrial inner membrane protein) were identified. The same observation regarding proliferating cells and extract exposure was recorded in this case. Additionally, three proteins directly involved in ossification (PDZ and LIM domain protein 7, prolyl 3-hydroxylase 1, and transmembrane glycoprotein NMB) were detected.

A



4. Results

B



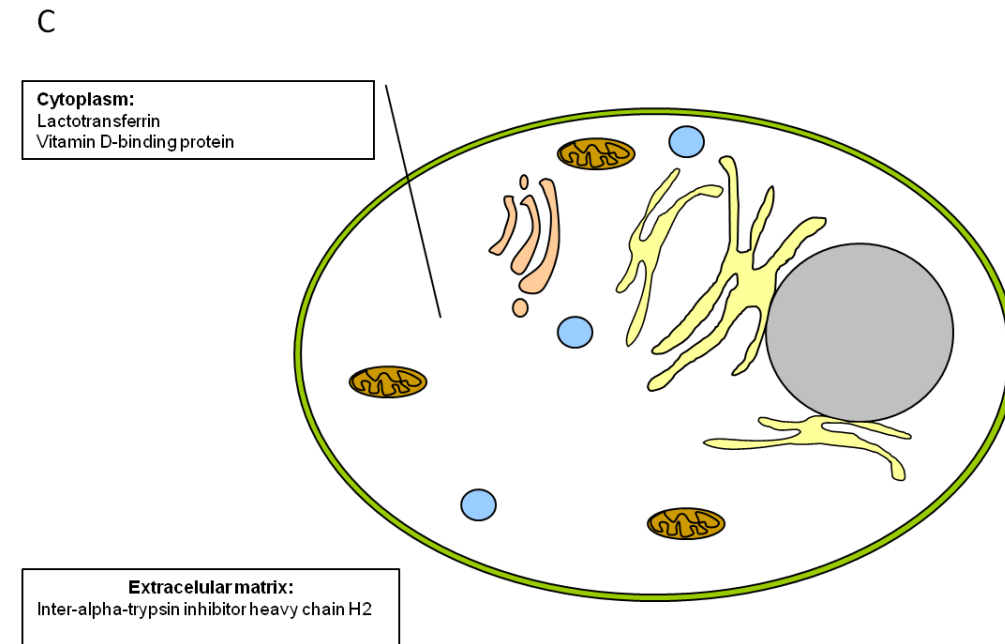


Figure 30. Overview of the locations of expressed proteins found with proteomics.

Summary of the locations of the proteins found with proteomics. The proteins are arranged according to their cellular functions. Presented are the results obtained for primary human osteoblasts grown on tissue culture plastic (A), after magnesium-based extract exposure (B) and after direct contact with degrading magnesium (C). Only the proteins that were exclusively expressed under the examined condition are indicated.

Among all of the analysed proteins, there were two magnesium binding proteins, 14 proteins that use magnesium as a cofactor and eight proteins that require calcium as a cofactor. Additionally, > 40 calcium (Ca) binding proteins were found. As calcium and magnesium are both important in bone metabolism [84], some of these proteins were further analysed by qPCR for the most interesting conditions (*i.e.*, extract, extract supplemented with differentiating medium and direct contact with the material). These proteins are involved in different processes of the cell. For example, alpha-actinin-1 (ACTN1) is part of the cytoskeleton that was increased after $MgCl_2$ and extract addition in primary human osteoblasts (Fig. 8, 13, 19, 23; Tables 9, 12, 15, 17). Furthermore, two proteins that are involved in osteoblast maturation were further analysed by qPCR (Annexin A1 and A2). These proteins were found in various approaches, and their translation was investigated, as osteoblast maturation is significant for bone formation. The initiation of Annexin A4 translation was examined under the analysed conditions, as this protein is involved in homeostasis. The other analysed proteins are involved in cell motility (MYL6B) and cell adhesion (PCDHA1), which are both important activities for bone formation after a fracture. The qPCR analysis revealed similar results in comparison to the proteomics study. Gene expression was induced significantly for nearly all genes investigated after extract exposure and direct contact with degrading magnesium samples in proliferating primary human osteoblasts (Fig. 31). No significant induction of gene expression was recorded in cells

exposed to titanium samples and differentiating primary human osteoblasts exposed to magnesium-based extracts.

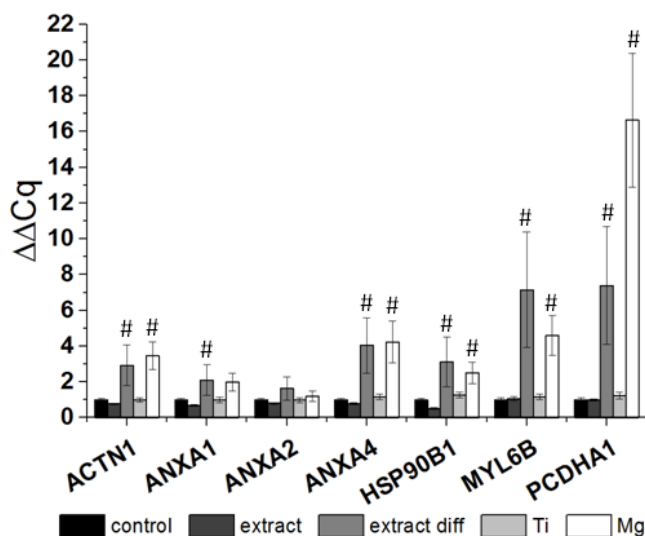
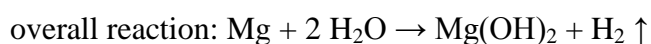
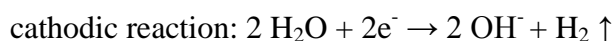


Figure 31. Gene expression of proteins identified with proteomics.

Gene expression of proteins identified using the proteomics approach after incubation under cell culture conditions (control) and after the addition of magnesium-based extracts, extracts supplemented with differentiating medium and growth on metal samples (1 week) for primary human osteoblasts. Gene expression was normalised to the expression of GAPDH and β -Actin and additionally to the control condition ($\Delta\Delta Cq$). The expression under cell culture conditions was set as the control (= 1). GAPDH: glyceraldehyde 3-phosphate dehydrogenase; ACTN1: alpha-actinin-1; ANXA1-4: annexin A1-4; HSP90B1: endoplasmic; MYL6B: myosin light chain 6B; and PCDHA1: protocadherin alpha-1. Significant differences between the control and the indicated conditions are shown by hash tags (# = $p < 0.05$).

5. DISCUSSION

Magnesium implants are considered to have a functional aspect that might lead to osteoinductive properties, as described *in vivo* [1, 2]. Therefore, different parameters that are important for bone growth were analysed under different magnesium corrosion conditions (*i.e.*, magnesium salt, magnesium-based extracts and direct contact with the degrading material). Proliferating and differentiating cells were used. The following corrosion reaction of pure magnesium was considered for the characterization of the medium and magnesium-based extracts [85]:



The anodic and cathodic reactions generate gaseous substances, whereas the overall reaction forms a protection layer on top of the magnesium sample (solid $\text{Mg}(\text{OH})_2$). This corrosion layer slows down the degradation [86].

Medium and extract characterisation

First, osmolality and pH values were determined after MgCl_2 addition to the cell culture medium or extract preparation to guarantee that the cells were not dying due to osmotic shock or high toxicity. In the case of the extracts, the magnesium concentrations were also examined.

As expected, the addition of MgCl_2 did not change the pH in experiments with and without cells (data not shown). The osmolality increased (0.06 osmol/kg in McCoy's 5A) with the supplementation of up to 25 mM MgCl_2 . This increase resulted in a 25-fold higher magnesium concentration in comparison to the standard medium (Fig. 5). All osmolality values are known to be not toxic for the cells [73]. The content of Cl^{-} in human plasma is approximately 100 mmol/L and thereby many fold higher than that of Mg^{2+} [87]. Thus, it was proven that the results obtained for the examined cell types are based solely on increased Mg^{2+} concentrations and not caused by additional factors, such as increased pH or toxic effects.

The concentrations of magnesium in the original extracts were up to 35.6 times higher than those present in commonly used cell culture media. Interestingly, the osmolalities did not increase in the same manner (Table 14). During the corrosion of pure magnesium, not all magnesium ions were dissolved in the solution, as some corrosion products were generated and Mg^{2+} ions were bound in the corrosion layer. However, the osmolalities were above the critical level of 0.4 osmol/kg, for which a decrease in cell viability was shown experimentally [73]. The pH was increased in magnesium-based extracts and was in the alkaline range (Table

14). However, if cells were present during corrosion, especially differentiating primary human osteoblasts, cellular metabolism reduced both the osmolality and pH values (Fig. 15, 16). Similar observations have been reported previously for magnesium alloys [10]. Thus, under conditions with low oxygen or high metabolic activity, cells regulate both pH and osmolality via the gluconeogenic pathway. The cells produce enhanced amounts of lactate at higher pH values in order to enable the uptake of glucose [88]. This tendency could also be shown in the proteomics data (*e.g.*, pyruvate dehydrogenase E1 component subunit beta, mitochondrial and phosphoglycerate kinase 1 were expressed when a magnesium-based extract was added to the environment). These proteins are both involved in the gluconeogenic pathway. Furthermore, it could be proven that the degradation of magnesium reduces the amount of surrounding oxygen [89]. Moreover, if pyruvate comes into contact with hydrogen, it dissolves, resulting in the generation of carbon dioxide, water and acetic acid [90], which acidifies the medium. Additionally, CO₂ from the incubator is also responsible for the acidification of the medium. In conclusion, the osmolality is reduced as a result of cellular metabolism, as well as the formation of a corrosion layer on top of the magnesium layer, which slows down further corrosion.

5.1 CELL COUNTS AFFECTED BY MAGNESIUM

As one of the first determining factors, the cell number was investigated. Magnesium is involved in many processes in the cell (*e.g.*, as cofactor). Therefore, an enhancement of the magnesium concentration in the environment should increase the cellular metabolism and cause an increased cell number.

Magnesium chloride

Magnesium salt had inhibitory effects on the number of proliferating cells. The primary cells appeared to be more affected than the cell lines, as the reduction of the cell count of primary cells was approximately 50% (Fig. 6 A). A similar effect was observed with differentiating cells (Fig. 11 A) after the addition of differentiation medium. As expected, the cell count was reduced. This reduction was caused primarily by growth arrest and the onset of matrix production [91]. The cell count was further decreased when MgCl₂ was added to the cells. This finding led to the conclusion that the addition of magnesium salt did not accelerate the progress of primary human osteoblast differentiation. SaoS2 cells and primary human osteoblasts appeared to have a similar sensitivity, as both cell types exhibited a comparable sensitivity to magnesium salt. Similar results were observed for primary human cartilage cells [92], as well as for mouse macrophages and stem cells from the umbilical cord [93].

Nevertheless, for mammary epithelial cells, it was shown that proliferation was stimulated at concentrations of magnesium of up to 40 mM [94].

Magnesium-based extracts

The influence of magnesium-based extracts on the number of proliferating cells was remarkably different in comparison to the results obtained with magnesium salt (Fig. 17 A). Magnesium-based extracts have positive effects on primary human osteoblasts with respect to proliferation (Fig. 17 A), in contrast to the analysed cell lines and to previously analysed magnesium salt conditions (Fig. 6 A). In another publication, it was reported that a magnesium alloy had no negative effect on the proliferation of primary human osteoblasts [95]. Based on this results the selection of the test material appears to impact cell proliferation. In contrast to the study performed by Willbold *et al.* [95], pure magnesium was used without alloying elements in this study. The observed increase in cell counts may serve as a first indicator of the “osteoinductive properties” of magnesium in primary human osteoblasts [82]. Moreover, this finding indicated that factors other than magnesium, such as the rough corrosion layer and the alkaline pH that was recorded under these conditions, are relevant for the described osteoinductivity [96, 97].

Direct contact with the material

Although the pH and osmolality are increased due to corrosion (Table 14), the cells are able to reduce both of these factors, as discussed previously (medium and extract characterisation). Similar findings in comparison to magnesium-based extracts were obtained with cells growing on implant material (Fig. 25). Interestingly, in all cases, the cell count decreased when the cells grew on titanium samples. The adhesion strength of the cells is dependent on the roughness of the implant's surface. The attachment is weaker on polished surfaces, such as the titanium samples used in this study, than on rough isotropic surfaces [98]. This result suggests that in addition to enhanced Mg^{2+} concentrations in the environment (as detected with $MgCl_2$), corrosion factors and an alkaline pH (magnesium extracts) are involved in the bone-inducing quality of such implants. Moreover, the surface itself had an impact. The surface of the polished titanium samples did not change at all during the study, whereas the pure magnesium samples underwent various changes. The surface became rougher, and the composition changed over the time.

If only Mg^{2+} was present at enhanced concentrations (> 10 mM), an inhibitory effect on the proliferation of the cells was determined, as observed in previous studies [99].

The increased proliferation after extract exposure indicates the positive influences of pH and corrosion products on the cells. Additionally, pure magnesium implants exhibit the advantage

of surface roughness induced by degradation, which may allow for stronger adhesion of the cells. Thus, magnesium is the preferred material in comparison to titanium, as an increased cell count is advantageous for osteoinduction [100]. This conclusion was also supported by the exerted appearance of the cells on titanium samples (Fig. 27).

5.2 VIABILITY INFLUENCED BY MAGNESIUM EXPOSURE

Cell viability is a very important parameter for medical implants. The mechanical properties may be ideal, but if the cells are dying due to contact with the material, the implant will never obtain authorisation to be placed on the market.

Magnesium chloride

The viability of the cell lines was not influenced significantly by exposure to magnesium salt (Fig. 6 B). Although the viability was reduced for proliferating cells, it remained above 90%; thus, no toxic effect was observed. However, primary human osteoblasts were much more sensitive to enhanced MgCl_2 concentrations in the medium. A significant reduction of primary human osteoblast viability was observed. This decrease was not caused by elevated osmolality but was instead directly related to the presence of Mg^{2+} . However, it should be mentioned that in this experiment, the viability of the primary human osteoblasts was already quite low under the control conditions without increasing concentrations of MgCl_2 . In other studies, primary cells were more stable than cell lines after exposure to high magnesium concentrations [73]. However, one very important issue for reliable and reproducible results is the source of primary human osteoblasts. In this experiment, the primary human osteoblasts were extracted from humans and thus showed a strong patient-dependency and variability depending on age, gender and diseases, such as osteoporosis [101]. This effect must be considered when evaluating and comparing results obtained with primary human osteoblasts. In differentiating cells, the viability was comparable to that observed for the control for U2OS cells or higher than that observed for the control for MG63 cells (Fig. 11 B). However, extensive proliferation was observed in the control, resulting in cell death because not enough space was provided for growth. Thus, the increased viability at higher magnesium concentrations is a false positive result.

Again, primary human osteoblasts were the most sensitive cell type, with a generally low viability. The reduction caused by the addition of MgCl_2 was not as dramatic for differentiating cells as for proliferating cells. The cells switched their metabolism to produce extracellular matrix [16]; thus, the influence of enhanced Mg^{2+} concentrations was not as

dramatic as that observed for proliferating cells. Thus, magnesium does not have a strong influence on the viability of mature osteoblasts that have already started mineralisation.

In conclusion, if only the concentration of Mg^{2+} ions is increased without any other changes in the medium (*e.g.*, pH or the occurrence of corrosion products), magnesium has negative effects on the viability of primary human osteoblasts [79].

Magnesium-based extracts

A slightly different viability pattern was observed with magnesium-based extracts in comparison to magnesium salt (Fig. 17 B).

In conclusion, primary human osteoblasts appeared to be more robust in the presence of enhanced magnesium concentrations in the medium in experiments with magnesium-based extracts, where additional factors (increased pH and corrosion products) are present [82]. It is possible that the cells were able to metabolise the magnesium differently and were thus less affected with respect to viability.

Direct contact with the material

On implant materials, the cell lines showed a uniform viability pattern (Fig. 25 B). However, the viability of primary human osteoblasts was much higher than that observed in the other experiments with magnesium salt and magnesium-based extracts. A rough surface like that of magnesium results in integrin expression and thus increased cell adhesion [102-104]. The most interesting result was the composition of the surface of the magnesium samples. The detection of single cells was difficult, as the cells appeared to be embedded in a corrosion layer, which was formed on top of the sample. This corrosion layer on magnesium samples appeared to have advantageous properties for cell growth in comparison to titanium samples (Fig. 25 C). The rough surface of the magnesium allows the cells to adhere more easily to the material; thus, cell counts and viability were increased in comparison to titanium [98].

Primary human osteoblasts appeared to be less affected with respect to viability when not only was Mg^{2+} enhanced but other factors, such as an alkaline pH and corrosion products, were present [105]. Moreover, the corrosion layer slows down degradation, and amino acids can bind to the surface, enabling the cells to grow on the surface [81].

Taking the results obtained with magnesium-based extracts and direct contact with degrading magnesium material together, the constant viability can be counted as the second “osteoinductive property” in primary human osteoblasts (see cell count for magnesium-based extracts). Moreover, the best results regarding cell viability were obtained with direct contact with the material.

In conclusion, magnesium-based extracts and direct contact with the material are favourable *in vitro* models for testing cell viability. In contrast, magnesium salt is not an appropriate model for examining the viability of cells [79, 82].

5.3 CELL SIZE AFFECTED BY MAGNESIUM CORROSION

The cell size was first determined with trypsinised cells in suspension. This analysis was performed in parallel to the investigation of cell count and viability. As significant differences were observed, the cells were also examined in the adherent state.

Magnesium chloride

The size and shape of the cells have been reported to be important for the fate of the cell (*i.e.*, if the cell exhibits a large spreading area in combination with an extensive cytoskeleton, the cell tends to enter the differentiation phase faster) [80]. This effect could be one explanation for the reduced viability discussed in Chapter 5.2 in combination with an enlarged cell size for primary human osteoblasts [79].

Magnesium-based extracts and direct contact with the material

Proliferating primary human osteoblasts became very large after extract addition in suspension and in the adherent state (Fig. 18, 19, Table 15). This increase in size of proliferating primary human osteoblasts again indicated “osteoinductive properties,” as an increased size is an indicator that the cells will enter the differentiation phase earlier [80]. Magnesium appears to have an effect on this pathway. However, this effect was only observed after extract addition and not after direct contact with the material (Fig. 26, Table 18). Differentiating primary human osteoblasts are generally larger than proliferating primary human pre-osteoblasts [106]. Due to mineralisation, mature primary human osteoblasts exhibit a larger size. This difference was also observed in this *in vitro* study of adhered primary human osteoblasts (Table 12). As shown previously it is very likely that Mg^{2+} increased the expression of proteins involved in differentiation, adhesion and the cytoskeleton, as shown in a previous study [107].

It has been shown previously that the presence of divalent cations, such as magnesium, stimulates cell adhesion [47]. In this study, SaoS2 cells and primary human osteoblasts adhered more strongly to tissue culture plastic with increasing extracellular magnesium concentrations. In the presence of concentrations higher than 10 mM $MgCl_2$ and after the addition of magnesium-based extracts, the use of cell scrapers was necessary to remove the cells from the surface, whereas MG63 and U2OS cells could be easily detached from the tissue culture plastic by trypsinisation.

There is a possible correlation between increased cell size and enhanced adhesion behaviour. Divalent cations, such as Mg^{2+} , are responsible for higher expression of integrins, which are part of focal adhesions. Cells can bind directly to the material via these proteins [83, 108]. Thus, a larger spreading area leads to increased adhesion.

Moreover, Mg^{2+} was reported to regulate the organisation of integrins in focal adhesions [109], which are important for cell adhesion to implant materials [110]. Stronger cell adhesion could be hypothesised to be related to a larger number of focal adhesion contacts. Unfortunately, no relation between the number of focal adhesions and the strength of adhesion was observed. No increase in the number of focal adhesions was recorded after exposure to magnesium samples (Fig. 27, Table 19). Surprisingly, the number of focal adhesions appeared to decrease with incubation length.

Nonetheless, it was reported that an increased cell-material area in combination with well-defined focal adhesions and a comprehensive cytoskeleton provokes the cells to abort proliferation and enter the differentiation phase earlier [80]. This intensified adhesion behaviour of primary human osteoblasts in contact with extracts could be regarded as the next indicator of the “osteoinductive properties” of magnesium.

Nevertheless, integrin protein expression was observed via proteomics, as discussed in Chapter 5.6, indicating that magnesium influences the building of extracellular matrix contacts.

In conclusion, free Mg^{2+} has positive effects on cell size and cell adhesion in SaoS2 cells and primary human osteoblasts, as it is involved in adhesion (*e.g.*, because of expression and involvement in the organisation of integrins). This effect was observed best with magnesium salt concentrations higher than 10 mM and with magnesium-based extracts. In the case of cell size, magnesium-based extracts are the preferred method because the results can be easily evaluated and the conditions are closer to the *in vivo* conditions than those obtained with the magnesium salt [79, 82].

5.4 GENE EXPRESSION REVEALS OSTEOINDUCTIVE PROPERTIES

In addition to cell number, viability and cell size, the expression of genes involved in bone and matrix formation can indicate whether high magnesium concentrations may be involved in mineralisation.

RT-PCR

A first qualitative approach was performed using RT-PCR and increased $MgCl_2$ concentrations. The genes whose expression levels were expected to show the greatest

influence by enhanced MgCl_2 concentrations in the environment using RT-PCR were chosen for qPCR. The application of qPCR revealed more detailed changes in gene expression than RT-PCR (discussed in the following chapter).

Genes involved in different maturation phases of osteoblasts were analysed by RT-PCR. The transcription factor *Cbfa1* induces osteoblast maturation. Therefore, it was investigated whether magnesium has a further impact on the expression of this factor. The expression of the *Cbfa1* was determined in all cells. As the gene expression of this factor did not show great variations due to the addition of magnesium and appeared to be unresponsive to increased magnesium concentrations, *Cbfa1* was not analysed further.

ALP is already present in pre-osteoblasts [111] and is therefore accepted as an early marker of osteoblast differentiation. Enhanced gene expression of ALP would indicate the initiation of osteoblast maturation. The gene expression of ALP was weak in MG63 cells but stronger in the other cells (Fig. 9 A). The initiation of maturation was induced differently in the various investigated cell types. Maturation was induced most strongly in SaoS2 cells.

Several genes were examined as markers of mature osteoblasts: BSP, OC and OPN [112-114]. The expression of these genes could be detected in primary human osteoblasts, but in the cell lines, different gene expression patterns were observed (Fig. 9 A). U2OS and MG63 cells revealed no genotype that was comparable to that of mature human osteoblasts. Thus, magnesium addition did not lead to maturation in those cells.

Two genes were selected as components of the matrix: Col 1 and Col 10. As a negative control, collagen type 2 (Col 2) was chosen, as this protein should not be present in osteoblasts [115]. The gene expression levels of Col 1 and Col 10 were comparable. There may be a link between cell size and increased adhesion behaviour. However, gene expression did not change after exposure to MgCl_2 (Fig. 9 A). Col 2 was not detected in any condition or cell type, as expected. Thus, these three genes were not further analysed by qPCR.

Cell adhesion to the extracellular matrix is initiated by HPSE [116]. The gene expression of HPSE was not analysed further because no change was observed in any cell type after the addition of magnesium salt. It appeared that the enhanced adhesion strength that was observed for SaoS2 cells and primary human osteoblasts was caused not by increased expression of this gene but by an augmented adhesion area, which was observed for the adherent cells (Fig. 8 and 9 A).

Moreover, OPG and RANKL, which are antagonists in the bone remodelling process [46, 117, 118], were analysed. The balance of the gene expression of these proteins is important for bone health and turnover [109]. The over-expression of OPG leads to increased inhibition

of osteoclast progenitor cells and therefore favours osteoblast activity. This effect may lead to new bone apposition. On the other hand, the over-expression of RANKL indicates increased recruitment and activation of osteoclasts. In other words, the upregulation of bone-related markers in combination with an OPG/RANKL ratio below 1 would indicate a bone remodelling effect, and an OPG/RANKL ratio above 1 would indicate an osteoinductive effect [58, 68]. Both parameters were therefore analysed based on the qPCR results. OPG/RANKL ratios > 1 were determined for most of the examined conditions and primary human osteoblasts (Tables 11, 16, 20).

Clear differences in gene expression were found by comparing the results obtained from RT-PCR and qPCR. The use of these two different methods may explain the variations. RT-PCR was applied as a qualitative method to investigate the presence/absence of gene expression under an examined condition. Nevertheless, the sensitivity of this method is limited. In contrast, qPCR is a method that is more sensitive. In addition, two housekeeping genes (GAPDH and β -Actin) were used to normalise gene expression. Both housekeeping genes were selected because they are constitutively expressed genes in a large number of cell types. Moreover, the employed housekeeping genes are involved in significant cellular processes (*e.g.*, glycolysis (GAPDH) or cell structure (β -Actin)).

qPCR

Magnesium chloride

The results of qPCR after exposure to enhanced MgCl_2 concentrations were heterogeneous for all cell types (Fig. 10). It is very complicated to determine a marker for osteoblastic maturation under enhanced extracellular magnesium salt conditions. The expression pattern of MG63 differed most significantly from that of primary human osteoblasts, whereas similarities between U2OS cells and to some extent, SaoS2 cells were observed. Thus, no cell line is a completely suitable model for studying the impact of magnesium salt on bone cells using gene expression. Magnesium accessibility is important for bone formation, and magnesium deficiency was found to cause OPG/RANKL ratios that promote osteoclastogenesis (in primary human osteoblasts, up to 16-fold in comparison to the control after a 50% magnesium nutrition diet for six months) [58]. In contrast, magnesium addition increases serum OPG and leads to variations in the OPG/RANKL ratios, which appears to support bone formation [119]. In this case, the OPG/RANKL ratios are heterogeneous after MgCl_2 addition for proliferating cells (Table 11). MgCl_2 revealed no magnesium-based stimulation of the OPG/RANKL ratio, indicating no clear osteoinductive effect for the analysed cell lines. In the case of primary human osteoblasts, the OPG/RANKL ratio is < 1 .

The addition of 15 mM MgCl₂, when the OPG/RANKL ratio is > 1, would indicate bone formation. However, as the rest of the gene expression pattern is heterogeneous, no general conclusion can be made.

Regarding differentiating cells, the gene expression was less heterogeneous after MgCl₂ addition (Fig. 14). Most of the genes increased their expression with enhanced magnesium in the environment, indicating an impact of magnesium on differentiation and bone formation.

In conclusion, enhanced MgCl₂ revealed no clear osteogenic trend when investigating the gene expression of important genes involved in matrix formation, which should be expressed at elevated magnesium concentrations. Therefore, it is not advisable to use gene expression as an indicator of osteoinduction when using magnesium salt as a model system.

Magnesium-based extracts and direct contact with the material

The influence of magnesium-based extracts on the gene expression of primary human osteoblasts was clearer than that observed with magnesium salt (Fig. 20). An increase of ALP, indicating an induction of primary human osteoblast maturation, was observed for proliferating primary human osteoblasts after 1 week of extract addition and for differentiating primary human osteoblasts after 2 weeks of extract addition. Moreover, ALP was induced significantly when primary human osteoblasts were exposed to pure magnesium samples (Fig. 28). Increased ALP expression was observed in another study using human bone marrow-derived stromal cells after increased Mg²⁺ concentrations, indicating primary human osteoblast differentiation [120]. Thus, the increased expression of ALP that is induced by magnesium corrosion could serve as an indicator of osteoinduction when analysing magnesium-based extracts and direct contact with the material with primary human osteoblasts.

As expected, BSP, OC and OPN were expressed, especially in cells cultured with extracts and differentiation factors (Fig. 24). Direct contact with pure magnesium samples also induced a significant increase (Fig. 28), indicating the induction of mineralisation in the cells. These proteins are markers of mature osteoblasts [121] and therefore indicate bone formation.

In MG63 and U2OS cells, the genes were induced to a lower extent in comparison to the other differentiating cells. It was reported in the literature that these cells are unable to build a calcified matrix and that their gene expression differs from that of primary cells [27, 38]. However, in this study, a highly significant induction of the expression of nearly all genes was observed in differentiating cells for U2OS and MG63 cells (Fig. 24 A + B), indicating a strong influence of magnesium on bone- and matrix-related genes.

OPG/RANKL ratios < 1 were observed for all investigated conditions in primary human osteoblasts, except for the addition of 15 mM $MgCl_2$ and longer extract exposure in proliferating cells (Tables 11, 13, 16, and 20). These conditions have positive effects on bone remodelling [122]. The influences of magnesium on bone and matrix-related genes that were observed for magnesium-based extracts and direct contact with simultaneously degrading material are summarized in Figure 32. Magnesium induces gene expression in immature and mature osteoblasts, resulting in enhanced matrix formation. Due to the presence of OPG/RANKL ratios < 1, osteoclast maturation is initiated. These activities keep the events of bone formation and bone resorption in balance (bone remodelling).

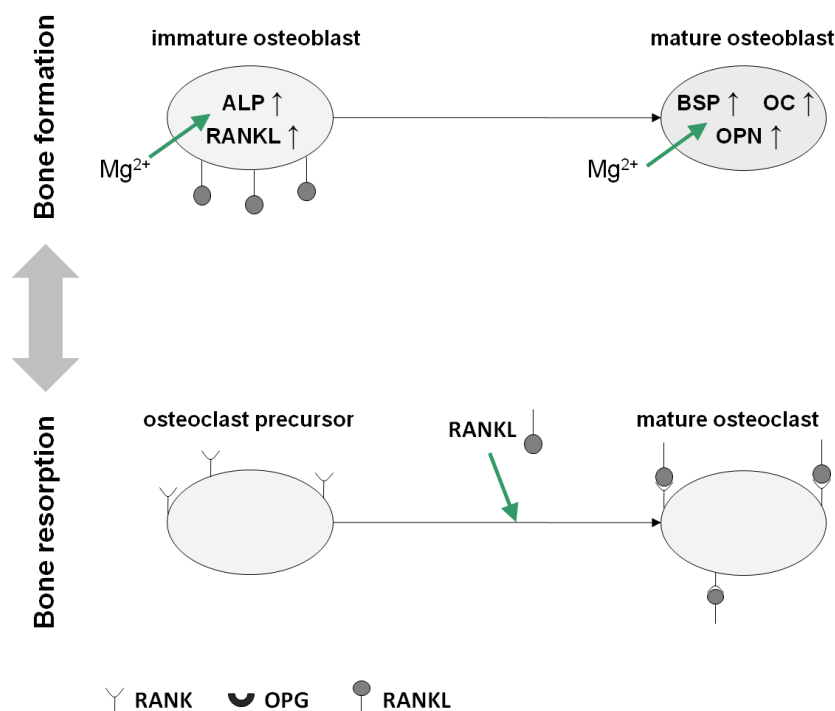


Figure 32. Influence of magnesium on genes involved in bone and matrix formation.

The effects of magnesium on bone- and matrix-related genes were analysed under different conditions. Magnesium has positive effects on immature and mature osteoblasts. Because of the OPG/RANKL ratio, bone resorption is also influenced by the activation of osteoclasts via RANKL.

In conclusion, some “osteoinductive properties” were observed in primary human osteoblasts. The upregulated gene expression of bone-related markers after short-term extract exposure, extract addition to differentiating cells and direct contact with degrading material revealed a gene expression pattern that favours bone formation.

In contrast to short-term extract exposure, long-term exposure triggered a decrease in gene expression patterns. This observation suggests that the extract and its ingredients initiate osteoinduction. A further analysis of the extract composition is needed to understand this phenomenon.

Direct contact with the material had distinct influences on the cells. U2OS cells, MG63 cells and primary human osteoblasts had similar expression patterns. The expression was much higher after exposure to pure magnesium samples than after exposure to titanium. Moreover, the bone remodelling gene expression pattern could be investigated for primary human osteoblasts. Regarding Saos2 cells, the opposite was observed. Contact with pure magnesium appeared to inhibit the expression of bone-related genes in SaoS2 cells (Fig. 28).

Overall, the stimulation caused by pure magnesium was more obvious than that caused by magnesium-based extracts, with a gene expression pattern favouring bone formation in primary human osteoblasts. This effect is due to the combination of an alkaline pH and corrosion products (*e.g.*, Mg(OH)₂) that are generated during degradation while the cells are growing on the sample.

5.5 SUITABLE OSTEOBLASTIC *IN VITRO* CELL MODEL FOR MAGNESIUM INVESTIGATION

Cell lines are commonly used as models for analysing cell behaviour *in vitro*. Regarding the investigation of magnesium, MG63 cells are the most frequently examined cell model [30-33]. In this study, four cell types were analysed. The use of these different cell types makes it possible to draw conclusions about their feasibility as model systems for osteoinductivity *in vitro*.

Considering the origin of the cell lines - osteosarcoma - it is not a surprise that the cells exhibit different behaviour with respect to cell counts in comparison to primary human osteoblasts [25] because these cell lines are known to be fast growing.

The addition of extracellular magnesium had no effect on the size of U2OS and MG63 cells because these cells are unable to form a calcified matrix on their own [27]. The expression of marker genes for mature osteoblasts is reduced or not measurable (Fig. 9) [121]. Thus, a comparison to primary human osteoblasts is not possible.

Furthermore, as the osteosarcoma-derived cell lines exhibit characteristics that are more fibroblast-like (*e.g.*, MG63 and U2OS cells [29, 35]), the differences in gene expression patterns in comparison to primary human osteoblasts can be explained.

In contrast, SaoS2 cells exhibit mineralisation and even osteoinductive potential *in vitro* [39]. Accordingly, the enhancement of extracellular magnesium has an effect on various processes within this cell line, as indicated by increased cell sizes. Free Mg²⁺ may induce collagen expression [123]. This induction could lead to the observed enhanced cell size.

Overall, the results obtained with the cell lines under the different magnesium conditions were too heterogeneous in comparison to primary human osteoblasts; thus, reliable results will only

be achieved with primary human osteoblasts [79, 82]. MG63 and U2OS cells yielded results that differed most in comparison to primary human osteoblasts. Depending on the analysed condition, SaoS2 cells may be feasible as an osteoblastic model *in vitro*. Several additional cell types with the potential to serve as an alternative model to primary human osteoblasts were investigated in another study [121]. Those authors concluded that osteoblasts of animal origin, such as MC3T3-E1 cells from mice (representative of a pre-osteoblastic phenotype), might serve as an alternative. It would be interesting to compare this finding with the test design used in this study.

5.6 PROTEOMICS CONFIRMED PHENOTYPIC AND GENOTYPIC STUDIES FOR OSTEOINDUCTIVE FEATURES

The addition of magnesium-based extracts and direct contact with simultaneously degrading magnesium samples revealed some osteoinductive features, as described in the previous chapters of this discussion. However, the obtained results were only related to phenotypic or genotypic effects. To verify whether measurable influences of magnesium are also detectable at the protein level, all previously applied conditions were analysed with a proteomic approach and primary human osteoblasts.

Distinct differences in the 2-DE gel patterns of the various conditions were determined (Fig. 29). Many different proteins were detected, including many calcium binding proteins, demonstrating the importance of calcium for osteoinduction. The expression of those genes was also increased, indicating an important role of calcium-binding proteins under the examined conditions. These proteins might serve as calcium storage. Another possibility is that this induction is a mechanism to preserve the calcium/magnesium balance under high extracellular magnesium conditions. The cells might be able to keep calcium inside the cell to provide calcium during metabolism and prevent hypocalcaemia [124]. Examples of detected proteins involved in the regulation of Ca^{2+} homeostasis are calcium/calmodulin-dependent protein kinase type II subunit delta, nucleobindin-2 and sarcoplasmic/endoplasmic reticulum calcium ATPase 2. These genes were only expressed after extract addition when the magnesium concentrations were high (up to 2.9 mM; Table 14) in combination with other corrosion factors.

Some of the calcium-binding proteins detected via 2-DE were further analysed at the gene expression level. Among these proteins are proteins of the cytoskeleton (ACTN1), proteins involved in osteoblast maturation (ANXA1 and ANXA2), a protein associated with homeostasis (ANXA4), a chaperone (HSP90B1) and proteins involved in cell motility

(MYL6B) and adhesion (PCDHA1). The significant increase in gene expression after all magnesium exposure conditions highlights the importance of these proteins (Fig. 31). ACTN1 is a binding protein that is associated with adhesion [125]. The observed upregulation of this gene explains the strong adhesion that was observed on magnesium samples in the experiments performed in this study. ACTN1 is a part of focal adhesions, and it was discussed previously that the addition of magnesium has a positive influence on integrin, which is a mediator for the extracellular matrix.

ANXA1 gene expression was increased on magnesium samples (Fig. 31). This effect was a result of the reaction to high Mg^{2+} concentrations and pH caused by simultaneous degradation of the sample because this protein plays a role in anti-inflammatory signalling and apoptosis [126].

The second protein of the annexin family (ANXA2) performs functions in pre-osteoblast proliferation and matrix maturation [127]. Since no significant increase in gene expression was examined in this study, ANXA2 is suggested to have no major influence on matrix maturation under increased magnesium conditions.

ANXA4 was analysed as the third protein of the annexin family. This protein is located in the cell membrane to determine Ca^{2+} concentrations in the cytosol [128]. The significant induction of ANXA4 indicates the great importance of calcium homeostasis under high magnesium conditions [129].

HSP90B1 is a chaperone of the endoplasmic reticulum, which is suggested to control osteogenesis [130]. A significant increase in the gene expression of this chaperone indicates that this protein is important for correct protein folding in primary human osteoblasts in the presence of high magnesium concentrations and under conditions that favour osteoinduction (magnesium samples). The uptake of magnesium will change the intracellular concentration, an increase of chaperones occurs to ensure correct protein folding.

It is thought that myosin 6, where MYL6B belongs to, is localised to the leading edge of the cells; thus, increased expression of this gene could lead to the enhanced cell sizes measured in this study. Thus, this protein is involved in cell motility [131], and direct contact with degrading material has a positive influence on the attachment of the leading edges of the cells and therefore the spreading of the cells.

PCDHA1 is involved in cell adhesion [132]. Stronger adhesion was observed under conditions for which increased gene expression was observed (*i.e.*, extract diff and magnesium samples). This finding is consistent with the examinations of integrin and ACTN1.

In addition to the calcium-binding proteins, a second group of proteins was detected in the 2-DE gels. A significant number of proteins involved in cell structure were identified. This observation was consistent with the increased cell size observed after MgCl_2 and extract addition (Fig. 7, 8, 12, 13, 18, 19, 22, 23; Tables 9, 12, 15, 17). This finding was not only a phenotypic phenomenon in this study but was also confirmed at the protein level by this result. Thus, this result was a confirmation of the previously observed "osteoinductive properties" (*i.e.*, increased cell size and augmented adhesion behaviour after 10 mM magnesium salt or extract exposure).

In addition, many proteins involved in cell metabolism were detected. It was striking that many proteins were expressed after exposure to magnesium-based extracts, which were not found under the other conditions (> 140 ; Fig. 29 and 30). In particular, these proteins are responsible for cell growth and proliferation (*e.g.*, 11 amino acid ligases and proteins involved in glycolysis). This finding was consistent with the increased proliferation measured after magnesium-based extract addition (Fig. 17 A) and thus verified that magnesium-based extract is a more reliable model system than magnesium salt.

Only a few proteins were identified after direct contact with degrading magnesium samples. The low cell number ($< 10,000$ cells) could be a reason for this result. The limit of detection for slightly expressed proteins might have been too low. However, housekeeping proteins (*e.g.*, GAPDH and actin) were determined. Thus, the experiment itself was successful. Nevertheless, some proteins, such as the vitamin D-binding protein, which is an important protein for bone metabolism [133, 134], were only expressed after direct contact with magnesium, indicating that this condition has an effect on bone metabolism. In addition, lactotransferrin was also only detected under this condition. This protein is thought to support osteogenesis [135]. Thus, the conditions present during corrosion (*i.e.*, an alkaline pH and corrosion products such as $\text{Mg}(\text{OH})_2$) induce osteogenesis via the overexpression of proteins involved in this process (lactotransferrin and vitamin D-binding protein).

Together with the other positive effects (viability, cell size and adhesion, and gene expression) that occurred under these conditions, this result shows the suitability of this *in vitro* model for analysing magnesium corrosion. Thus, this condition appears to be suitable for analysing the influence of magnesium materials *in vitro*.

The proteomic approach underlined the findings of previous investigations at the phenotypic and genotypic level. The osteoinductive features observed after magnesium-based extract addition and direct contact with a corroding magnesium material were also observed in the protein expression patterns. Moreover, it became clear that Mg^{2+} is not the only factor

important for enhanced bone formation, as most effects were observed after extract addition and direct contact with the degrading material. However, many proteins that require magnesium as a cofactor were detected (*e.g.*, ATP-citrate synthase, alpha-enolase, transketolase, and cytoplasmic isocitrate dehydrogenase [NADP]). This finding shows the importance of magnesium for the cell and its metabolism [11, 44, 45].

Figure 33 summarizes the results of the various proteomic approaches and the table from Appendix 1. This figure presents the cellular processes that are most affected by incubation with increased magnesium concentrations. Most processes are involved in proliferation (translation, transcription, cell division, cell growth and proliferation) or cell adhesion (proteins relating to the cytoskeleton and the adhesion of the cell).

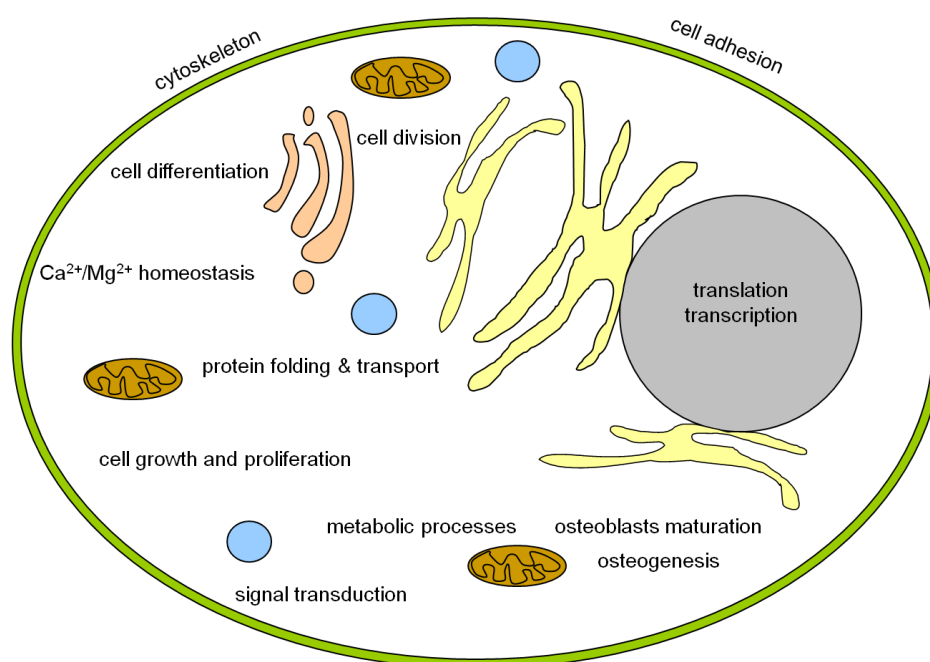


Figure 33. Influence of magnesium on main processes according to the number of regulated proteins.

Overview of the cellular processes affected by enhanced magnesium concentrations. Various processes are influenced, including osteogenesis, cell differentiation, and cell adhesion.

In conclusion, a significant influence of magnesium exposure was observed at the protein level. An important influence on calcium-binding proteins was observed, suggesting that the cells attempt to store Ca^{2+} and maintain $\text{Ca}^{2+}/\text{Mg}^{2+}$ homeostasis during osteoinduction. The osteoinductive properties identified in previous phenotypic and genotypic studies (*i.e.*, cell count, cell size, and gene expression) were confirmed at the protein level. In addition, it was confirmed that exposure to magnesium-based extracts and pure magnesium samples are best suited for analysing magnesium degradation *in vitro*.

6. SUMMARY AND OUTLOOK

In the present study, the influence of magnesium on bone-derived cells was investigated by analysing different parameters of bone metabolism. Different *in vitro* model systems have been used. The most important conclusions are outline below.

A) Osteoinductive indicators were observed for primary human osteoblasts:

- I. increased cell numbers after magnesium-based extract addition indicated a higher proliferation rate;
- II. increased cell sizes in combination with increased adhesion behaviour after MgCl_2 and magnesium-based extract supplementation suggested an early switch to differentiation;
- III. bone-inducing gene expression patterns were observed for magnesium-based extracts and direct contact with simultaneously corroding material.

B) The experiments revealed that primary cells of the investigated tissue should be used as an *in vitro* model if magnesium is analysed:

- I. the results obtained using the cell lines were heterogeneous and showed no specific stimulation by magnesium;
- II. primary human osteoblasts yielded consistent results, with clear influences of magnesium on proliferation, cell size, and gene and protein expression.

C) Mg^{2+} is not the only factor important for enhanced bone formation *in vivo*:

- I. the results obtained with MgCl_2 were very heterogeneous;
- II. magnesium-based extracts and direct contact tests revealed clear osteoinductive features, indicating that other factors, such as an alkaline pH, calcium/magnesium balance and corrosion products, are involved in this phenomenon.

D) Examinations of magnesium as an implant material should be performed with the direct test.

A thorough characterisation of the extracts must be performed to analyse the detailed composition of the corrosion products in order to identify the component that triggers the positive effects observed in this study. Moreover, further studies analysing the osteoinductive features of magnesium implant materials must be performed with direct contact with simultaneously degrading material and primary human osteoblasts to obtain reliable results.

7. REFERENCES

- 1) Witte, F., Kaese, V., Haferkamp, H., Switzer, E., Meyer-Lindenberg, A., Wirth, C. and Windhagen, H., *In vivo corrosion of four magnesium alloys and the associated bone response*. *Biomaterials*, 2005. 26(17): 3557-3563.
- 2) Kraus, T., Fischerauer, S.F., Hänzi, A.C., Uggowitz, P.J., Löffler, J.F. and Weinberg, A.M., *Magnesium alloys for temporary implants in osteosynthesis: in vivo studies of their degradation and interaction with bone*. *Acta biomaterialia*, 2012. 8(3): 1230-1238.
- 3) Witte, F., *The history of biodegradable magnesium implants: a review*. *Acta biomaterialia*, 2010. 6(5): 1680-1692.
- 4) Zartner, P., Cesnjevar, R., Singer, H. and Weyand, M., *First successful implantation of a biodegradable metal stent into the left pulmonary artery of a preterm baby*. *Catheterization and Cardiovascular Interventions*, 2005. 66(4): 590-594.
- 5) Erbel, R., Di Mario, C., Bartunek, J., Bonnier, J., de Bruyne, B., Eberli, F.R., Erne, P., Haude, M., Heublein, B. and Horrigan, M., *Temporary scaffolding of coronary arteries with bioabsorbable magnesium stents: a prospective, non-randomised multicentre trial*. *The Lancet*, 2007. 369(9576): 1869-1875.
- 6) Windhagen, H., Radtke, K., Weizbauer, A., Diekmann, J., Noll, Y., Kreimeyer, U., Schavan, R., Stukenborg-Colsman, C. and Waizy, H., *Biodegradable magnesium-based screw clinically equivalent to titanium screw in hallux valgus surgery: short term results of the first prospective, randomized, controlled clinical pilot study*. *Biomed Eng Online*, 2013. 12: 62.
- 7) Lensing, R., Behrens, P., Müller, P.P., Lenarz, T. and Stieve, M., *In vivo testing of a bioabsorbable magnesium alloy serving as total ossicular replacement prostheses*. *Journal of biomaterials applications*, 2014. 28(5): 688-696.
- 8) Staiger, M.P., Pietak, A.M., Huadmai, J. and Dias, G., *Magnesium and its alloys as orthopedic biomaterials: a review*. *Biomaterials*, 2006. 27(9): 1728-1734.

- 9) Wolf, F.I. and Cittadini, A., *Chemistry and biochemistry of magnesium*. Molecular aspects of medicine, 2003. 24(1): 3-9.
- 10) Seuss, F., Seuss, S., Turhan, M., Fabry, B. and Virtanen, S., *Corrosion of Mg alloy AZ91D in the presence of living cells*. Journal of Biomedical Materials Research Part B: Applied Biomaterials, 2011. 99(2): 276-281.
- 11) Wolf, F.I. and Cittadini, A., *Magnesium in cell proliferation and differentiation*. Front Biosci, 1999. 4: D607-617.
- 12) Yamamoto, A. and Hiromoto, S., *Effect of inorganic salts, amino acids and proteins on the degradation of pure magnesium in vitro*. Materials Science and Engineering: C, 2009. 29(5): 1559-1568.
- 13) Kanczler, J. and Oreffo, R., *Osteogenesis and angiogenesis: the potential for engineering bone*. Eur Cell Mater, 2008. 15(2): 100-114.
- 14) Karsenty, G., *Transcriptional regulation of osteoblast differentiation during development*. Front Biosci, 1998. 3: 834-837.
- 15) Stein, G.S., Lian, J.B. and Owen, T.A., *Relationship of cell growth to the regulation of tissue-specific gene expression during osteoblast differentiation*. The FASEB journal, 1990. 4(13): 3111-3123.
- 16) Lian, J.B. and Stein, G.S., *Concepts of osteoblast growth and differentiation: basis for modulation of bone cell development and tissue formation*. Critical Reviews in Oral Biology & Medicine, 1992. 3(3): 269-305.
- 17) Dougall, W.C., Glaccum, M., Charrier, K., Rohrbach, K., Brasel, K., De Smedt, T., Daro, E., Smith, J., Tometsko, M.E. and Maliszewski, C.R., *RANK is essential for osteoclast and lymph node development*. Genes & development, 1999. 13(18): 2412-2424.
- 18) Katakura, Y., Alam, S. and Shirahata, S., *Immortalization by gene transfection*. Methods Cell Biol, 1998. 57(1): 69.

- 19) Moran, E., *Interaction of adenoviral proteins with pRB and p53*. The FASEB journal, 1993. 7(10): 880-885.
- 20) Lincks, J., Boyan, B., Blanchard, C., Lohmann, C., Liu, Y., Cochran, D., Dean, D. and Schwartz, Z., *Response of MG63 osteoblast-like cells to titanium and titanium alloy is dependent on surface roughness and composition*. Biomaterials, 1998. 19(23): 2219-2232.
- 21) Cenni, E., Granchi, D., Ciapetti, G., Stea, S., Savarino, L. and Corradini, A., *Interleukin-6 expression by osteoblast-like MG63 cells challenged with four acrylic bone cements*. Journal of Biomaterials Science, Polymer Edition, 2001. 12(2): 243-253.
- 22) Xu, P., Liang, J., Dong, G., Zheng, L. and Ye, L., *Cytotoxicity of RealSeal on human osteoblast-like MG63 cells*. Journal of endodontics, 2010. 36(1): 40-44.
- 23) Bethesda, M., *PubMed Help [Internet]*. 2005-: National Center for Biotechnology Information (US). Available from: <http://www.ncbi.nlm.nih.gov/books/NBK3827/>.
- 24) Bodnar, A.G., Ouellette, M., Frolkis, M., Holt, S.E., Chiu, C.-P., Morin, G.B., Harley, C.B., Shay, J.W., Lichtsteiner, S. and Wright, W.E., *Extension of life-span by introduction of telomerase into normal human cells*. Science, 1998. 279(5349): 349-352.
- 25) Hasegawa, T., Hirose, T., Kudo, E., Hizawa, K., Usui, M. and Ishii, S., *Immunophenotypic heterogeneity in osteosarcomas*. Human pathology, 1991. 22(6): 583-590.
- 26) Pautke, C., Schieker, M., Tischer, T., Kolk, A., Neth, P., Mutschler, W. and Milz, S., *Characterization of osteosarcoma cell lines MG-63, Saos-2 and U-2 OS in comparison to human osteoblasts*. Anticancer research, 2004. 24(6): 3743-3748.
- 27) Isfort, R.J., Cody, D.B., Lovell, G. and Doersen, C.J., *Analysis of oncogenes, tumor suppressor genes, autocrine growth-factor production, and differentiation state of human osteosarcoma cell lines*. Molecular carcinogenesis, 1995. 14(3): 170-178.

- 28) Orimo, H., Goseki-Sone, M., Hosoi, T. and Shimada, T., *Functional assay of the mutant tissue-nonspecific alkaline phosphatase gene using U2OS osteoblast-like cells*. Molecular genetics and metabolism, 2008. 94(3): 375-381.
- 29) Niforou, K.N., Anagnostopoulos, A.K., Vougas, K., Kittas, C., Gorgoulis, V.G. and Tsangaris, G.T., *The proteome profile of the human osteosarcoma U2OS cell line*. Cancer Genomics-Proteomics, 2008. 5(1): 63-77.
- 30) Torricelli, P., Fini, M., Borsari, V., Lenger, H., Bernauer, J., Tschon, M., Bonazzi, V. and Giardino, R., *Biomaterials in orthopedic surgery: effects of a nickel-reduced stainless steel on in vitro proliferation and activation of human osteoblasts*. The International journal of artificial organs, 2003. 26(10): 952-957.
- 31) Wang, Y., Xie, X., Li, H., Wang, X., Zhao, M., Zhang, E., Bai, Y., Zheng, Y. and Qin, L., *Biodegradable CaMgZn bulk metallic glass for potential skeletal application*. Acta biomaterialia, 2011. 7(8): 3196-3208.
- 32) Zomorodian, A., Garcia, M., Moura e Silva, T., Fernandes, J., Fernandes, M. and Montemor, M., *Corrosion resistance of a composite polymeric coating applied on biodegradable AZ31 magnesium alloy*. Acta biomaterialia, 2013. 9(10): 8660-8670.
- 33) Krüger, R., Seitz, J.-M., Ewald, A., Bach, F.-W. and Groll, J., *Strong and tough magnesium wire reinforced phosphate cement composites for load-bearing bone replacement*. Journal of the mechanical behavior of biomedical materials, 2013. 20: 36-44.
- 34) Dedhar, S., Mitchell, M.D. and Pierschbacher, M.D., *The osteoblast-like differentiated phenotype of a variant of MG-63 osteosarcoma cell line correlated with altered adhesive properties*. Connective tissue research, 1989. 20(1-4): 49-61.
- 35) Billiau, A., Edy, V., Heremans, H., Van Damme, J., Desmyter, J., Georgiades, J. and De Somer, P., *Human interferon: mass production in a newly established cell line, MG-63*. Antimicrobial agents and chemotherapy, 1977. 12(1): 11-15.

- 36) Pangalos, M., Bintig, W., Schlingmann, B., Feyerabend, F., Witte, F., Begandt, D., Heisterkamp, A. and Ngezahayo, A., *Action potentials in primary osteoblasts and in the MG-63 osteoblast-like cell line*. Journal of bioenergetics and biomembranes, 2011. 43(3): 311-322.
- 37) Bilbe, G., Roberts, E., Birch, M. and Evans, D., *PCR phenotyping of cytokines, growth factors and their receptors and bone matrix proteins in human osteoblast-like cell lines*. Bone, 1996. 19(5): 437-445.
- 38) Czekanska, E.M., Stoddart, M.J., Ralphs, J.R., Richards, R.G. and Hayes, J.S., *A phenotypic comparison of osteoblast cell lines versus human primary osteoblasts for biomaterials testing*. Journal of Biomedical Materials Research Part A, 2014. 102(8): 2636-2643.
- 39) Yu, Y., Harris, R.I., Yang, J.-L., Anderson, H.C. and Walsh, W.R., *Differential expression of osteogenic factors associated with osteoinductivity of human osteosarcoma cell lines*. Journal of Biomedical Materials Research Part A, 2004. 70(1): 122-128.
- 40) Elin, R., *Assessment of magnesium status*. Clinical chemistry, 1987. 33(11): 1965-1970.
- 41) Moe, S.M., *Disorders involving calcium, phosphorus, and magnesium*. Primary Care: Clinics in Office Practice, 2008. 35(2): 215-237.
- 42) Bohl, C.H. and Volpe, S.L., *Magnesium and exercise*. Critical reviews in food science and nutrition, 2002. 42(6): 533-563.
- 43) Martindale, L. and Heaton, F., *Magnesium deficiency in the adult rat*. Biochemical Journal, 1964. 92(1): 119-126.
- 44) Swaminathan, R., *Magnesium metabolism and its disorders*. The Clinical Biochemist Reviews, 2003. 24(2): 47-66.
- 45) Jahnen-Dechent, W. and Ketteler, M., *Magnesium basics*. Clinical kidney journal, 2012. 5(Suppl 1): i3-14.

- 46) Noronha, L. and Matuschak, G., *Magnesium in critical illness: metabolism, assessment, and treatment*. Intensive Care Medicine, 2002. 28(6): 667-679.
- 47) Paul, W. and Sharma, C.P., *Effect of calcium, zinc and magnesium on the attachment and spreading of osteoblast like cells onto ceramic matrices*. Journal of Materials Science: Materials in Medicine, 2007. 18(5): 699-703.
- 48) Patterson, K.C., Yang, R., Zeng, B., Song, B., Wang, S., Xi, N. and Basson, M.D., *Measurement of cationic and intracellular modulation of integrin binding affinity by AFM-based nanorobot*. Biophysical journal, 2013. 105(1): 40-47.
- 49) Fuhrmann, A., Li, J., Chien, S. and Engler, A.J., *Cation Type Specific Cell Remodeling Regulates Attachment Strength*. PloS one, 2014. 9(7): e102424.
- 50) Gilmore, A.P. and Burridge, K., *Molecular mechanisms for focal adhesion assembly through regulation of protein-protein interactions*. Structure, 1996. 4(6): 647-651.
- 51) Cary, L.A., Chang, J.F. and Guan, J.-L., *Stimulation of cell migration by overexpression of focal adhesion kinase and its association with Src and Fyn*. Journal of cell science, 1996. 109(7): 1787-1794.
- 52) Hammerschmidt, M. and Wedlich, D., *Regulated adhesion as a driving force of gastrulation movements*. Development, 2008. 135(22): 3625-3641.
- 53) Zebda, N., Dubrovskiy, O. and Birukov, K.G., *Focal adhesion kinase regulation of mechanotransduction and its impact on endothelial cell functions*. Microvascular research, 2012. 83(1): 71-81.
- 54) Porter, R.S., *The Merck Manual of Diagnosis and Therapy, 19th Edition*. 2011: Whitehouse Station, NJ. 949-986.
- 55) Rude, R., Gruber, H., Wei, L., Frausto, A. and Mills, B., *Magnesium deficiency: effect on bone and mineral metabolism in the mouse*. Calcified tissue international, 2003. 72(1): 32-41.

- 56) Whang, R., Oei, T.O. and Watanabe, A., *Frequency of hypomagnesemia in hospitalized patients receiving digitalis*. Archives of internal medicine, 1985. 145(4): 655-656.
- 57) Gruber, H.E., Rude, R.K., Wei, L., Frausto, A., Mills, B.G. and Norton, H.J., *Magnesium deficiency: effect on bone mineral density in the mouse appendicular skeleton*. BMC musculoskeletal disorders, 2003. 4(1): 7.
- 58) Rude, R.K., Gruber, H.E., Wei, L.Y. and Frausto, A., *Immunolocalization of RANKL is increased and OPG decreased during dietary magnesium deficiency in the rat*. Nutrition & metabolism, 2005. 2(1): 24.
- 59) Saggese, G., Bertelloni, S., Baroncelli, G., Federico, G., Calisti, L. and Fusaro, C., *Bone demineralization and impaired mineral metabolism in insulin-dependent diabetes mellitus. A possible role of magnesium deficiency*. Helvetica paediatrica acta, 1989. 43(5-6): 405-414.
- 60) Zofková, I. and Kancheva, R., *The relationship between magnesium and calciotropic hormones*. Magnesium research: official organ of the International Society for the Development of Research on Magnesium, 1995. 8(1): 77-84.
- 61) Carpenter, T., *Disturbances of vitamin D metabolism and action during clinical and experimental magnesium deficiency*. Magnesium research: official organ of the International Society for the Development of Research on Magnesium, 1988. 1(3-4): 131-139.
- 62) Castiglioni, S., Cazzaniga, A., Albisetti, W. and Maier, J.A., *Magnesium and osteoporosis: current state of knowledge and future research directions*. Nutrients, 2013. 5(8): 3022-3033.
- 63) Belluci, M.M., Schoenmaker, T., Rossa-Junior, C., Orrico, S.R., de Vries, T.J. and Everts, V., *Magnesium deficiency results in an increased formation of osteoclasts*. The Journal of nutritional biochemistry, 2013. 24(8): 1488-1498.
- 64) Seo, J.W. and Park, T.J., *Magnesium metabolism*. Electrolyte & Blood Pressure, 2008. 6(2): 86-95.

- 65) Rozen, S. and Skaletsky, H., *Primer3 on the WWW for general users and for biologist programmers*, Krawetz, S. and Misener, S., 2000: Humana Press. New Jersey, Clifton, N.J. 365-386.
- 66) Kamata, N., Fujimoto, R., Tomonari, M., Taki, M., Nagayama, M. and Yasumoto, S., *Immortalization of human dental papilla, dental pulp, periodontal ligament cells and gingival fibroblasts by telomerase reverse transcriptase*. *Journal of oral pathology & medicine*, 2004. 33(7): 417-423.
- 67) Smith, P.N., Freeman, C., Yu, D., Chen, M., Gatenby, P.A., Parish, C.R. and Li, R.W., *Heparanase in primary human osteoblasts*. *Journal of orthopaedic research*, 2010. 28(10): 1315-1322.
- 68) Maddi, A., Hai, H., Ong, S.-T., Sharp, L., Harris, M. and Meghji, S., *Long wave ultrasound may enhance bone regeneration by altering OPG/RANKL ratio in human osteoblast-like cells*. *Bone*, 2006. 39(2): 283-288.
- 69) Mauney, J.R., Blumberg, J., Pirun, M., Volloch, V., Vunjak-Novakovic, G. and Kaplan, D.L., *Osteogenic differentiation of human bone marrow stromal cells on partially demineralized bone scaffolds in vitro*. *Tissue engineering*, 2004. 10(1-2): 81-92.
- 70) Gallagher, J.A., *Human osteoblast culture*. *Methods in molecular medicine*, 2003. 80: 3-18.
- 71) Kim, T.-K., Sharma, B., Williams, C., Ruffner, M., Malik, A., McFarland, E. and Elisseeff, J., *Experimental model for cartilage tissue engineering to regenerate the zonal organization of articular cartilage*. *Osteoarthritis and Cartilage*, 2003. 11(9): 653-664.
- 72) Koch, F.P., Merkel, C., Ziebart, T., Smeets, R., Walter, C. and Al-Nawas, B., *Influence of bisphosphonates on the osteoblast RANKL and OPG gene expression in vitro*. *Clinical oral investigations*, 2012. 16(1): 79-86.

- 73) Fischer, J., Pröfrock, D., Hort, N., Willumeit, R. and Feyerabend, F., *Improved cytotoxicity testing of magnesium materials*. Materials Science and Engineering: B, 2011. 176(20): 1773-1777.
- 74) Tan, S.C., Carr, C.A., Yeoh, K.K., Schofield, C.J., Davies, K.E. and Clarke, K., *Identification of valid housekeeping genes for quantitative RT-PCR analysis of cardiosphere-derived cells preconditioned under hypoxia or with prolyl-4-hydroxylase inhibitors*. Molecular biology reports, 2012. 39(4): 4857-4867.
- 75) Klose, J. and Kobalz, U., *Two-dimensional electrophoresis of proteins: an updated protocol and implications for a functional analysis of the genome*. Electrophoresis, 1995. 16(1): 1034-1059.
- 76) Zimny-Arndt, U., Schmid, M., Ackermann, R. and Jungblut, P.R., *Classical proteomics: two-dimensional electrophoresis/MALDI mass spectrometry*, 2009: Humana Press. Totowa, NJ. 65-91.
- 77) Meganathan, K., Jagtap, S., Wagh, V., Winkler, J., Gaspar, J.A., Hildebrand, D., Trusch, M., Lehmann, K., Hescheler, J. and Schlüter, H., *Identification of thalidomide-specific transcriptomics and proteomics signatures during differentiation of human embryonic stem cells*. PloS one, 2012. 7(8): e44228.
- 78) Consortium, U., *UniProt: a hub for protein information*. Nucleic Acids Research, 2014. gku989.
- 79) Burmester, A., Luthringer, B., Willumeit, R. and Feyerabend, F., *Comparison of the reaction of bone-derived cells to enhanced MgCl₂-salt concentrations*. Biomatter, 2014. 4(1): e967616.
- 80) Bacáková, L., Filova, E., Rypáček, F., Svorčík, V. and Starý, V., *Cell adhesion on artificial materials for tissue engineering*. Physiol Res, 2004. 53(Suppl 1): 35-45.

- 81) Willumeit, R., Fischer, J., Feyerabend, F., Hort, N., Bismayer, U., Heidrich, S. and Mihailova, B., *Chemical surface alteration of biodegradable magnesium exposed to corrosion media*. Acta biomaterialia, 2011. 7(6): 2704-2715.
- 82) Burmester, A., Willumeit-Römer, R. and Feyerabend, F., *Behavior of bone cells in contact with magnesium implant material*. Journal of Biomedical Materials Research Part B: Applied Biomaterials, 2015.
- 83) Zreiqat, H., Howlett, C., Zannettino, A., Evans, P., Schulze-Tanzil, G., Knabe, C. and Shakibaei, M., *Mechanisms of magnesium-stimulated adhesion of osteoblastic cells to commonly used orthopaedic implants*. Journal of biomedical materials research, 2002. 62(2): 175-184.
- 84) Nieves, J.W., *Osteoporosis: the role of micronutrients*. The American journal of clinical nutrition, 2005. 81(5): 1232S-1239S.
- 85) Zeng, R.-C., Qi, W.-C., Zhang, F. and Li, S.-Q., *In vitro corrosion of pure magnesium and AZ91 alloy-the influence of thin electrolyte layer thickness*. Regenerative Biomaterials, 2016. 3(1): 49-56.
- 86) Song, G.L. and Atrens, A., *Corrosion mechanisms of magnesium alloys*. Advanced engineering materials, 1999. 1(1): 11-33.
- 87) Kirkland, N. and Birbilis N., *Magnesium Biomaterials: Design, Testing, and Best Practice*. 2014: Heidelberg, Springer International Publishing, 54.
- 88) Ivarsson, M., Noh, H., Morbidelli, M. and Soos, M., *Insights into pH-induced metabolic switch by flux balance analysis*. Biotechnology Progress, 2015. 31(2): 347-357.
- 89) Feyerabend, F., Drücker, H., Laipple, D., Vogt, C., Stekker, M., Hort, N. and Willumeit, R., *Ion release from magnesium materials in physiological solutions under different oxygen tensions*. Journal of Materials Science: Materials in Medicine, 2012. 23(1): 9-24.

- 90) Tsau, J.-L., Guffanti, A.A. and Montville, T.J., *Conversion of pyruvate to acetoin helps to maintain pH homeostasis in Lactobacillus plantarum*. Applied and environmental microbiology, 1992. 58(3): 891-894.
- 91) Lian, J.B. and Stein, G.S., *Development of the osteoblast phenotype: molecular mechanisms mediating osteoblast growth and differentiation*. The Iowa orthopaedic journal, 1995. 15: 118-140.
- 92) Feyerabend, F., Witte, F., Kammal, M. and Willumeit, R., *Unphysiologically high magnesium concentrations support chondrocyte proliferation and redifferentiation*. Tissue engineering, 2006. 12(12): 3545-3556.
- 93) Feyerabend, F., Fischer, J., Holtz, J., Witte, F., Willumeit, R., Drücker, H., Vogt, C. and Hort, N., *Evaluation of short-term effects of rare earth and other elements used in magnesium alloys on primary cells and cell lines*. Acta biomaterialia, 2010. 6(5): 1834-1842.
- 94) Sgambato, A., Wolf, F.I., Faraglia, B. and Cittadini, A., *Magnesium depletion causes growth inhibition, reduced expression of cyclin D1, and increased expression of P27Kip1 in normal but not in transformed mammary epithelial cells*. Journal of cellular physiology, 1999. 180(2): 245-254.
- 95) Willbold, E., Kalla, K., Bartsch, I., Bobe, K., Brauneis, M., Remennik, S., Shechtman, D., Nellesen, J., Tillmann, W. and Vogt, C., *Biocompatibility of rapidly solidified magnesium alloy RS66 as a temporary biodegradable metal*. Acta biomaterialia, 2013. 9(10): 8509-8517.
- 96) Weizbauer, A., Kieke, M., Rahim, M.I., Angrisani, G.L., Willbold, E., Diekmann, J., Flörkemeier, T., Windhagen, H., Müller, P.P., Behrens, P. and Budde, S., *Magnesium-containing layered double hydroxides as orthopaedic implant coating materials-An in vitro and in vivo study*. Journal of Biomedical Materials Research Part B: Applied Biomaterials, 2016. 104(3): 525-531.
- 97) Iskandar, M.E., Aslani, A., Tian, Q. and Liu, H., *Nanostructured calcium phosphate coatings on magnesium alloys: characterization and cytocompatibility with mesenchymal stem cells*. Journal of Materials Science: Materials in Medicine, 2015. 26(5): 1-18.

- 98) Anselme, K. and Bigerelle, M., *Topography effects of pure titanium substrates on human osteoblast long-term adhesion*. Acta biomaterialia, 2005. 1(2): 211-222.
- 99) Nguyen, T.Y., Liew, C.G. and Liu, H., *An in vitro mechanism study on the proliferation and pluripotency of human embryonic stems cells in response to magnesium degradation*. PloS one, 2013. 8(10): e76547.
- 100) Adkisson, H.D., Strauss-Schoenberger, J., Gillis, M., Wilkins, R., Jackson, M. and Hruska, K.A., *Rapid quantitative bioassay of osteoinduction*. Journal of orthopaedic research, 2000. 18(3): 503-511.
- 101) Watts, N.B., *Clinical utility of biochemical markers of bone remodeling*. Clinical chemistry, 1999. 45(8): 1359-1368.
- 102) Anselme, K., *Osteoblast adhesion on biomaterials*. Biomaterials, 2000. 21(7): 667-681.
- 103) Anselme, K., Bigerelle, M., Noel, B., Dufresne, E., Judas, D., Iost, A. and Hardouin, P., *Qualitative and quantitative study of human osteoblast adhesion on materials with various surface roughnesses*. Journal of biomedical materials research, 2000. 49(2): 155-166.
- 104) Anselme, K., Linez, P., Bigerelle, M., Le Maguer, D., Le Maguer, A., Hardouin, P., Hildebrand, H., Iost, A. and Leroy, J., *The relative influence of the topography and chemistry of TiAl6V4 surfaces on osteoblastic cell behaviour*. Biomaterials, 2000. 21(15): 1567-1577.
- 105) Arnett, T., *Regulation of bone cell function by acid-base balance*. Proceedings of the Nutrition Society, 2003. 62(02): 511-520.
- 106) Erlebacher, A., Filvaroff, E.H., Gitelman, S.E. and Derynck, R., *Toward a molecular understanding of skeletal development*. cell, 1995. 80(3): 371-378.
- 107) Zreiqat, H., Evans, P. and Howlett, C.R., *Effect of surface chemical modification of bioceramic on phenotype of human bone-derived cells*. Journal of biomedical materials research, 1999. 44(4): 389-396.

- 108) Gronowicz, G. and McCarthy, M., *Response of human osteoblasts to implant materials: Integrin-mediated adhesion*. Journal of orthopaedic research, 1996. 14(6): 878-887.
- 109) Stuiver, I., Ruggeri, Z. and Smith, J.W., *Divalent cations regulate the organization of integrins alpha v beta 3 and alpha v beta 5 on the cell surface*. Journal of cellular physiology, 1996. 168(3): 521-531.
- 110) Goto, T., Yoshinari, M., Kobayashi, S. and Tanaka, T., *The initial attachment and subsequent behavior of osteoblastic cells and oral epithelial cells on titanium*. Bio-medical materials and engineering, 2004. 14(4): 537-544.
- 111) Weinreb, M., Shinar, D. and Rodan, G.A., *Different pattern of alkaline phosphatase, osteopontin, and osteocalcin expression in developing rat bone visualized by in situ hybridization*. Journal of Bone and Mineral Research, 1990. 5(8): 831-842.
- 112) Bianco, P., Fisher, L.W., Young, M.F., Termine, J.D. and Robey, P.G., *Expression of bone sialoprotein (BSP) in developing human tissues*. Calcified tissue international, 1991. 49(6): 421-426.
- 113) Hauschka, P.V., Lian, J.B., Cole, D. and Gundberg, C.M., *Osteocalcin and matrix Gla protein: vitamin K-dependent proteins in bone*. Physiol Rev, 1989. 69(3): 990-1047.
- 114) Sodek, J., Chen, J., Nagata, T., Kasugai, S., Todescan, R., Li, I.W. and Kim, R.H., *Regulation of osteopontin expression in osteoblasts*. Annals of the New York Academy of Sciences, 1995. 760(1): 223-241.
- 115) Van der Rest, M. and Garrone, R., *Collagen family of proteins*. The FASEB journal, 1991. 5(13): 2814-2823.
- 116) Goldschmidt, O., Zcharia, E., Cohen, M., Aingorn, H., Cohen, I., Nadav, L., Katz, B.Z., Geiger, B. and Vlodavsky, I., *Heparanase mediates cell adhesion independent of its enzymatic activity*. The FASEB journal, 2003. 17(9): 1015-1025.

117) Kohli, S.S. and Kohli, V.S., *Role of RANKL-RANK/osteoprotegerin molecular complex in bone remodeling and its immunopathologic implications*. Indian journal of endocrinology and metabolism, 2011. 15(3): 175.

118) Lacey, D., Timms, E., Tan, H.-L., Kelley, M., Dunstan, C., Burgess, T., Elliott, R., Colombero, A., Elliott, G. and Scully, S., *Osteoprotegerin ligand is a cytokine that regulates osteoclast differentiation and activation*. cell, 1998. 93(2): 165-176.

119) Bae, Y.J. and Kim, M.-H., *Calcium and magnesium supplementation improves serum OPG/RANKL in calcium-deficient ovariectomized rats*. Calcified tissue international, 2010. 87(4): 365-372.

120) Leem, Y.H., Lee, K.S., Kim, J.H., Seok, H.K., Chang, J.S. and Lee, D.H., *Magnesium ions facilitate integrin alpha 2- • and alpha 3- • mediated proliferation and enhance alkaline phosphatase expression and activity in hBMSCs*. Journal of tissue engineering and regenerative medicine, 2014.

121) Czekanska, E., Stoddart, M., Richards, R. and Hayes, J., *In search of an osteoblast cell model for in vitro research*. Eur Cell Mater, 2012. 24(4): 1-17.

122) Tat, S.K., Pelletier, J.-P., Velasco, C.R., Padrines, M. and Martel-Pelletier, J., *New perspective in osteoarthritis: the OPG and RANKL system as a potential therapeutic target?* The Keio journal of medicine, 2009. 58(1): 29-40.

123) Yoshizawa, S., Brown, A., Barchowsky, A. and Sfeir, C., *Magnesium ion stimulation of bone marrow stromal cells enhances osteogenic activity, simulating the effect of magnesium alloy degradation*. Acta biomaterialia, 2014. 10(6): 2834-2842.

124) Fong, J. and Khan, A., *Hypocalcemia Updates in diagnosis and management for primary care*. Canadian Family Physician, 2012. 58(2): 158-162.

125) Otey, C.A. and Carpen, O., *Alpha-actinin revisited: A fresh look at an old player*. Cell motility and the cytoskeleton, 2004. 58(2): 104-111.

- 126) Parente, L. and Solito, E., *Annexin I: more than an anti-phospholipase protein*. Inflammation Research, 2004. 53(4): 125-132.
- 127) Genetos, D.C., Wong, A., Weber, T.J., Karin, N.J. and Yellowley, C.E., *Impaired Osteoblast Differentiation in Annexin A2- and -A5-Deficient Cells*. PloS one, 2014. 9(9): e107482.
- 128) Mohiti, J., Caswell, A. and Walkert, J., *Calcium-induced relocation of annexins IV and V in the human osteosarcoma cell line MG-63*. Molecular membrane biology, 1995. 12(4): 321-329.
- 129) Hoorn, E.J. and Zietse, R., *Disorders of calcium and magnesium balance: a physiology-based approach*. Pediatric Nephrology, 2013. 28(8): 1195-1206.
- 130) Loones, M.T. and Morange, M., *Hsp and chaperone distribution during endochondral bone development in mouse embryo*. Cell stress & chaperones, 1998. 3(4): 237-244.
- 131) Buss, F., Kendrick-Jones, J., Lionne, C., Knight, A.E., Côté, G.P. and Luzio, J.P., *The localization of myosin VI at the Golgi complex and leading edge of fibroblasts and its phosphorylation and recruitment into membrane ruffles of A431 cells after growth factor stimulation*. The Journal of cell biology, 1998. 143(6): 1535-1545.
- 132) Yagi, T. and Takeichi, M., *Cadherin superfamily genes: functions, genomic organization, and neurologic diversity*. Genes & development, 2000. 14(10): 1169-1180.
- 133) Papiha, S., Allcroft, L., Kanan, R., Francis, R. and Datta, H., *Vitamin D binding protein gene in male osteoporosis: association of plasma DBP and bone mineral density with (TAAA) n-Alu polymorphism in DBP*. Calcified tissue international, 1999. 65(4): 262-266.
- 134) Bhan, I., *Vitamin D Binding Protein and Bone Health*. International journal of endocrinology, 2014.

135) Li, W., Zhu, S. and Hu, J., *Bone Regeneration Is Promoted by Orally Administered Bovine Lactoferrin in a Rabbit Tibial Distraction Osteogenesis Model*. *Clinical Orthopaedics and Related Research*, 2015. 473(7): 2383-2393.

8. ABBREVIATIONS

ACTN1	alpha-actinin-1
ALP	alkaline phosphatase
ANXA1	annexin A1
ANXA2	annexin A2
ANXA4	annexin A4
Ar	argon
BSA	bovine serum albumin
BSP	bone sialoprotein
Ca	calcium
Cbfa1	runt-related transcription factor 2
cDNA	complementary deoxyribonucleic acid
Cl	chloride
Cl ⁻	chloride ion
Col	collagen
CO ₂	carbon dioxide
DAPI	4,6-diamidino-2-phenylindole dihydrochloride
dATP	deoxyadenosine triphosphate
dCTP	deoxycytidine triphosphate
dGTP	deoxyguanosine triphosphate
dTTP	deoxythymidine triphosphate
ddH ₂ O	double-distilled water
diff	differentiated
DMEM	Dulbecco's Modified Eagle Medium
DNA	deoxyribonucleic acid
DTT	dithiothreitol
EDTA	ethylenediamine tetraacetic acid
FA	focal adhesion
FBS	foetal bovine serum
Fig.	Figure
FITC	fluorescein isothiocyanate
GAPDH	glyceraldehyde-3-phosphate dehydrogenase
HPSE	heparanase
HPLC	high-performance liquid chromatography

HSP90B1	endoplasmic
IAA solution	iodoacetamide solution
IEF	isoelectric focusing
KCl	potassium chloride
KH ₂ PO ₄	potassium dihydrogen phosphate
L-AA	L-ascorbic acid
LC	liquid chromatography
LC/MS	liquid chromatography–mass spectrometry
MagIC	Magnesium Innovation Center
M-CSF	macrophage colony-stimulating factor
Mg	magnesium
Mg ²⁺	magnesium ion
MgCl ₂	magnesium chloride
Mg(OH) ₂	magnesium hydroxide
MS	mass spectrometry
MS-H ₂ O	water for mass spectrometry
MS/MS	tandem mass spectrometry
MYL6	myosin light chain 6B
NaCl	sodium chloride
Na ₂ HPO ₄	disodium hydrogen phosphate
NH ₄ HCO ₃	ammonium bicarbonate
OB	osteoblast
OC	osteocalcin
OPG	osteoprotegerin
OPN	osteopontin
PBS	phosphate-buffered saline
PCDHA1	protocadherin alpha-1
PCR	polymerase chain reaction
qPCR	real-time polymerase chain reaction
RNA	ribonucleic acid
ROI	region of interest
RANK	receptor Activator of NF-κB
RANKL	receptor Activator of NF-κB ligand
TexasRed	sulforhodamine 101 acid chloride

8. Abbreviations

Ti	titanium
Tris	tris(hydroxymethyl)aminomethane
Vit-D3	1 α ,25 dihydroxyvitamin D3
v/v	volume per volume
w/v	weight per volume
2-D	two-dimensional
β -GP	β -glycerolphosphate

9. LIST OF TABLES

Table 1. Mechanical properties of bone and biomaterials.	1
Table 2. Applied media and their compositions. DMEM GlutaMAX was used for primary human osteoblasts and MG63 cells, DMEM was used for U2OS cells and McCoy's 5A was used for SaoS2 cells.	8
Table 3. Reverse transcription-PCR (RT-PCR) primer sequences.	9
Table 4. Real-time PCR (qPCR) primer sequences.	10
Table 5. Cell culture conditions for different exposure conditions.	12
Table 6. Initial cell counts for the various proliferation experiments.	13
Table 7. CASY Model TT adjustments for different cell types.	13
Table 8. Fluorescent microscope filters and the corresponding spectra.	13
Table 9. Cell dimensions in μm of adherent cells (length (\leftrightarrow) and width (\updownarrow)) under control conditions and proliferating cells supplemented with MgCl_2	26
Table 10. Changes in relative density (% of control) after exposure to 25 mM MgCl_2	28
Table 11. OPG/RANKL gene expression ratios examined by qPCR at different MgCl_2 concentrations.	30
Table 12. Cell dimensions in μm of adherent cells (length (\leftrightarrow) and width (\updownarrow)) under control conditions and differentiating cells (diff) supplemented with MgCl_2 (0 - 25 mM).	32
Table 13. OPG/RANKL gene expression ratios examined by qPCR at different MgCl_2 concentrations for differentiating cells.	33
Table 14. Cell culture media and corresponding extract compositions (osmolality, pH and amount of Mg in the extract) for DMEM GlutaMAX I, DMEM and McCoy's 5A.	35
Table 15. Cell dimensions in μm of adherent cells (length (\leftrightarrow) and width (\updownarrow)) under cell control conditions and after magnesium-based extract addition.	39
Table 16. OPG/RANKL gene expression ratios determined by qPCR after exposure to magnesium-based extract for 1 and 2 weeks (OB 4 weeks).	41
Table 17. Cell dimensions in μm of adherent cells (length (\leftrightarrow) and width (\updownarrow)) under cell control conditions and after extract addition supplemented with differentiating medium (extract diff).	43
Table 18. Cell dimensions in μm of adherent cells (length (\leftrightarrow) and width (\updownarrow)) under cell control conditions and on titanium and pure magnesium samples. The mean values and standard deviations are presented].	47
Table 19. Vinculin particle counts for the control, titanium and pure magnesium samples after exposure of primary human osteoblasts for 1 day, 3 days, 1 week and 2 weeks.	48

Table 20. OPG/RANKL gene expression ratios determined by qPCR after exposure to titanium (Ti) and pure magnesium (Mg)..... 51

10. LIST OF FIGURES

Figure 1. Schematic presentation of chondral ossification.	2
Figure 2. Schematic presentation of the genes involved in bone formation and resorption.	3
Figure 3. Schematic presentation of the focal adhesion complex.	5
Figure 4. Overview of cell culture conditions.	12
Figure 5. Influence of increased MgCl ₂ concentrations on the osmolality of the media.	22
Figure 6. Cell count, viability, division and proliferation rates of osteoblastic cells after MgCl ₂ addition.	23
Figure 7. Size of cells from the bone system in suspension and adherent cells.	24
Figure 8. Cell size of adherent cells from the bone system after the addition of MgCl ₂	25
Figure 9. Comparison of the gene expression of various genes involved in bone formation. .	27
Figure 10. Gene expression of genes involved in bone metabolism after the addition of MgCl ₂	29
Figure 11. Cell counts and viability of differentiating cells from the bone system incubated with MgCl ₂	30
Figure 12. Cell size of differentiating cells from the bone system incubated with MgCl ₂	31
Figure 13. Cell size of adherent differentiating cells from the bone system incubated with MgCl ₂	32
Figure 14. Gene expression of genes involved in bone metabolism in differentiating cells incubated with MgCl ₂	34
Figure 15. Differences in extract osmolalities vs. the control.	36
Figure 16. Differences in extract pH values vs. the control.	37
Figure 17. Cell count and viability of cells from the bone system after the addition of magnesium-based extracts.	38
Figure 18. Size of cells from the bone system after the addition of magnesium-based extract.	38
Figure 19. Size of adherent cells from the bone system after the addition of magnesium-based extract.	39
Figure 20. Gene expression of genes involved in bone metabolism after the addition of magnesium-based extract.	40
Figure 21. Cell counts and viability of differentiating cells from the bone system after the addition of magnesium-based extract.	41

Figure 22. Cell size of differentiating cells from the bone system after the addition of magnesium-based extract.	42
Figure 23. Size of adherent differentiating cells from the bone system after the addition of magnesium-based extract.	42
Figure 24. Gene expression of genes involved in bone metabolism in differentiating cells after the addition of magnesium-based extract.	44
Figure 25. Cell counts and viability of cells from the bone system in direct contact with the material.	46
Figure 26. Size of adherent cells from the bone system after direct contact with the material.	47
Figure 27. Focal adhesions of primary human osteoblasts.	49
Figure 28. Expression of genes involved in bone metabolism in cells after direct contact with the materials.	50
Figure 29. Merged 2-DE image of all analysed conditions with proteomics.	52
Figure 30. Overview of the locations of expressed proteins found with proteomics.	55
Figure 31. Gene expression of proteins identified with proteomics.	56
Figure 32. Influence of magnesium on genes involved in bone and matrix formation.	67
Figure 33. Influence of magnesium on main processes according to the number of regulated proteins.	72

11. APPENDIX

Appendix 1

Identified proteins analysed under different magnesium exposure conditions. The proteins are sorted alphabetically by biological function. If the protein is expressed under an examined condition, it is marked in grey.

Biological process	Protein name	Additional information	control	5 mM MgCl ₂	diff	diff + 5 mM MgCl ₂	extract	extract diff	Mg sample
1-carbon metabolism	Putative adenosylhomocysteinase 2								
A	Actin, cytoplasmic 1								
	Actin-related protein 2/3 complex subunit 1B								
	Actin-related protein 2/3 complex subunit 2								
	Actin-related protein 2/3 complex subunit 4								
	Actin-related protein 3								
	Adenylyl cyclase-associated protein 1								
	Band 4.1-like protein 2								
actin cytoskeleton organisation	Coactosin-like protein								
	Cofilin-1								
	F-actin-capping protein subunit alpha-1								
	F-actin-capping protein subunit alpha-2								
	F-actin-capping protein subunit beta								
	Filamin-A								
	Filamin-B								
	Inverted formin-2								
	Profilin-1								
actin cytoskeleton reorganisation	Src substrate cortactin								
	Fascin								
	Unconventional myosin-Ib								
actin filament bundle assembly	Alpha-actinin-4	Ca ²⁺ binding							
	Dihydropyrimidinase-related protein 3								
	Ezrin								
	LIM domain and actin-binding protein 1								
	Moesin								

Biological process	Protein name	Additional information	control	5 mM MgCl ₂	diff	diff + 5 mM MgCl ₂	extract	extract diff	Mg sample
actin filament capping	Spectrin alpha chain, non-erythrocytic 1	Ca ²⁺ binding							
	Spectrin beta chain, non-erythrocytic 1								
actin filament depolymerisation	Cofilin-2								
	Destrin								
actin filament organisation	Drebrin								
	Thymosin beta-4								
actin filament polymerisation	Gelsolin	Ca ²⁺ binding							
activation of MAPKK activity (negative regulator of osteogenesis)	14-3-3 protein beta/alpha								
actomyosin structure organisation	Calponin-3								
amino-acid biosynthesis	Phosphoserine aminotransferase								
apoptotic process	14-3-3 protein epsilon								
	14-3-3 protein eta								
	14-3-3 protein gamma								
	14-3-3 protein theta								
	14-3-3 protein zeta/delta								
	Galectin-1								
	Heme oxygenase 1								
	Inhibitor of nuclear factor kappa-B kinase-interacting protein								
	Insulin-like growth factor-binding protein 3								
	Niban-like protein 1								
	PRA1 family protein 3								
	PRKC apoptosis WT1 regulator protein								
	Programmed cell death 6-interacting protein								
	Voltage-dependent anion-selective channel protein 1								
ATP metabolic process	ATP-citrate synthase	Cofactor Mg ²⁺							
	V-type proton ATPase subunit B, brain isoform								
	Adenylate kinase isoenzyme 1								
ATP/ADP antiporter	ADP/ATP translocase 3								
B bone development	Plastin-3	Ca ²⁺ binding							
C Ca-dependent activities in ER region	Reticulocalbin-1	Ca ²⁺ binding							

Biological process	Protein name	Additional information	control	5 mM MgCl ₂	diff	diff + 5 mM MgCl ₂	extract	extract diff	Mg sample
calcium homeostasis	Nucleobindin-1	Ca ²⁺ binding							
	Nucleobindin-2	Ca ²⁺ binding							
	Sarcoplasmic/endoplasmic reticulum calcium ATPase 2	Mg ²⁺ /Ca ²⁺ binding; Mg ²⁺ -dependent							
carbohydrate metabolic process	6-phosphogluconate dehydrogenase, decarboxylating								
	6-phosphogluconolactonase								
	Aflatoxin B1 aldehyde reductase member 2								
	Citrate synthase, mitochondrial								
	Transketolase	Cofactor Mg ²⁺ /Ca ²⁺							
	Transaldolase								
cell activation	CD59 glycoprotein								
cell adhesion	Alpha-parvin								
	Integrin beta-1	Mg ²⁺ /Ca ²⁺ binding							
	Lysosome membrane protein 2								
	Myosin-9								
	PDZ and LIM domain protein 2								
	Thrombospondin-1	Ca ²⁺ binding							
	Vinculin								
	Zyxin								
	Connective tissue growth factor								
	Fibronectin								
cell differentiation	Alpha-internexin								
	Chloride intracellular channel protein 4								
	Cullin-associated NEDD8-dissociated protein 1								
	Four and a half LIM domains protein 1								
	Nucleoside diphosphate kinase A	Cofactor Mg ²⁺							
Aminopeptidase N									
cell division	Microtubule-associated protein 4								
	Septin-11								

Biological process	Protein name	Additional information	control	5 mM MgCl ₂	diff	diff + 5 mM MgCl ₂	extract	extract diff	Mg sample
	Septin-2								
	Septin-7								
	Septin-9								
	Serine/threonine-protein phosphatase PP1-gamma catalytic subunit								
	Tubulin beta chain								
	cell junction assembly	Filamin-C							
cell migration	Caldesmon								
	Coronin-1B								
	Prelamin-A/C								
	Reticulon-4								
cell proliferation	28 kDa heat- and acid-stable phosphoprotein								
	Dipeptidyl peptidase 4								
	Disabled homolog 2								
	Dynactin subunit 2								
	Glia-derived nexin								
	Guanine nucleotide-binding protein G(i) subunit alpha-2								
	Mitogen-activated protein kinase 1	Cofactor Mg ²⁺							
	Peroxiredoxin-1								
	Tumor protein D54								
	Ubiquitin carboxyl-terminal hydrolase isozyme L1								
	Annexin A1	Ca ²⁺ binding							
Annexin A7	Ca ²⁺ binding								
cell redox homeostasis	Glutaredoxin-1								
	Glutathione reductase, mitochondrial								
	Thioredoxin domain-containing protein 5								
	Thioredoxin reductase 1, cytoplasmic								
cell-cell junction assembly	Talin-1								
cellular lipid metabolic process	Isocitrate dehydrogenase [NADP] cytoplasmic	Cofactor Mg ²⁺							
	Acetyl-CoA acetyltransferase, mitochondrial								
	Enoyl-CoA hydratase, mitochondrial								
cellular metabolic process	Aconitate hydratase,								

Biological process	Protein name	Additional information	control	5 mM MgCl ₂	diff	diff + 5 mM MgCl ₂	extract	extract diff	Mg sample
	mitochondrial								
	ATP synthase subunit alpha, mitochondrial								
	ATP synthase subunit beta, mitochondrial								
	ATP synthase subunit gamma, mitochondrial								
	ATP synthase subunit O, mitochondrial								
	ATP synthase-coupling factor 6, mitochondrial								
	Cytochrome b-c1 complex subunit 1, mitochondrial								
	Cytochrome c oxidase subunit 5B, mitochondrial								
	Dihydrolipoyllysine-residue succinyltransferase component of 2-oxoglutarate dehydrogenase complex, mitochondrial								
	Electron transfer flavoprotein subunit beta								
	NADH dehydrogenase [ubiquinone] iron-sulfur protein 3, mitochondrial								
cellular protein metabolic process	Beta-galactosidase								
	Arylsulfatase A	Cofactor Ca ²⁺							
	Glucosidase 2 subunit beta	Ca ²⁺ binding							
	UPF0556 protein C19orf10								
cellular response to calcium ion	Aspartyl/asparaginyl beta-hydroxylase	Ca ²⁺ binding							
	Calcium/calmodulin-dependent protein kinase type II subunit delta	regulation of Ca ²⁺ homeostatis							
	Ras GTPase-activating-like protein IQGAP1	Ca ²⁺ binding							
cellular response to osmotic stress	Serpin B6								
cellular response to oxidative stress	Thioredoxin-dependent peroxide reductase, mitochondrial								
chromatin organisation	Histone H2B type 1-J								
	Histone H2B type 1-K								
	Histone H3.1								
	Histone H4								
collagen fibril organisation	Prolyl 4-hydroxylase								

Biological process	Protein name	Additional information	control	5 mM MgCl ₂	diff	diff + 5 mM MgCl ₂	extract	extract diff	Mg sample
	subunit alpha-1								
cytokinesis	Annexin A11	Ca ²⁺ binding							
cytoplasmic transport	Actin-related protein 2								
cytoskeleton	Cytoskeleton-associated protein 4								
cytoskeleton organisation	Calpain-2 catalytic subunit	Cofactor Ca ²⁺							
	Calponin-2	Ca ²⁺ binding							
	Palladin								
	Tropomyosin alpha-1 chain								
D degradation of ubiquitinated proteins	26S protease regulatory subunit 4								
	26S protease regulatory subunit 6A								
	26S protease regulatory subunit 7								
	26S proteasome non-ATPase regulatory subunit 3								
diaphragm development	Brain acid soluble protein 1								
DNA metabolic process	5'-nucleotidase								
DNA repair	Transitional endoplasmic reticulum ATPase								
DNA synthesis	Prohibitin								
D-ribose catabolic process	ADP-sugar pyrophosphatase	Cofactor Mg ²⁺							
E endocytosis	Prolow-density lipoprotein receptor-related protein	Ca ²⁺ binding							
	Early endosome antigen 1								
	EH domain-containing protein 1	Ca ²⁺ binding							
epithelial cell differentiation	EH domain-containing protein 2	Ca ²⁺ binding							
	Transgelin								
ethanol catabolic process	Transgelin-2								
	Alcohol dehydrogenase class-3								
exocytosis	Secernin-1								
extracellular matrix organisation	Alpha-2-macroglobulin								
	Alpha-actinin-1	Ca ²⁺ binding							
	Calpain small subunit 1	Ca ²⁺ binding							
	Calpain-1 catalytic subunit	Cofactor Ca ²⁺							
	Cathepsin B								
	Cathepsin D								
	CD44 antigen								
	Collagen alpha-1(I) chain	Ca ²⁺ binding							

Biological process	Protein name	Additional information	control	5 mM MgCl ₂	diff	diff + 5 mM MgCl ₂	extract	extract diff	Mg sample
	Collagen alpha-1(VI) chain								
	Collagen alpha-1(XII) chain								
	Collagen alpha-1(XIV) chain								
	Collagen alpha-2(I) chain	Ca ²⁺ binding							
	Collagen alpha-2(VI) chain								
	Collagen alpha-3(VI) chain								
	Galectin-3								
	Plectin								
	Procollagen galactosyltransferase 1								
	Procollagen-lysine,2-oxoglutarate 5-dioxygenase 2								
	Matrix metalloproteinase-14	Ca ²⁺ binding							
	Metalloproteinase inhibitor 1								
	Serpin H1								
F	fatty acid beta-oxidation	Delta(3,5)-Delta(2,4)-dienoyl-CoA isomerase, mitochondrial							
		Trifunctional enzyme subunit alpha, mitochondrial							
		Trifunctional enzyme subunit beta mitochondrial							
fatty acid metabolic process	Fatty acid synthase								
	Fatty acid-binding protein, heart								
	Peroxisomal multifunctional enzyme type 2								
	Prostacyclin synthase								
	Very long-chain specific acyl-CoA dehydrogenase, mitochondrial								
fatty acid transport	Aspartate aminotransferase, mitochondrial								
focal adhesion assembly	Protein S100-A10	Ca ²⁺ binding							
	Thy-1 membrane glycoprotein								
G	glucose metabolic process	1,4-alpha-glucan-branching enzyme							
		6-phosphofructokinase type C	Cofactor Mg ²⁺						
		Alcohol dehydrogenase [NADP(+)]							

Biological process	Protein name	Additional information	control	5 mM MgCl ₂	diff	diff + 5 mM MgCl ₂	extract	extract diff	Mg sample
	Alpha-enolase	Cofactor Mg ²⁺							
	Fructose-bisphosphate aldolase A								
	Fructose-bisphosphate aldolase C								
	Glucose-6-phosphate 1-dehydrogenase								
	Glucose-6-phosphate isomerase								
	Glyceraldehyde-3-phosphate dehydrogenase								
	Glycogen phosphorylase, brain form								
	Glycogen phosphorylase, liver form								
	Hexokinase-1								
	L-lactate dehydrogenase A chain								
	L-lactate dehydrogenase B chain								
	Lysosomal alpha-glucosidase								
	Malate dehydrogenase, cytoplasmic								
	Malate dehydrogenase, mitochondrial								
	Phosphoglucomutase-1	Cofactor Mg ²⁺							
	Phosphoglycerate kinase 1								
	Phosphoglycerate mutase 1								
	Pyruvate dehydrogenase E1 component subunit beta, mitochondrial								
	Pyruvate kinase PKM	Cofactor Mg ²⁺							
	UTP-glucose-1-phosphate uridylyltransferase								
H	hyaluronan metabolic process	Inter-alpha-trypsin inhibitor heavy chain H2							
I	intermediate filament organisation	Desmoplakin							
	intermediate filament organisation	Vimentin							
	intracellular protein transport	AP-2 complex subunit alpha-1							
		AP-2 complex subunit beta							
		AP-2 complex subunit mu							
		AP-3 complex subunit beta-							

Biological process	Protein name	Additional information	control	5 mM MgCl ₂	diff	diff + 5 mM MgCl ₂	extract	extract diff	Mg sample
	1								
	Ras-related protein Rab-11B								
	Ras-related protein Rab-14								
	Ras-related protein Rab-1B								
	Ras-related protein Rab-23								
	Ras-related protein Rab-2A								
	Ras-related protein Rab-5C								
	Ras-related protein Rab-7a								
	Vacuolar protein sorting-associated protein 26A								
	Vacuolar protein sorting-associated protein 35								
	Clathrin heavy chain 1								
	Coatomer subunit alpha								
	Coatomer subunit beta								
	Coatomer subunit beta'								
	Coatomer subunit delta								
	Coatomer subunit gamma-1								
	GTP-binding protein SAR1a								
	Protein SEC13 homolog								
	Protein transport protein Sec23A								
	Protein transport protein Sec31A	Ca ²⁺ dependent protein binding							
	Sorting nexin-1								
	Sorting nexin-3								
	Sorting nexin-9								
	Target of Myb protein 1								
intracellular transport	Kinesin-1 heavy chain								
ion transmembrane transport	Annexin A6	Ca ²⁺ binding							
ion transport	LIM and SH3 domain protein 1								
	Sideroflexin-3								
	Sodium/potassium-transporting ATPase subunit alpha-1								
K keratinisation	Periplakin								
L leukotriene biosynthetic process	Aminopeptidase B								
lipid catabolic process	Putative phospholipase B-like 2								

Biological process	Protein name	Additional information	control	5 mM MgCl ₂	diff	diff + 5 mM MgCl ₂	extract	extract diff	Mg sample
lipid metabolism	Vigilin								
lipid transport	Extended synaptotagmin-1								
M membrane organisation	Unconventional myosin-Ic								
methylation	Adenosylhomocysteinase								
	Mitochondrial 10-formyltetrahydrofolate dehydrogenase								
	Nicotinamide N-methyltransferase								
microtubule bundle formation	Microtubule-associated protein 1B								
microtubule cytoskeleton organisation	Microtubule-associated protein 1A								
microtubule depolymerisation	Stathmin								
mitochondrial calcium ion homeostasis	Mitochondrial inner membrane protein								
mitochondrial fusion	Synaptic vesicle membrane protein VAT-1 homolog								
movement of cell or subcellular component	Tropomyosin alpha-3 chain	Ca ²⁺ binding							
	Tropomyosin alpha-4 chain								
mRNA processing	ATP-dependent RNA helicase DDX39A								
	Heterogeneous nuclear ribonucleoprotein F								
	Heterogeneous nuclear ribonucleoprotein H								
	Heterogeneous nuclear ribonucleoprotein M								
	Heterogeneous nuclear ribonucleoprotein Q								
	Heterogeneous nuclear ribonucleoprotein U								
	Heterogeneous nuclear ribonucleoprotein A2/B1								
	Heterogeneous nuclear ribonucleoprotein C1/C2								
	Nuclease-sensitive element-binding protein 1								
	Poly(rC)-binding protein 1								
	Poly(rC)-binding protein 2								
	Polyadenylate-binding protein 1								
	Polypyrimidine tract-binding protein 1								
	Ribonuclease inhibitor								
	RNA binding motif protein,								

Biological process	Protein name	Additional information	control	5 mM MgCl ₂	diff	diff + 5 mM MgCl ₂	extract	extract diff	Mg sample
	X-linked-like-1								
	RNA-binding protein FUS								
	Serine/arginine-rich splicing factor 1								
	Serine-threonine kinase receptor-associated protein								
muscle contraction	Actin, gamma-enteric smooth muscle								
	Myoferlin	Cofactor Ca ²⁺							
muscle filament sliding	Tropomyosin beta chain								
N nuclear lamina	Lamin-B2								
nuclear membrane organisation	Torsin-1A-interacting protein 1								
	Histone H1x								
	Histone H2A type 1-H								
nucleosome assembly	Core histone macro-H2A.1								
	Nucleosome assembly protein 1-like 1								
	Nucleosome assembly protein 1-like 4								
nucleosome disassembly	Protein SET								
nucleotide binding	Voltage-dependent anion-selective channel protein 2								
O organelle organisation	Cytoplasmic dynein 1 heavy chain 1								
	PDZ and LIM domain protein 7								
ossification	Prolyl 3-hydroxylase 1								
	Transmembrane glycoprotein NMB								
osteoblast differentiation	ATP-dependent RNA helicase A								
	1,25-dihydroxyvitamin D(3) 24-hydroxylase, mitochondrial								
osteoclast development	Annexin A2	Ca ²⁺ binding							
osteogenesis	Lactotransferrin								
oxidation-reduction process	4-trimethylaminobutyraldehyde dehydrogenase								
	Thioredoxin domain-containing protein 17								
P pathogenesis	N-acetylglucosamine-6-sulfatase	Cofactor Ca ²⁺							
peptidyl-proline hydroxylation	Prolyl 4-hydroxylase subunit alpha-2								

Biological process	Protein name	Additional information	control	5 mM MgCl ₂	diff	diff + 5 mM MgCl ₂	extract	extract diff	Mg sample
platelet activation	WD repeat-containing protein 1								
	Calumenin								
platelet aggregation	Cysteine and glycine-rich protein 1								
	Myosin regulatory light chain 12A								
prenylcysteine metabolic process	Prenylcysteine oxidase 1								
protease inhibitor	Calpastatin								
	Phosphatidylethanolamine-binding protein 1								
protein complex assembly	Macrophage-capping protein								
protein folding	10 kDa heat shock protein, mitochondrial	Ca ²⁺ binding							
	60 kDa heat shock protein, mitochondrial								
	78 kDa glucose-regulated protein								
	Alpha-crystallin B chain								
	BAG family molecular chaperone regulator 2	Ca ²⁺ binding							
	Calnexin								
	Calreticulin	Ca ²⁺ binding							
	Endoplasmic reticulum resident protein 29								
	Endoplasmic reticulum resident protein 44								
	Endoplasmin								
	Neutral alpha-glucosidase AB								
	Peptidyl-prolyl cis-trans isomerase A								
	Peptidyl-prolyl cis-trans isomerase B								
	Peptidyl-prolyl cis-trans isomerase FKBP10	Ca ²⁺ binding							
	Peptidyl-prolyl cis-trans isomerase FKBP9	Ca ²⁺ binding							
	Peroxiredoxin-4								
	Prefoldin subunit 2								
	Prefoldin subunit 4								
	Protein disulfide-isomerase A3								
	Protein disulfide-isomerase A4								

Biological process	Protein name	Additional information	control	5 mM MgCl ₂	diff	diff + 5 mM MgCl ₂	extract	extract diff	Mg sample
	Protein disulfide-isomerase A5								
	Protein disulfide-isomerase A6								
	Protein disulfide-isomerase Stress-70 protein, mitochondrial								
	T-complex protein 1 subunit alpha								
	T-complex protein 1 subunit beta								
	T-complex protein 1 subunit delta								
	T-complex protein 1 subunit eta								
	T-complex protein 1 subunit gamma								
	T-complex protein 1 subunit theta								
	T-complex protein 1 subunit zeta								
	Tubulin alpha-1B chain								
	Tubulin beta-3 chain								
	Tubulin beta-4B chain								
	UDP-glucose:glycoprotein glucosyltransferase 1	Cofactor Ca ²⁺							
protein homooligomerisation	Atlastin-3								
	Erythrocyte band 7 integral membrane protein	Cofactor Ca ²⁺							
protein modification	Protein-glutamine gamma-glutamyltransferase 2	Cofactor Ca ²⁺							
	LIM domain only protein 7								
	Protein-lysine 6-oxidase								
	Puromycin-sensitive aminopeptidase								
protein oligomerisation	Ubiquitin carboxyl-terminal hydrolase 5								
	Ubiquitin-like modifier-activating enzyme 1								
protein stabilisation	Neuroblast differentiation-associated protein AHNAK								
	Nucleophosmin								
protein transport	Lysosome-associated membrane glycoprotein 1								
	Protein canopy homolog 2								
	ADP-ribosylation factor 3								

Biological process	Protein name	Additional information	control	5 mM MgCl ₂	diff	diff + 5 mM MgCl ₂	extract	extract diff	Mg sample
	ADP-ribosylation factor 4								
	General vesicular transport factor p115								
	Golgi resident protein GCP60								
	GTP-binding nuclear protein Ran								
	Importin subunit beta-1								
	Importin-5								
	Major vault protein								
	Nascent polypeptide-associated complex subunit alpha								
	Rab GDP dissociation inhibitor beta								
	Ribosome-binding protein 1								
	Transmembrane emp24 domain-containing protein 9								
	Transportin-1								
	Vesicle-trafficking protein SEC22b								
	Proteasome activator complex subunit 1								
	Proteasome subunit alpha type-1								
	Proteasome subunit alpha type-5								
	Proteasome subunit alpha type-6								
	Proteasome subunit alpha type-7								
	Proteasome subunit beta type-1								
	Cathepsin Z								
	Cytosol aminopeptidase								
	pyrimidine biosynthesis	UMP-CMP kinase							Cofactor Mg ²⁺
R	regulation of cell shape	Protein S100-A13							Ca ²⁺ binding
	regulation of synapse assembly	PDZ and LIM domain protein 5							
	response to oxidative stress	Peroxiredoxin-2							
		Peroxiredoxin-5, mitochondrial							
		Peroxiredoxin-6							
S	signal transduction	Annexin A4							Ca ²⁺ binding
		Annexin A5							Ca ²⁺ binding

Biological process	Protein name	Additional information	control	5 mM MgCl ₂	diff	diff + 5 mM MgCl ₂	extract	extract diff	Mg sample
	Chloride intracellular channel protein 1								
	Coronin-1C								
	Dihydropyrimidinase-related protein 2								
	N(G),N(G)-dimethylarginine dimethylaminohydrolase 2								
	Protein S100-A11	Ca ²⁺ binding							
	Protein S100-A4	Ca ²⁺ binding							
	Protein S100-A6	Ca ²⁺ binding							
	Rho GDP-dissociation inhibitor 1								
	Rho GTPase-activating protein 1								
	SH3 domain-binding glutamic acid-rich-like protein								
skeletal muscle tissue development	Myosin light polypeptide 6								
	Glutaminase kidney isoform, mitochondrial								
	Glutamine-fructose-6-phosphate aminotransferase [isomerizing]								
	Glutathione S-transferase omega-1								
	Glutathione S-transferase P								
	Leukotriene A-4 hydrolase								
	Ornithine aminotransferase, mitochondrial								
	Prosaposin								
small molecule metabolic process	Sulfide:quinone oxidoreductase, mitochondrial								
	UDP-glucose 6-dehydrogenase								
	Aldo-keto reductase family 1 member C1								
	Aldo-keto reductase family 1 member C3								
	Alpha-aminoadipic semialdehyde dehydrogenase								
	Bifunctional purine biosynthesis protein PURH								

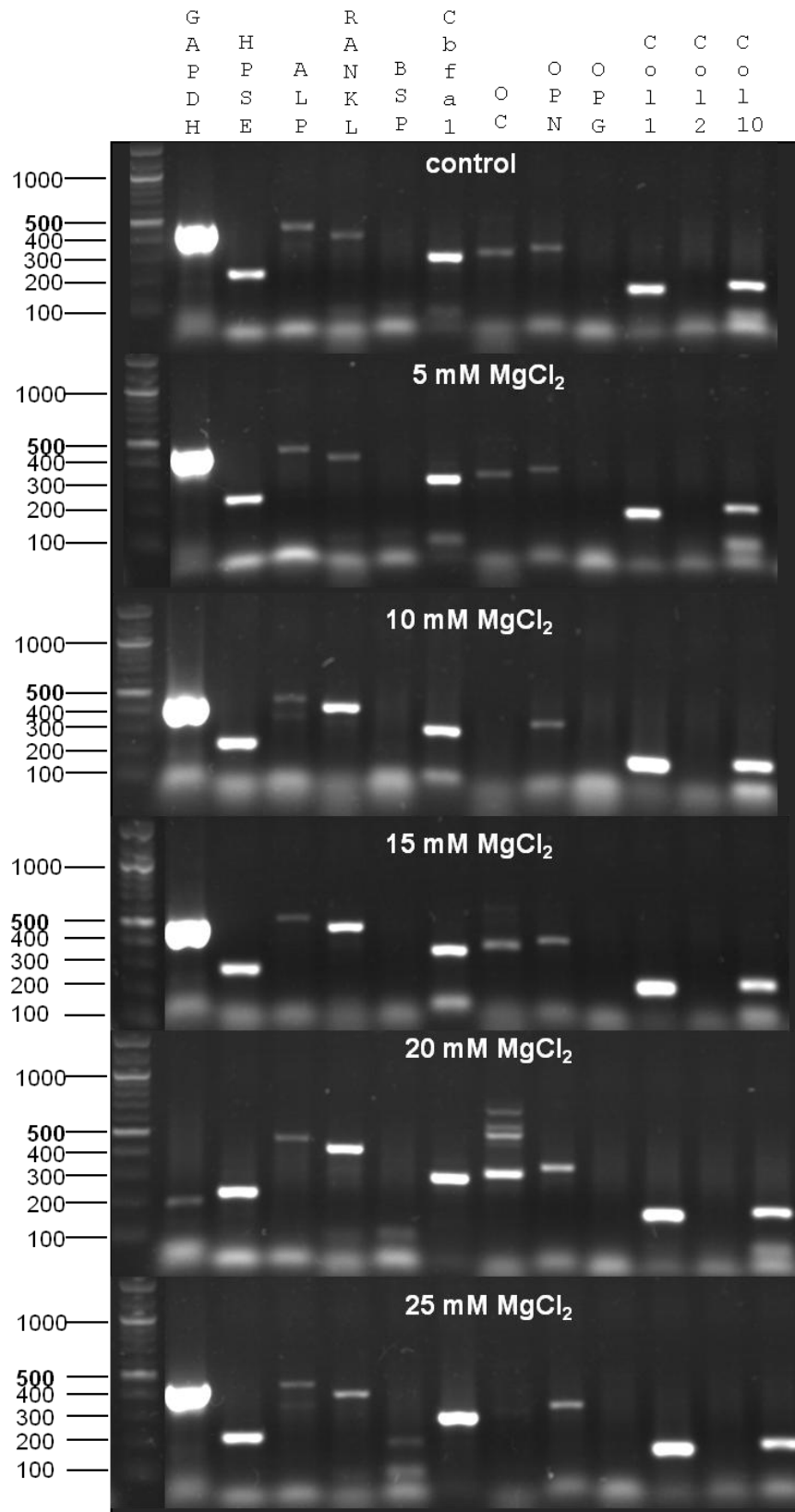
Biological process	Protein name	Additional information	control	5 mM MgCl ₂	diff	diff + 5 mM MgCl ₂	extract	extract diff	Mg sample
	Biliverdin reductase A								
	Carbonyl reductase [NADPH] 1								
	Creatine kinase B-type								
	Cytosolic non-specific dipeptidase								
	Glucosylceramidase								
	Lysosomal protective protein								
	Myristoylated alanine-rich C-kinase substrate								
	NADH-cytochrome b5 reductase 3								
	Persulfide dioxygenase ETHE1, mitochondrial								
steroid hormone mediated signaling pathway	Membrane-associated progesterone receptor component 2								
	Heat shock 70 kDa protein 1A/1B								
	Heat shock 70 kDa protein 4								
	Heat shock cognate 71 kDa protein								
	Heat shock protein 105 kDa								
	Heat shock protein beta-1								
	Heat shock protein beta-6								
stress response	Heat shock protein beta-7								
	Heat shock protein HSP 90-alpha								
	Heat shock protein HSP 90-beta								
	Hypoxia upregulated protein 1								
	Protein DJ-1								
	Stress-induced-phosphoprotein 1								
superoxide metabolic process	Superoxide dismutase [Cu-Zn]								
	Superoxide dismutase [Mn], mitochondrial								
T	ATP-dependent RNA helicase DDX1								
transcription	ATP-dependent RNA helicase DDX3Y								
	Complement component 1 Q subcomponent-binding								

Biological process	Protein name	Additional information	control	5 mM MgCl ₂	diff	diff + 5 mM MgCl ₂	extract	extract diff	Mg sample
	protein, mitochondrial								
	Far upstream element-binding protein 1								
	Far upstream element-binding protein 2								
	Four and a half LIM domains protein 2								
	Heterogeneous nuclear ribonucleoprotein D0								
	Heterogeneous nuclear ribonucleoprotein D-like								
	High mobility group protein HMG-I/HMG-Y								
	Interleukin enhancer-binding factor 3								
	MICOS complex subunit MIC19								
	Nucleolin								
	Polymerase I and transcript release factor								
	Probable ATP-dependent RNA helicase DDX17								
	Protein LYRIC								
	Signal transducer and activator of transcription 1-alpha/beta								
	Staphylococcal nuclease domain-containing protein 1								
	Transcription intermediary factor 1-beta								
	X-ray repair cross-complementing protein 5								
	X-ray repair cross-complementing protein 6								
translation	40S ribosomal protein S10								
	40S ribosomal protein S11								
	40S ribosomal protein S12								
	40S ribosomal protein S13								
	40S ribosomal protein S14								
	40S ribosomal protein S15a								
	40S ribosomal protein S16								
	40S ribosomal protein S17-like								
	40S ribosomal protein S19								
	40S ribosomal protein S2								

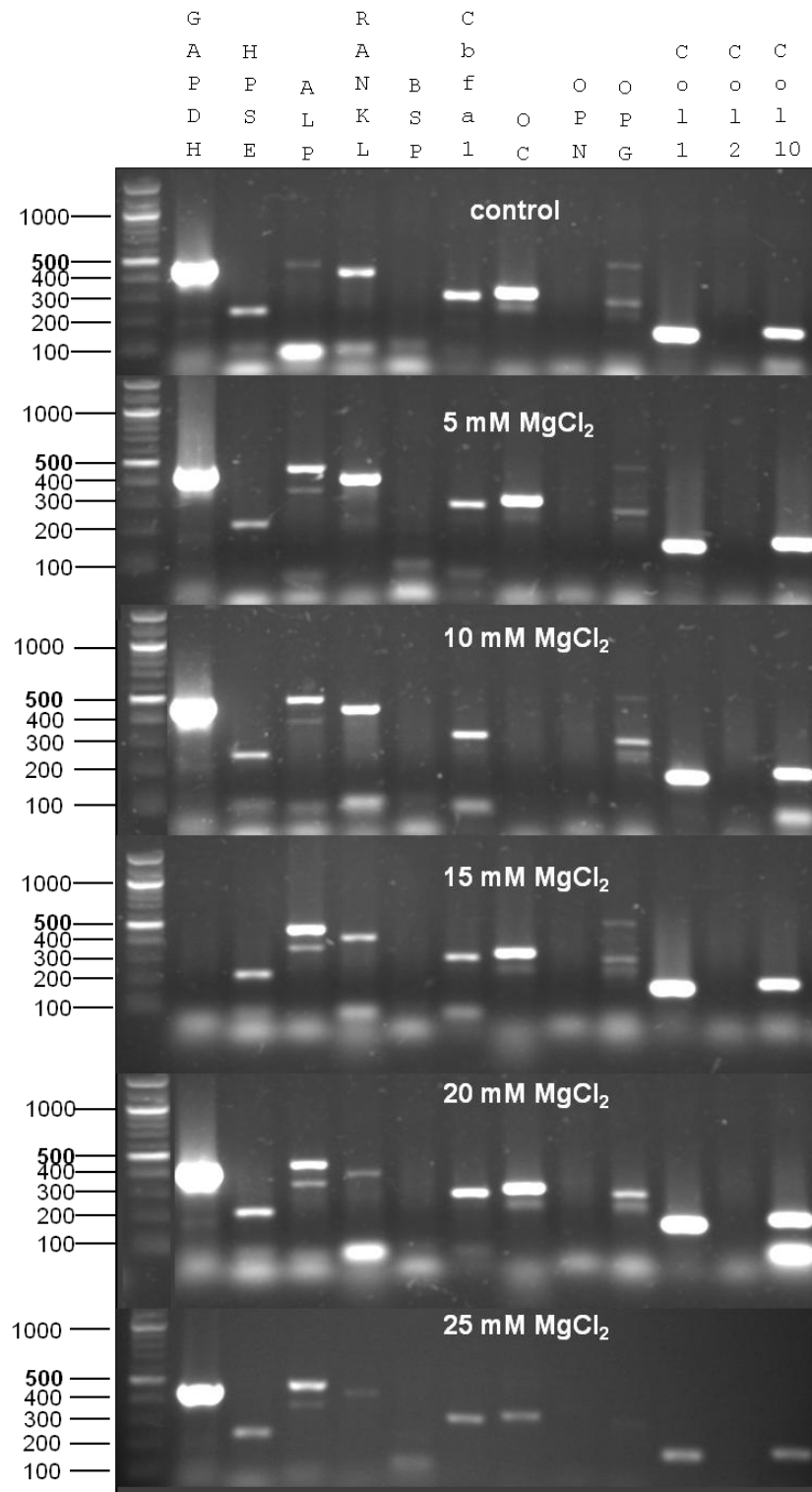
Biological process	Protein name	Additional information	control	5 mM MgCl ₂	diff	diff + 5 mM MgCl ₂	extract	extract diff	Mg sample
	40S ribosomal protein S20								
	40S ribosomal protein S25								
	40S ribosomal protein S3								
	40S ribosomal protein S3a								
	40S ribosomal protein S4								
	40S ribosomal protein S5								
	40S ribosomal protein S6								
	40S ribosomal protein S7								
	40S ribosomal protein S8								
	40S ribosomal protein S9								
	40S ribosomal protein SA								
	60S acidic ribosomal protein P0								
	60S acidic ribosomal protein P2								
	60S ribosomal protein L10a								
	60S ribosomal protein L11								
	60S ribosomal protein L12								
	60S ribosomal protein L13								
	60S ribosomal protein L13a								
	60S ribosomal protein L14								
	60S ribosomal protein L18								
	60S ribosomal protein L18a								
	60S ribosomal protein L22								
	60S ribosomal protein L23								
	60S ribosomal protein L23a								
	60S ribosomal protein L24								
	60S ribosomal protein L26								
	60S ribosomal protein L27								
	60S ribosomal protein L27a								
	60S ribosomal protein L28								
	60S ribosomal protein L30								
	60S ribosomal protein L4								
	60S ribosomal protein L6								
	60S ribosomal protein L7								
	60S ribosomal protein L7a								
	60S ribosomal protein L9								
	Alanine-tRNA ligase, cytoplasmic								
	Asparagine-tRNA ligase, cytoplasmic								

Biological process	Protein name	Additional information	control	5 mM MgCl ₂	diff	diff + 5 mM MgCl ₂	extract	extract diff	Mg sample
	Aspartate-tRNA ligase, cytoplasmic								
	Cysteine-tRNA ligase, cytoplasmic								
	Dolichyl-diphosphooligosaccharide-protein glycosyltransferase subunit 1								
	Dolichyl-diphosphooligosaccharide-protein glycosyltransferase subunit 2								
	Elongation factor 1-alpha 1								
	Elongation factor 1-beta								
	Elongation factor 1-delta								
	Elongation factor 1-gamma								
	Elongation factor 2								
	Elongation factor Tu								
	Eukaryotic initiation factor 4A-II								
	Eukaryotic peptide chain release factor subunit 1								
	Eukaryotic translation initiation factor 2 subunit 3								
	Eukaryotic translation initiation factor 4 gamma 1								
	Eukaryotic translation initiation factor 4H								
	Eukaryotic translation initiation factor 5A-1								
	Eukaryotic translation initiation factor 6								
	Glycine-tRNA ligase								
	Histidine-tRNA ligase, cytoplasmic								
	Inorganic pyrophosphatase	Cofactor Mg ²⁺							
	Isoleucine-tRNA ligase, cytoplasmic								
	Leucine-tRNA ligase, cytoplasmic								
	Myotrophin								
	Signal peptidase complex catalytic subunit SEC11A								
	Threonine-tRNA ligase, cytoplasmic								
	Tryptophan-tRNA ligase,								

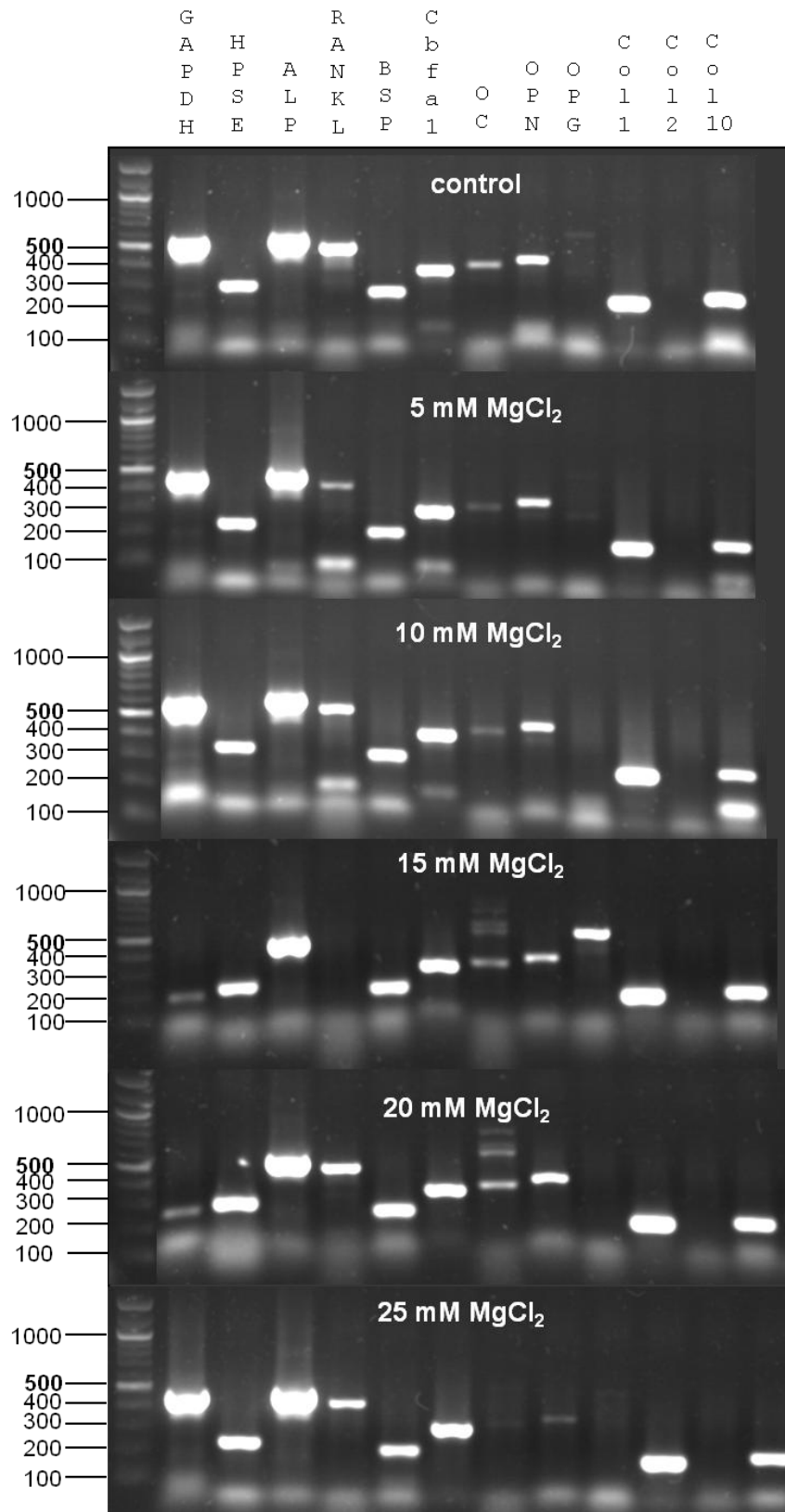
Biological process	Protein name	Additional information	control	5 mM MgCl ₂	diff	diff + 5 mM MgCl ₂	extract	extract diff	Mg sample
	cytoplasmic Tyrosine-tRNA ligase, cytoplasmic Valine-tRNA ligase								
tRNA processing	3-hydroxyacyl-CoA dehydrogenase type-2								
U unknown	Nodal modulator 3								
	PDZ and LIM domain protein 4								
	Protein AHNAK2								
	Protein canopy homolog 4								
	Putative protein FAM10A4								
	Putative tropomyosin alpha- 3 chain-like protein								
	Reticulocalbin-3	Ca ²⁺ binding							
vesicle-mediated transport	Perilipin-3								
V vesicular transport	Vesicle-associated membrane protein 3								
	Vesicle-fusing ATPase	Cofactor Mg ²⁺							
vitamin D metabolic process	Vitamin D-binding protein								
vitamin metabolic process	Pyridoxal kinase	Cofactor Mg ²⁺							



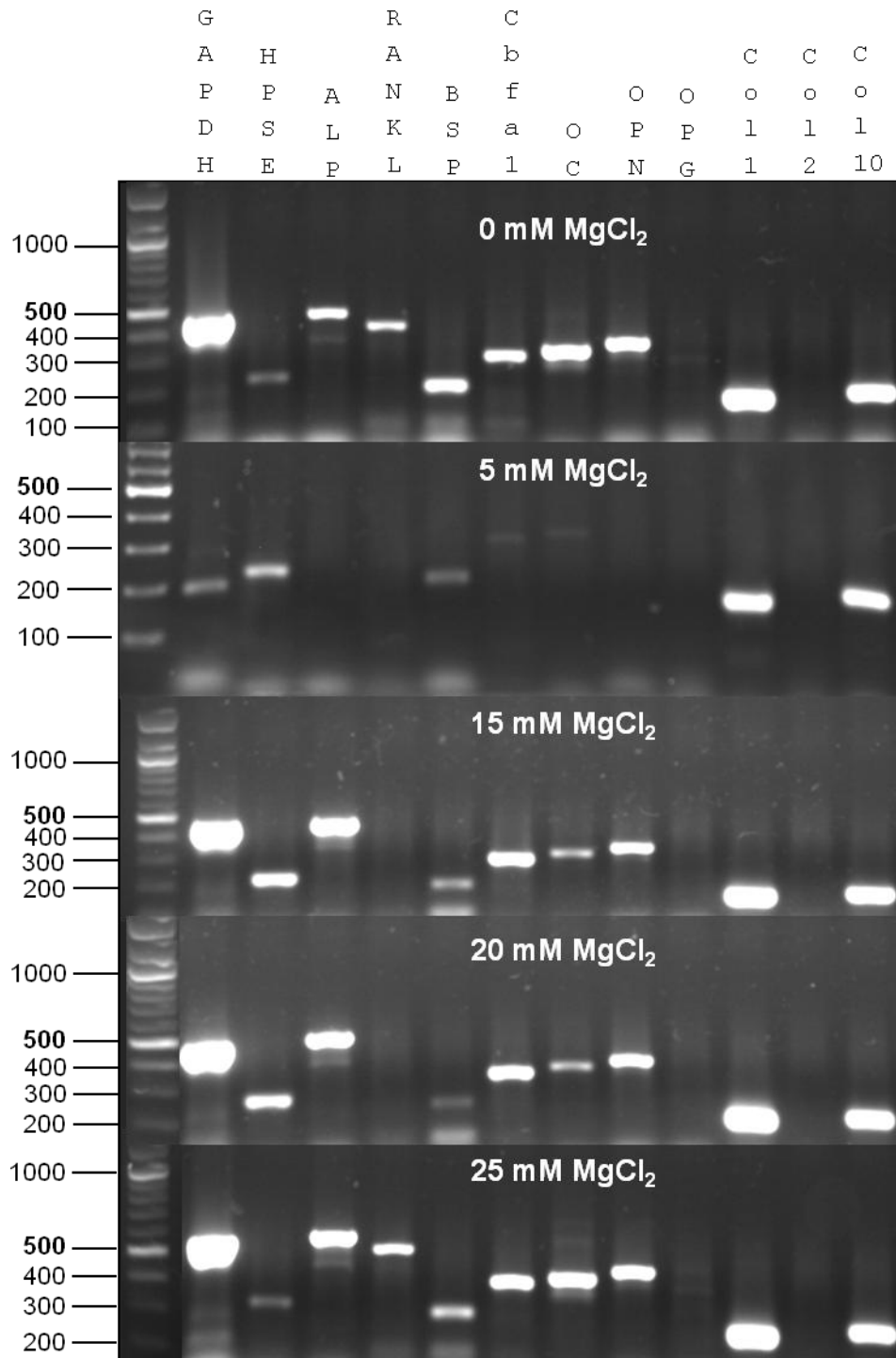
Appendix 2. Comparison of the qualitative gene expression of various genes involved in bone formation in U2OS cells under cell culture conditions and after incubation with 5-25 mM MgCl₂ for one week. The sizes of the DNA ladder are indicated. GAPDH: glyceraldehyde-3-phosphate dehydrogenase; HPSE: heparanase; ALP: alkaline phosphatase; RANKL: RANK ligand; BSP: bone sialoprotein; Cbfa1: runt-related transcription factor 2; OC: osteocalcin, OPN: osteopontin; OPG: osteoprotegerin; and Col: collagen.



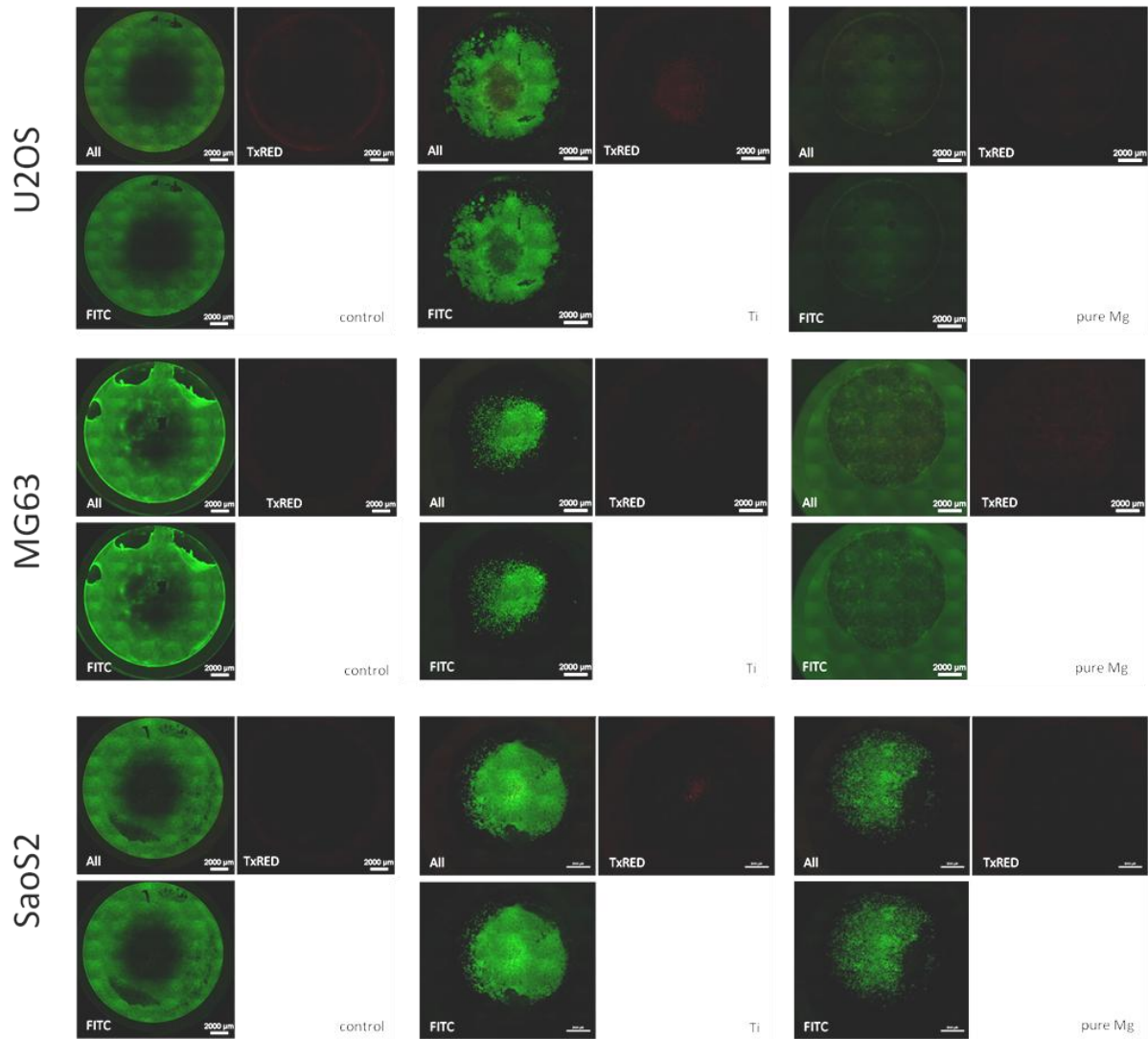
Appendix 3. Comparison of the qualitative gene expression of various genes involved in bone formation in MG63 cells under cell culture conditions and after incubation with 5-25 mM MgCl₂ for one week. The sizes of the DNA ladder are indicated. GAPDH: glyceraldehyde-3-phosphate dehydrogenase; HPSE: heparanase; ALP: alkaline phosphatase; RANKL: RANK ligand; BSP: bone sialoprotein; Cbfa1: runt-related transcription factor 2; OC: osteocalcin, OPN: osteopontin; OPG: osteoprotegerin; and Col: collagen.



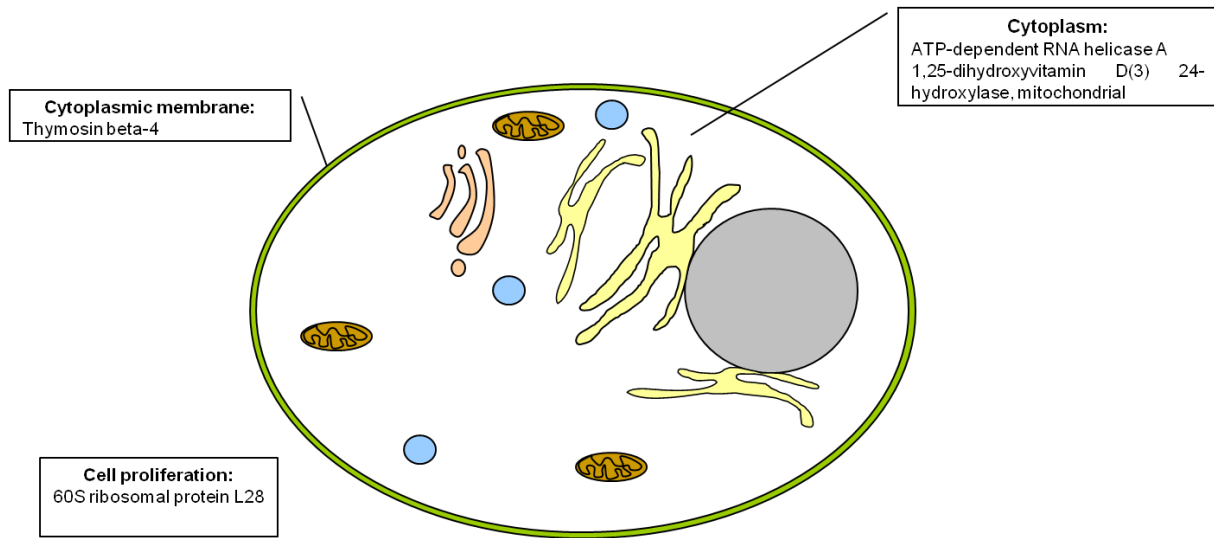
Appendix 4. Comparison of the qualitative gene expression of various genes involved in bone formation in SaoS2 cells under cell culture conditions and after incubation with 5-25 mM MgCl₂ for one week. The sizes of the DNA ladder are indicated. GAPDH: glyceraldehyde-3-phosphate dehydrogenase; HPSE: heparanase; ALP: alkaline phosphatase; RANKL: RANK ligand; BSP: bone sialoprotein; Cbfa1: runt-related transcription factor 2; OC: osteocalcin, OPN: osteopontin; OPG: osteoprotegerin; and Col: collagen.



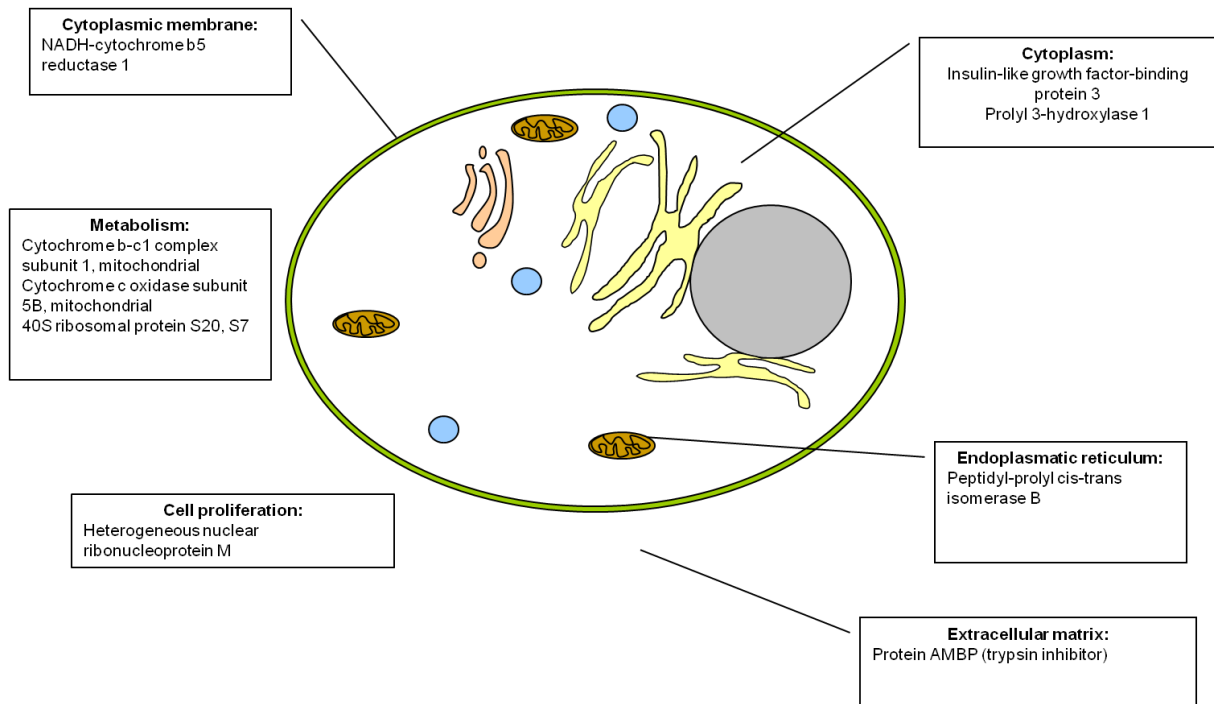
Appendix 5. Comparison of the qualitative gene expression of various genes involved in bone formation in primary human osteoblasts under cell culture conditions and after incubation with 5-25 mM MgCl₂ for one week. No results are available for 10 mM MgCl₂, as no PCR products could be detected. The sizes of the DNA ladder are indicated. GAPDH: glyceraldehyde-3-phosphate dehydrogenase; HPSE: heparanase; ALP: alkaline phosphatase; RANKL: RANK ligand; BSP: bone sialoprotein; Cbfa1: runt-related transcription factor 2; OC: osteocalcin, OPN: osteopontin; OPG: osteoprotegerin; and Col: collagen.



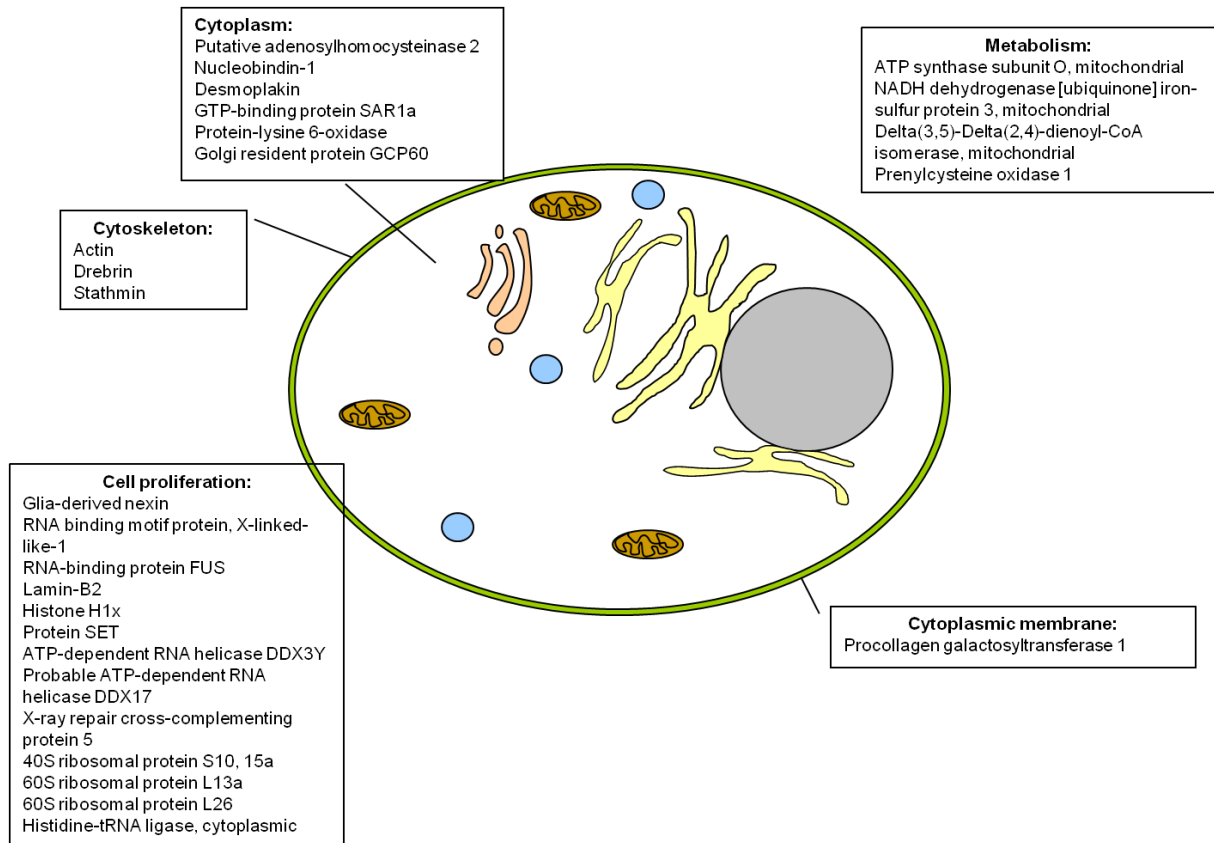
Appendix 6. Live/Dead staining of cells cultured on different materials to visualise the viability of the cells. Living cells were stained green (FITC) and dead cells appeared red (TexasRED); ALL: merged images. Presented are the results for the cell lines U2OS, MG63, and SaoS2.



Appendix 7. Overview of the locations of expressed proteins found with proteomics after the addition of $MgCl_2$. The proteins are arranged according to their cellular functions. Only the proteins that were exclusively expressed under the examined condition are indicated.



Appendix 8. Overview of the locations of expressed proteins found with proteomics after the addition of $MgCl_2$ to differentiating cells. The proteins are arranged according to their cellular functions. Only the proteins that were exclusively expressed under the examined condition are indicated.



Appendix 9. Overview of the locations of expressed proteins found with proteomics after the addition of magnesium-based extract to differentiating cells. The proteins are arranged according to their cellular functions. Only the proteins that were exclusively expressed under the examined condition are indicated.

12. PUBLICATION LIST

12.1 JOURNAL ARTICLES

Burmester A., Luthringer B., Willumeit R., Feyerabend F., *Comparison of the reaction of bone-derived cells to enhanced MgCl₂-salt concentrations*. Biomatter, 2014. 4(1): e967616.

Burmester A., Willumeit-Römer R., Feyerabend F., *Behavior of bone cells in contact with magnesium implant material*. Journal of Biomedical Materials Research Part B: Applied Biomaterials, 2015. doi: 10.1002/jbm.b.33542.

12.2 CONFERENCE CONTRIBUTIONS

Oral presentations

Burmester A., Feyerabend F., Luthringer B., Willumeit R., *Genetic regulation of cells from the bone system in reaction to magnesium corrosion environment*.

Seminar at the Institute of Biochemistry and Molecular Biology, University Hamburg, Hamburg, 26 November 2012.

Burmester A., Feyerabend F., Luthringer B., Willumeit R., *Comparison of osteoblasts and osteosarcoma cell lines in reaction to enhanced Mg²⁺ concentrations*.

National Conference “Jahrestagung der Deutschen Gesellschaft für Biomaterialien”, Hamburg, 1 - 3 November 2012.

Burmester A., Feyerabend F., Luthringer B., Willumeit R., *Genetic regulation of bone cells upon increased magnesium salt concentrations*.

International Conference “Materials Science Engineering”, Darmstadt, 25 - 27 September 2012.

Burmester A., Feyerabend F., Luthringer B., Willumeit R., *Comparison of the reaction of bone-derived cells to high magnesium concentrations*.

International Conference “4th Symposium on Biodegradable Metals”, Maratea, Italy. 27 August - 1 September 2012.

Poster presentations

Omidi M., **Burmester A.**, Schütz D., Wurlitzer M., Kwiatkowski M., Luthringer B., Willumeit-Römer R., Schlüter H., *Application of proteomics on bone cells in response to Mg-alloys compared to Ti-Implants*. National Conference “49. Jahrestagung der DGMS”, Hamburg, 28 February – 2 March 2016

Burmester A., Feyerabend F., Willumeit R., *Influence of magnesium extracts on proliferating and differentiating bone-derived cells*. National Conference “Jahrestagung der Deutschen Gesellschaft für Biomaterialien”, Erlangen, 26 - 28 September 2013.

Burmester A., Feyerabend F., Willumeit R., *Influence of magnesium extracts on proliferating and differentiating bone-derived cells.*

3rd workshop “Neue Horizonte für metallische Biomaterialien”, Geesthacht, 28 - 29 May 2013

Burmester A., Feyerabend F., Luthringer B., Willumeit R., *Influence of MgCl₂ on bone cells.*








2nd Workshop “Neue Horizonte für metallische Biomaterialien”, Geesthacht, 2 - 3 May 2011

Burmester A., Feyerabend F., Luthringer B., Willumeit R., *Influence of MgCl₂ on bone cells.*











National conference “Jahrestagung der Deutschen Gesellschaft für Biomaterialien”, Gießen, 10 - 12 November 2011.

13. HAZARD STATEMENTS AND SAFETY PHRASES









Listing of potentially hazardous substances used in this study classified in accordance with the Globally Harmonized System of Classification, Labelling and Packaging of Chemicals GHS.

Substance	Chemical Abstract Service No.	Hazard Statement	Precautionary Statement	Danger Symbol
acetonitrile	75-05-8	225-302+312+332-319	210-240-302+352-305+351+338-403+233	 
alexa Fluor 488 phalloidin	17466-45-4	302-311-332	302+352-361-301+312-330-304+340-312-261-264-280	
ammonium bicarbonate	1066-33-7	302	301+312+330	
boric acid	10043-35-3	360	201-308+313	
chloroform	67-66-3	302-315-319-331-351-361d-372	302+352-304+340-305+351+338	 











13. Hazard statements and safety phrases

Substance	Chemical Abstract Service No.	Hazard Statement	Precautionary Statement	Danger Symbol
dexamethasone	50-02-2	315-317-319-334-335	261-280-305+351+338-342+311	 
dithiothreitol (DTT)	3483-12-3	302-315-319-335	261-305+351+338	
ethylenediamine tetra acetic acid-Na ₂ (EDTA)	6381-92-6	332-373	314	 
ethanol	64-17-5	225-319	210-240-305+351+338-403+233	 
formaldehyde	50-00-0	301+311+331-314-317-335-341-350-370	201-260-280-301+310+330-303+361+353-304+340+310-305+351+338-308+311	  







13. Hazard statements and safety phrases

Substance	Chemical Abstract Service No.	Hazard Statement	Precautionary Statement	Danger Symbol
formic acid	64-18-6	226-302-314-331	260-280-303+361+353-304+340+310-305+351+338-403+233	  
Hellmanex™		290-315-319-335	234-261-312-332+313-403+233-405	 
iodacetamide	144-48-9	301-317-334-413	261-280-301+310-342+311	 
magnesium	7439-95-4	250-260	222-223-231+232-370+378-422	 powder

13. Hazard statements and safety phrases

Substance	Chemical Abstract Service No.	Hazard Statement	Precautionary Statement	Danger Symbol
methanol	67-56-1	225-301+311+331+-370	210-240-280-302+352-304+340-308+310-403+233	  
QIAGEN buffer RLT		302-314-412	280-305+351+338-308+311	 
QIAGEN buffer RW1		226-314	210-280-305+351+338-308+311	 
sodium dodecyl sulfate (SDS)	151-21-3	228-302-315-318-332-335-412	261-264-280-301+312-330-302+352-305+351+338-310-321-332+313-362-273-501	  

13. Hazard statements and safety phrases

Substance	Chemical Abstract Service No.	Hazard Statement	Precautionary Statement	Danger Symbol
titanium	7440-32-6	250-252	210-222-280-235+410-420-422	 powder
Triton X-100	9002-93-1	302-319-411	273-280-301-312+330-337+313-391-501	 
TRITC-conjugated phalloidin	17466-45-4	300+310+330-371	260-262-264-270-271-308+311-301+310-330-310-361-363-304+340-302+351+338-337+313-403+233-405-501	
1 α ,25 dihydroxyvitamin D3	32222-06-3	300-310-330-361	260-264-280-284-301+310	 
2-phenylindole-4',6-dicarboxamidine dihydrochloride (DAPI)	28718-90-3		308+313-403+233-501	

Danger symbols were used from <http://www.kroschke.com>

GHS Hazard Statement

Physical hazards

H225	Highly flammable liquid and vapour
H226	Flammable liquid and vapour
H228	Flammable solid
H250	Catches fire spontaneously if exposed to air
H252	Self-heating in large quantities; may catch fire

H260	In contact with water releases flammable gases which may ignite spontaneously
H290	May be corrosive to metals

Health hazards

H300	Fatal if swallowed
H301	Toxic if swallowed
H302	Harmful if swallowed
H310	Fatal in contact with skin
H311	Toxic in contact with skin
H312	Harmful in contact with skin
H314	Causes severe skin burns and eye damage
H315	Causes skin irritation
H317	May cause an allergic skin reaction
H318	Causes serious eye damage
H319	Causes serious eye irritation
H330	Fatal if inhaled
H331	Toxic if inhaled
H332	Harmful if inhaled
H334	May cause allergy or asthma symptoms or breathing difficulties if inhaled
H335	May cause respiratory irritation
H341	Suspected of causing genetic defects
H350	May cause cancer
H351	Suspect of causing cancer
H360	May damage fertility or the unborn child
H361	Suspected of damaging fertility or the unborn child
H361d	Suspected of damaging the unborn child
H370	Causes damage to organs
H371	May cause damage to organs
H372	Causes damage to organs through prolonged or repeated exposure
H373	May cause damage to organs through prolonged or repeated exposure

Environmental hazards

H411	Toxic to aquatic life with long-lasting effects
H412	Harmful to aquatic life with long-lasting effects
H413	May cause long-lasting harmful effects to aquatic life

General precautionary statements

Prevention precautionary statements

P201	Obtain special instructions before use.
P210	Keep away from heat, hot surfaces, sparks, open flames and other ignition sources. No smoking.
P222	Do not allow contact with air.
P223	Do not allow contact with water.

P234	Keep only in original container.
P240	Ground/bond container and receiving equipment.
P260	Do not breathe dust/fumes/gas/mist/vapours/spray.
P261	Avoid breathing dust/fumes/gas/mist/vapours/spray.
P262	Do not get in eyes, on skin, or on clothing.
P264	Wash ... thoroughly after handling.
P270	Do not eat, drink or smoke when using this product.
P271	Use only outdoors or in a well-ventilated area.
P273	Avoid release to the environment.
P280	Wear protective gloves/protective clothing/eye protection/face protection
P284	[In case of inadequate ventilation] wear respiratory protection.
P231+232	Handle under inert gas. Protect from moisture
P235+410	Keep cool. Protect from sunlight

Response precautionary statements

P301	IF SWALLOWED:
P308	IF exposed or concerned:
P310	Immediately call a POISON CENTER/doctor/...
P312	Call a POISON CENTER/ doctor/.../if you feel unwell.
P314	Get Medical advice/attention if you feel unwell.
P321	Specific treatment (see ... on this label).
P330	Rinse mouth.
P361	Take off immediately all contaminated clothing.
P362	Take off contaminated clothing.
P363	Wash contaminated clothing before reuse.
P391	Collect spillage.
P301+310	IF SWALLOWED: Immediately call a POISON CENTER/doctor/...
P301+312	IF SWALLOWED: Call a POISON CENTER/doctor/.../if you feel unwell.
P301+310+330	IF SWALLOWED: Immediately call a POISON CENTER/doctor/...Rinse mouth.
P302+352	IF ON SKIN: Wash with plenty of water/...
P302+351+338	IF ON SKIN: Rinse cautiously with water for several minutes. Remove contact lenses if present and easy to do. Continue rinsing.
P303+361+353	IF ON SKIN (or hair): Take off immediately all contaminated clothing. Rinse skin with water/ shower.
P304+340	IF INHALED: Remove person to fresh air and keep comfortable for breathing.
P304+340+310	IF INHALED: Remove person to fresh air and keep comfortable for breathing. Immediately call a POISON CENTER/doctor/...
P305+351+338	IF IN EYES: Rinse cautiously with water for several minutes. Remove contact lenses if present and easy to do – continue rinsing.
P308+310	IF exposed or concerned: Immediately call a POISON CENTER/doctor/...

P308+311	IF exposed or concerned: Call a POISON CENTER/ doctor/...
P308+313	IF exposed: Call a POISON CENTER or doctor/physician.
P312+330	Call a POISON CENTER/ doctor/.../if you feel unwell. Rinse mouth.
P332+313	If skin irritation occurs: Get medical advice/attention.
P337+313	If eye irritation persists get medical advice/attention.
P342+311	If experiencing respiratory symptoms: Call a POISON CENTER/doctor/...
P370+378	In case of fire: Use ... to extinguish.

Storage precautionary statements

P405	Store locked up.
P420	Store away from other materials.
P422	Store contents under ...
P403+233	Store in a well ventilated place. Keep container tightly closed.

Disposal precautionary statements

P501	Dispose of contents/container to ... [... in accordance with local/regional/national/international regulation (to be specified)].
------	---

14. ACKNOWLEDGEMENTS

First, I would like to sincerely thank my advisor Prof. Regine Willumeit-Römer for her supervision, for giving me the opportunity to work in the interesting field of biodegradable magnesium and for educating me about medical devices. Moreover, I would like to thank her for her patience, motivation and guidance during my Ph.D.

Second, I would like to thank Prof. Uli Hahn for giving me the opportunity to defend my thesis in his department and present my research throughout my graduate work.

My thanks also go to Dr. Bérengère Luthringer and Dr. Frank Feyerabend for their supervision and help.

I would like to thank all members of WBB (formerly WPS) for having fun while doing lab work, for stimulating discussions and for all of their support. Special thanks go to Axel Deing, Daniela Lange and Lena Frenzel. I really appreciate your friendship.

I wish to thank all of my friends, simply for everything.

Last but not least, I would like to thank my parents and my husband, who always supported me.